

AD-A066 206

FOREIGN TECHNOLOGY DIV WRIGHT-PATTERSON AFB OHIO
SCIENTIFIC NOTES FROM THE CENTRAL AERO-HYDRODYNAMIC INSTITUTE (--ETC(U)
AUG 78

F/G 20/4

UNCLASSIFIED

FTD-ID(RS)T-1039-78

NL

1 of 4
AD
A066206



1

AD-A066206

FOREIGN TECHNOLOGY DIVISION



SCIENTIFIC NOTES FROM THE CENTRAL
AERO-HYDRODYNAMIC INSTITUTE
(SELECTED ARTICLES)

DDC
RECORDED
19 MAR 1979
E



Approved for public release;
distribution unlimited.

78 12 21 129

FTD- ID(RS)T-1039-78

UNEDITED MACHINE TRANSLATION

FTD-ID(RS)T-1039-78

10 August 1978

MICROFICHE NR: *FD-78-C-001085*

SCIENTIFIC NOTES FROM THE CENTRAL AERO-
HYDRODYNAMIC INSTITUTE (SELECTED ARTICLES)

English pages: 307

Source: Uchenyye Zapiski TSAGI, Moscow, Vol. 1,
Nr. 4, 1970, PP. 1-132.

Country of origin: USSR

This document is a machine translation.

Requester: FTD/TQTA

Approved for public release; distribution unlimited

ACCESSION for	
NTIS	White Section <input checked="" type="checkbox"/>
DDC	Ball Section <input type="checkbox"/>
UNANNOUNCED	<input type="checkbox"/>
JUSTIFICATION	
BY	
DISTRIBUTION/AVAILABILITY CODES	
Dist.	AVAIL. SPECIAL
<i>A</i>	

THIS TRANSLATION IS A RENDITION OF THE ORIGINAL FOREIGN TEXT WITHOUT ANY ANALYTICAL OR EDITORIAL COMMENT. STATEMENTS OR THEORIES ADVOCATED OR IMPLIED ARE THOSE OF THE SOURCE AND DO NOT NECESSARILY REFLECT THE POSITION OR OPINION OF THE FOREIGN TECHNOLOGY DIVISION.

PREPARED BY:

TRANSLATION DIVISION
FOREIGN TECHNOLOGY DIVISION
WP-AFB, OHIO.

FTD- ID(RS)T-1039-78

Date 10 Aug 1978

TABLE OF CONTENTS

U. S. Board on Geographic Names Transliteration System, Russian and English Trigonometric Functions.....	111
Region of Constant Vorticity in a Plane Potential Flow, by V. S. Sadovskiy.....	1
Uniqueness of the Solution of the Problem of Sonic Flow About a Profile, by Yu. B. Lifschitz.....	21
Optimum Distribution of Wing Thickness in a Supersonic Flow, By I. I. Burakov, Yu. L. Zhilin.....	35
The Similarity of Flows with Spraying Jets, by V. N. Gusev, V. V. Mikhaylov.....	53
The Simulation of Viscous Hypersonic Flows in Wind Tunnels, by V. S. Galkin, V. S. Nikolayev.....	62
Method of Calculation of the Turbulent Jets Near the Wall when the Longitudinal Gradient of Pressure is Present, by A. S. Ginevskiy, A. V. Kolesnikov, I. N. Podol'nyy.....	81
Calculation by the Method Monte-Carlo of Heat Flow Between Parallel Plates in the Rarefied Gas, by V. I. Vlasov.....	108
Interaction of Fast Particles with Solid Surface, by A. I. Yerofeyev.....	119
Criteria of the Longitudinal Stability of Aerodynamic Air-Cushion Vehicle, by R. D. Irodov.....	142
Irregular Optimum Trajectories of Craft During Flight in the Atmosphere, by V. V. Dikusar, A. A. Shilov.....	163
Equations of Rolling of an Plactic Tire, by V. S. Gozdek.....	183
The Account of Experience in Operation During the Determination of the Service Life of Construction, by V. D. Il'ichev.....	203
Approximation Method of the Calculation of Axisymmetric Interaction of the Freely Spraying Jet with Barrier by, V. I. Blagosklonov.....	220

78 12 21 129

Work of Gas Ejector in the Dissimilar Physical Parameters of the Mixed Gases, by P. A. Kukanov, I. I. Mezhirov.....	232
Effect of Wing Vortex System in the Absence of Lift on its Streamlining at Low Angles of Attack, by K. K. Fedyayevskiy, N. N. Pomin.....	249
Study of the Vortex System of Helicopter Rotor, by V. G. Kolkov.....	259
Fluctuations of Liquid in Cylindrical Container with Circular Baffle, by I. V. Kolin.....	271
Determination of the Required Accuracy of the Autonomous Angular Measurements and Wstimation Power Consumption for the Trajectory Correction of Space Vehicle During Approach to Planet, by S. V. Petukhov.....	285
References.....	305

U. S. BOARD ON GEOGRAPHIC NAMES TRANSLITERATION SYSTEM

Block	Italic	Transliteration	Block	Italic	Transliteration
А а	А а	A, a	Р р	Р р	R, r
Б б	Б б	B, b	С с	С с	S, s
В в	В в	V, v	Т т	Т т	T, t
Г г	Г г	G, g	У у	У у	U, u
Д д	Д д	D, d	Ф ф	Ф ф	F, f
Е е	Е е	Ye, ye; E, e*	Х х	Х х	Kh, kh
Ж ж	Ж ж	Zh, zh	Ц ц	Ц ц	Ts, ts
З з	З з	Z, z	Ч ч	Ч ч	Ch, ch
И и	И и	I, i	Ш ш	Ш ш	Sh, sh
Й й	Й й	Y, y	Щ щ	Щ щ	Shch, shch
К к	К к	K, k	Ъ ъ	Ъ ъ	"
Л л	Л л	L, l	Ы ы	Ы ы	Y, y
М м	М м	M, m	Ь ь	Ь ь	'
Н н	Н н	N, n	Э э	Э э	E, e
О о	О о	O, o	Ю ю	Ю ю	Yu, yu
П п	П п	P, p	Я я	Я я	Ya, ya

*ye initially, after vowels, and after ъ, ь; e elsewhere.
When written as ë in Russian, transliterate as yë or ë.

RUSSIAN AND ENGLISH TRIGONOMETRIC FUNCTIONS

Russian	English	Russian	English	Russian	English
sin	sin	sh	sinh	arc sh	sinh ⁻¹
cos	cos	ch	cosh	arc ch	cosh ⁻¹
tg	tan	th	tanh	arc th	tanh ⁻¹
ctg	cot	cth	coth	arc cth	coth ⁻¹
sec	sec	sch	sech	arc sch	sech ⁻¹
cosec	csc	csch	csch	arc csch	csch ⁻¹
		Russian	English		
		rot	curl		
		lg	log		

Page 1.

REGION OF CONSTANT VORTICITY IN A PLANE POTENTIAL FLOW.

V. S. Sadovskiy.

In the work obtained exact solution for flat/plane steady flow of the incompressible fluid with constant eddy/vortex, which borders on the dividing flow line on the potential flow. Is determined the form of the duct/contour, which limits the range of constant eddying, and also the flow line internal vortex flow. Are given the results of the calculations of the distribution of velocities along the axes x and y . Relation to the velocity on duct/contour in the point of its greatest thickening to velocity at infinity rendered/showed equal to

$$\frac{u}{u_{\infty}} = 1.67.$$

In hydrodynamics are known the solutions, which describe steady flow of the incompressible fluid with different from zero eddy/vortex in the closed domain on boundary of which it comes into contact with external potential flow. In the three-dimensional/space case - this is Hill's known spherical eddy/vortex. In the flat/plane case, if the

liquid duct/contour, which separate/liberates external irrotational flow from internal vortex flow, is circumference, then the conditions of the consistency of both flows it is possible to satisfy, assigning eddy/vortex Ω in the form $\Omega = A\psi$, where A - constant, ψ - function of current [1]. Is of interest to find such duct/contour which would satisfy all conditions of consistency on liquid boundary for the case of internal flow with the constant value of eddy/vortex. Specifically, this case is important in connection with the intensely developed/processed at present problem of the construction of the maximum flows of viscous fluid with the stationary separation zones when number $Re \rightarrow \infty$ (for example, see [2]).

Let us examine certain steady flow of the incompressible fluid with a speed of u_∞ in the undisturbed incident flow. Let the flow be such, what out of duct/contour ALBM (Fig. 1) it is potential, inside - vortex/eddy.

Page 2.

On the liquid boundary, which divides both flows, are fulfilled the conditions of their consistency, i.e., in each point of the duct/contour of velocity, are directed tangentially toward it, and their value from outer and inside of duct/contour are equal to:

$W_+ = W_-$. The value of eddy/vortex Ω let us assign according to the

law

$$\Omega = -\Omega_0 \operatorname{sign} y, \quad (1)$$

where Ω_0 - certain positive constant.

Introducing the function of current ψ by the relationship/ratios

$$\frac{\partial \psi}{\partial y} = u, \quad \frac{\partial \psi}{\partial x} = -v, \quad (2)$$

where u, v - component of vector of speed along the axes x and y , we come as is known (see [1]), to the equation

$$\Delta \psi = -\Omega, \quad (3)$$

where Δ - operator of Laplace.

Task consists of the determination of such duct/contour with given ones u_∞ and Ω_0 , on which "would be cemented" by continuous form as function of current ψ , satisfying the equation of Laplace out of duct/contour and the equation of Poisson - inside, so also its first-order derivatives (i.e. velocity).

Duct/contour subsequently searches for in the class of the closed curves, which possess dual symmetry (relative to the direction of velocity u_∞ and of the direction, perpendicular to it, which are

accepted for x and y axes respectively). For convenience subsequently, we consider that are assigned/prescribed the values of eddy/vortex Ω_0 and the linear dimension of field $2a_0$ along the axis x , and velocity u_∞ is subject to determination.

Transition to dimensionless variables is realized/accomplished with the aid of the relationship/ratios

$$\{x, y\} = \{\bar{x}, \bar{y}\} a_0; \quad \{u, v\} = \{\bar{u}, \bar{v}\} \Omega_0 a_0; \quad \psi = \bar{\psi} \Omega_0 a_0^2. \quad (4)$$

In these variables the eddy/vortex in the internal point of region is equal to

$$\Omega(x, y) = -\operatorname{sign} y, \quad (5)$$

and equation (3) is recorded/written in the form

$$\Delta\psi = \operatorname{sign} y \quad (6)$$

(line here and subsequently everywhere they are omitted).

In the coordinate system, driving/moving with speed u_∞ , the velocity at infinity is equal to zero, and the velocity in any end point of flow plane is created by the eddy/vortices which are distributed within duct/contour according to condition (5). The task of the determination of the velocity in liquid from the assigned/prescribed vorticity distribution in it is certain region

Σ , when liquid rests upon infinity, there were solved even in the middle of XIX century (Stokes, Helmholtz). Its solution is given by the logarithmic potential of area in the form

$$\psi_1(x, y) = \frac{1}{2\pi} \iint_V \text{sign } \eta_1 \ln r d\xi d\eta, \quad (7)$$

where (ξ, η) - the sliding point, on which is conducted the integration, and $r = \sqrt{(x-\xi)^2 + (y-\eta)^2}$ - distance between this point and a fixed point (x, y) .

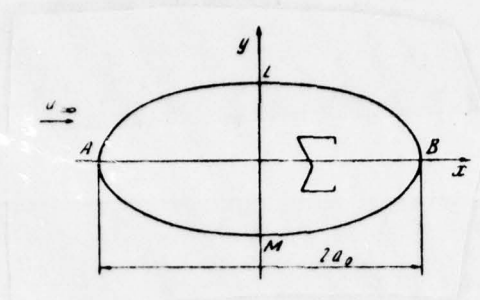


Fig. 1.

Page 3.

The function of current $\psi_1(x, y)$ satisfies the equation of Laplace out of region Σ , and within - to the equation of Poisson (6). If duct/contour consists of piecewise smooth curves, solution (7) is continuous together with its derivatives at any point of plane [4]. Passage to fixed coordinate system consists of addition to $\psi_1(x, y)$ the function of the current of uniform flow $\psi_0 = u_\infty y$.

Thus, the function of current $\psi = \psi_0 + \psi_1$ satisfies the equation of Laplace out of region Σ and equation (6) at point within it, and is also continuous with its derivative on duct/contour itself. It is easy to see that $\psi(x, 0) = 0$, x -axis is flow line. Let us require so that the unknown duct/contour would be also flow line $\psi(x, y) = 0$. This means that the duct/contour satisfies the integral equation

$$u_\infty y + \psi_1(x, y) = 0, \quad (8)$$

where $\psi_1(x, y)$ is given by expression (7), and

$$u_\infty = - \frac{\partial \psi_1}{\partial y} \Big|_{x=-1} = \frac{1}{2\pi} \int_{-1}^1 \int_{-1}^1 \frac{\eta \operatorname{sign} \eta d\xi d\eta}{(1+\xi)^2 + \eta^2}. \quad (9)$$

Thus, the boundary of the region, which satisfies all enumerated above requirements, it is the solution of integral equation (8), in which the integrals are taken from known functions, but on unknown unknown region Σ . However, dual integrals are reduced to usual, since one repeated integral can be fulfilled in quadratures, after which equation (8) is led in Cartesian system of coordinates to the form

$$\begin{aligned} y = \frac{1}{4\pi u_\infty} & \left\{ 2 \int_0^1 (\xi + x) \left(\operatorname{arctg} \frac{\eta_0 + y}{\xi + x} - \operatorname{arctg} \frac{\eta_0 - y}{\xi + x} \right) d\xi + \right. \\ & + 2 \int_0^1 (\xi - x) \left(\operatorname{arctg} \frac{\eta_0 + y}{\xi - x} - \operatorname{arctg} \frac{\eta_0 - y}{\xi - x} \right) d\xi + \\ & + \int_0^1 (\eta_0 + y) \{ \ln [(\xi - x)^2 + (\eta_0 + y)^2] + \ln [(\xi + x)^2 + (\eta_0 + y)^2] \} d\xi - \\ & \left. - \int_0^1 (\eta_0 - y) \{ \ln [(\xi - x)^2 + (\eta_0 - y)^2] + \ln [(\xi + x)^2 + (\eta_0 - y)^2] \} d\xi + I_0 \right\}, \quad (10) \end{aligned}$$

where

$$\begin{aligned}
I_0 = & 4y - 2y \{ (1+x) \ln [(1+x)^2 + y^2] + (1-x) \ln [(1-x)^2 + y^2] \} - \\
& - 2y^2 \left(\operatorname{arctg} \frac{1+x}{y} + \operatorname{arctg} \frac{1-x}{y} \right) - \\
& - 2(1+x)^2 \operatorname{arctg} \frac{y}{1+x} - 2(1-x)^2 \operatorname{arctg} \frac{y}{1-x}; \\
u_\infty = & \frac{1}{2\pi} \int_0^1 \left\{ \ln \left[1 + \left(\frac{\eta_0}{\xi-1} \right)^2 \right] + \ln \left[1 + \left(\frac{\eta_0}{\xi+1} \right)^2 \right] \right\} d\xi. \quad (11)
\end{aligned}$$

Here $[x, y=f(x)]$ - the fixed/recorded point of duct/contour, and $[\xi, \eta_0=f(\xi)]$ - the sliding point of duct/contour, on which is conducted the integration.

Page 4.

Extracted integral equation - nonlinear. Integrands have a special feature/peculiarity at point $\xi=x$ (all the special feature/peculiarities in the integrals, included into the large curly braces, removed). It is impossible to find the solution or to demonstrate its existence and by singularly analytical methods.

Therefore equation was solved numerically on EVM [computer] BESM-3M. For solution was utilized the method of successive approximations, which lies in the fact that is assigned the initial duct/contour $y=f_0(x)$ (in this case in the form of the table of values y at nodal points) :

$$\frac{0, x_1, x_2, \dots, x_{n-1}, 1}{y_0, y_1, y_2, \dots, y_{n-1}, y_n}.$$

For each point $[x_i, y_i=f_0(x_i)]$ are calculated all integrals, entering right side (10) when $\eta=f_0(t)$, and on relationship/ratio (10) is obtained the following approach/approximation $y=f_1(x)$, determined at the same nodal points. Values y and η at intermediate (not coinciding with node/units) points are determined by the method of quadratic interpolation (i.e. on the parabola, carried out through the nearest three node/units), and in the vicinity of point $x=1$, where is necessary the increased accuracy/precision in connection with the low values of y and large slope/inclinations curved, is utilized interpolation with the assigned/prescribed accuracy/precision (i.e. curve is given through more than three node/unit).

Initially after $y=f_0(x)$ was undertaken circle with radius of with a of $R=1$. The convergence of approach/approximations render/showed very rapid with $0.8 > x > 0$ and substantially slower with $x > 0.9$. (As it render/showed subsequently, circumference very strongly

differs from the obtained calculated duct/contour precisely in the vicinity of point $x=1$). Iterations ceased, when the subsequent approach/approximation differed from that preceding/previous in the vicinity of point $x=1$ in sixth significant digit. A quantity of node/units in interval $[0, 1]$ was undertaken equal to $n=38$, moreover their frequency in vicinity $x=1$ was sufficient high (see the given below table). After this as the initial duct/contour $\varphi=f_0(x)$ were accepted different curves and straight lines (moreover $y_i \ll 1$ and $y_i \gg 1$). However, iterations constant/invariably converge to one and the same curved. This gives some bases to assume that the obtained solution of equation (10) is singular (in the class of duct/contours with dual symmetry), although, of course, this cannot serve as completely strict proof, and a question concerning the uniqueness of solution requires more detailed examination.

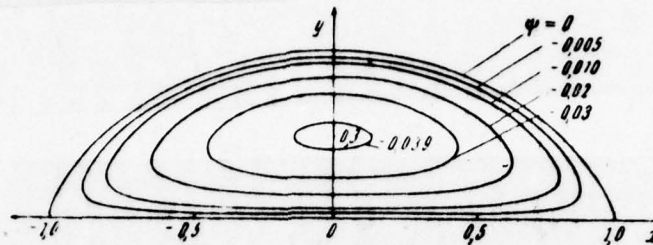


Fig. 2.

Page 5.

It is indisputable, it does remain the open and this question: is possible whether the solution of stated problem in the class of the duct/contours, which do not possess symmetry relative to y axis? The proposed in work method is made it possible beyond initial boundary of the region to take any asymmetric relative to y axis duct/contour and to obtain following approach/approximations. The work in this direction, connected with the high expenditures of machine time, is conducted.

As a result of calculations, were obtained the following coordinates of the duct/contour (last figure was rounded-off).

Value u_{∞} rendered/showed equal to 0.14158. Let us note that if we

velocity u_∞ consider equal to 1, then the value of eddy/vortex Ω_0 proves to be equal to $\Omega_0 = 1/0.14158 = 7.063$.

Having available the duct/contour, which separate/liberates the potential flow from the vortex/eddy, it is possible without the special work to calculate the parameters of internal and external flows. Fig. 2, depicts the pattern of lines of current $\psi = \text{const}$ of internal (vortex/eddy) flow and dividing duct/contour $\psi = 0$. The determination of velocities along the axes x and y is reduced to the simple calculation of the integrals:

$$\left. \begin{aligned} u(x=0) &= \left[u_\infty + \frac{1}{2\pi} \int \int \frac{(y-\eta) \operatorname{sign} \eta d\xi d\eta}{r^2} \right]_{x=0} = \\ &= u_\infty - \frac{1}{2\pi} \int_0^1 \{ \ln [\xi^2 + (\eta_0 - y)^2] + \ln [\xi^2 + (\eta_0 + y)^2] \} d\xi + \\ &\quad + \frac{1}{\pi} \left[\ln(1 + y^2) - 2 + 2y \operatorname{arctg} \frac{1}{y} \right]; \\ u(y=0) &= u_\infty - \frac{1}{2\pi} \int_0^1 \{ \ln [(\xi - x)^2 + \eta_0^2] + \ln [(\xi + x)^2 + \eta_0^2] \} d\xi + \\ &\quad + \frac{1}{2\pi} [(1-x) \ln(1-x)^2 + (1+x) \ln(1+x)^2 - 4]. \end{aligned} \right\} (12)$$

Calculation data according to the distribution of velocities are represented in Fig. 3 and 4.

x	y	x	y	x	y	x	y	x	y
0,00	0,5991	0,40	0,5349	0,70	0,3848	0,91	0,1826	0,993	0,02842
0,05	0,5981	0,45	0,5171	0,73	0,3628	0,93	0,1541	0,996	0,01835
0,10	0,5952	0,50	0,4967	0,76	0,3391	0,95	0,1220	0,998	0,01056
0,15	0,5903	0,55	0,4736	0,79	0,3134	0,96	0,1042	0,999	0,006025
0,20	0,5834	0,58	0,4582	0,82	0,2854	0,97	0,08473	0,9995	0,003419
0,25	0,5745	0,61	0,4418	0,85	0,2547	0,98	0,06296	1,000	0
0,30	0,5635	0,64	0,4242	0,87	0,2325	0,985	0,05080	--	--
0,35	0,5504	0,67	0,4052	0,89	0,2086	0,990	0,03738	--	--

Page 6.

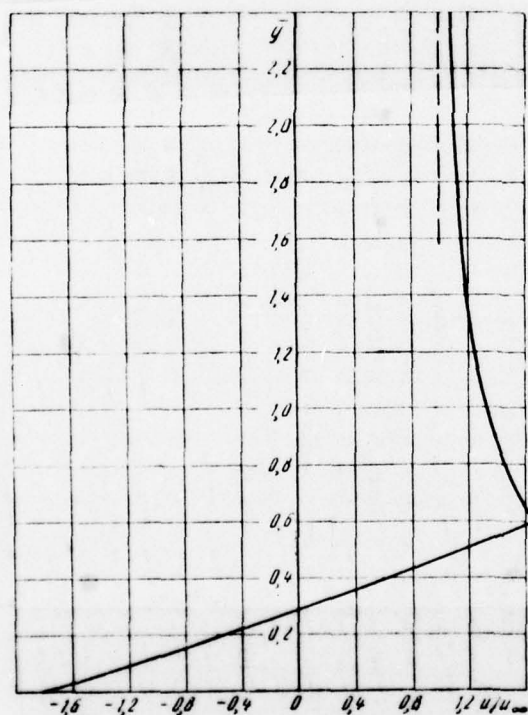


Fig. 3.

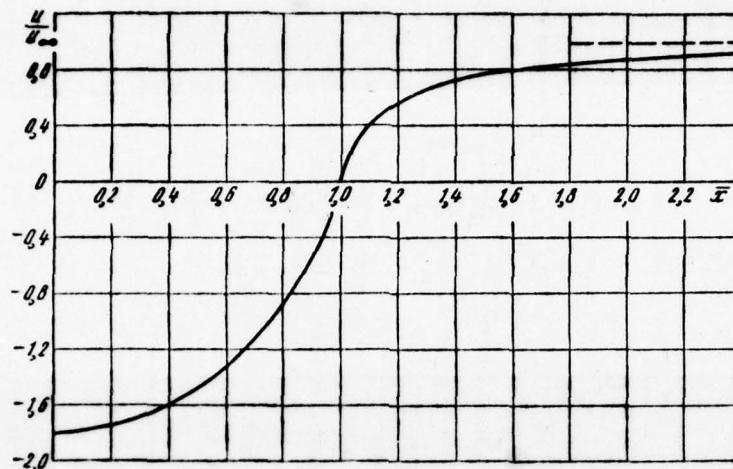


Fig. 4.

Page 7.

Let us examine some special feature/peculiarities of flow in the vicinity of critical point. Let point O be the branch point of flow line $\psi=0$ (Fig. 5). Planes flow in I and II regions are stationary and are with respect by potential and vortex/eddy, and the angle between the tangent to the dividing flow line OL at point O and the x-axis $\alpha_0 \neq 0$. It is obvious that in this case point O is critical, i.e., velocity W in it is equal to zero. Furthermore, the velocities in each of the regions possess evenly continuous derivatives. In that case it is easy to establish/install the direct coupling between derivatives at point O and the angle α_0 . In fact, it is obvious that

for II region

$$\left. \frac{\partial v}{\partial x} \right|_{0 II} = 0,$$

consequently,

$$\left. \frac{\partial u}{\partial y} \right|_{0 II} = -\Omega_0 \neq 0. \quad (13)$$

At point A on flow line $\left. \text{tg} \alpha = \frac{v}{u} \right|_{II}$. Fixing point A to critical point along flow line and opening indeterminacy/uncertainty according to l'Hopital's rule, we obtain:

$$\text{tg} \alpha_0 = \frac{\frac{\partial v}{\partial x} \frac{\partial x}{\partial l} + \frac{\partial v}{\partial y} \frac{\partial y}{\partial l}}{\frac{\partial u}{\partial x} \frac{\partial x}{\partial l} + \frac{\partial u}{\partial y} \frac{\partial y}{\partial l}}. \quad (14)$$

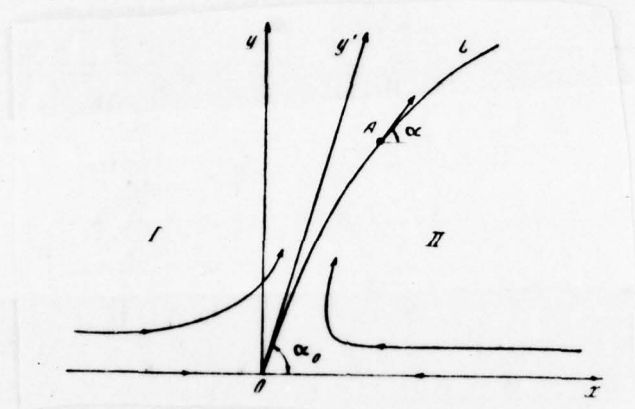


Fig. 5.

Page 8.

All derivatives must be taken at point O from the side of II regions. Taking into account (13) and the equation of continuity formula (14) we convert to the form

$$\operatorname{tg} \alpha_0 = \frac{-\frac{\partial u}{\partial x} \operatorname{tg} \alpha_0}{\frac{\partial u}{\partial x} + \frac{\partial u}{\partial y} \operatorname{tg} \alpha_0}$$

or, it is final, to the form

$$\left. \frac{\partial u}{\partial x} \right|_{011} = -\frac{1}{2} \Omega_0 \operatorname{tg} \alpha_0. \quad (15)$$

Repeating analogous lining/calculations for the irrotational flow in I of region and noting that $\left. \frac{\partial u}{\partial y} \right|_{01} = 0$ unlike (13), is easy

to arrive at the conclusion that with $\alpha \neq \pi/2$ relationship/ratio (14) can be satisfied only under the condition

$$\left. \frac{\partial u}{\partial x} \right|_{01} = 0, \quad (16)$$

i.e. in the case sufficient "smooth" irrotational flow everything first derivatives from composing the velocities in critical point with $\alpha_0 \neq \pi/2$ are equal to zero.

Since OL is the flow line, which separate/liberates irrotational flow from vortex/eddy with one and the same constant Bernoulli ($\alpha_0 \neq 0$), then at any point of this line $\left. \frac{\partial W}{\partial l} \right|_I = \left. \frac{\partial W}{\partial l} \right|_{II}$.

$$\left. \frac{\partial W}{\partial l} \right|_{01} = \left. \frac{\partial W}{\partial l} \right|_{011}. \quad (17)$$

Finally, it is easy to show that for I and II regions at point O they occur of the equality

$$\left. \begin{aligned} -\frac{\partial u}{\partial x} \Big|_{01} &= \frac{\partial W}{\partial l} \Big|_{01}; \\ -\frac{\partial u}{\partial x} \Big|_{011} &= \frac{\partial W}{\partial l} \Big|_{011}, \end{aligned} \right\} \quad (18)$$

where l - an element of length of flow line OAL. [Formulas (18) are the equations of continuity, written in oblique axes xy' , where y' - tangent to flow line OL at point O].

The comparison of formulas (17) and (18) gives the relationship/ratio

$$\left. \frac{\partial u}{\partial x} \right|_{01} = \left. \frac{\partial u}{\partial x} \right|_{011}, \quad (19)$$

however kinematic relationship/ratios (15) and (16), as can easily be seen that they contradict dynamic compatibility condition (19). This means that with $\alpha_0 \neq 0$ flat/plane stationary vortical irrotational flow with evenly continuous derivatives cannot be consistent on the dividing them flow line in the vicinity of the critical point [in the case $\alpha_0 = \pi/2$ the relationship/ratio, analogous (14), for vortex flow it is fulfilled only when $\left. \frac{\partial u}{\partial x} \right|_{0 \parallel} = \infty$, which contradicts the uniform continuity of derivatives], i.e., the potential and vortex flows, which border on liquid flow line, cannot be sufficiently smooth in the vicinity of critical point with $\alpha_0 \neq 0$.

Page 9.

This fact is located in accordance with the results, described above. It is real/actual, formula (12) for determining the velocity it is easy with the aid of Green's formula to convert to the logarithmic potential of the simple layer, for which at the critical point 0 are disrupted the conditions for existence of evenly-continuous derivatives (for example, the density of logarithmic potential does not satisfy Gelder's condition (see [3] and [4]).

It is necessary to note that during the solution of integral

equation (10) the special attention was allctted to the vicinity of critical point, was required a considerable increase of the accuracy/precision of ccunt and quantity of nodal points in this region. The investigation of the analytical properties of the function of current ψ in the vicinity of critical point shows that $\alpha_0 = \pi/2$. The proof of this affirmation will be given in following article.

The author is grateful to G. I. Tagancv for the proposed theme and cnsultations.

REFERENCES.

1. G. Lamb. Hydrodynamics. M., Gostekhtheorizdat, 1947.
2. G. K. Batchelor. On steady laminar flcw with closed streamlines at large Reynolds number. "J of Fluid Mech", v 1, p 2, 1956.
3. N. M. Gunter. Theory of potential and its application/use to the basic tasks of mathematical physics. M., Gostekhtheorizdat, 1953.
4. G. N. Polozhiy. Equations of mathematical physics. M., "higher school", 1964.

5. N. Ye. Kochin, I. A. Kibel', N. V. Roze. Theoretical hydromechanics. H. 1. M., Fizmatgiz, 1963.

Received 15/VIII 1969.

Page 10.

UNIQUENESS OF THE SOLUTION OF THE PROBLEM OF SONIC FLOW ABOUT A
PROFILE.

Yu. B. Lifschitz.

Is proven the uniqueness of solution, placed by F. I. Frankl, the task of the flow of gas about airfoil/profile with number $M_\infty = 1$.

Examining the task of the flow of gas about the airfoil/profile, close to datum, with number $M=1$ at infinity, F. I. Frankl clashed with the possible nonuniqueness of obtained solutions [1]. Analogous situation appeared in the nozzle theory of Laval [2], where it was connected with the nonuniqueness of the flow of the gas, taking place through the assigned/prescribed nozzle. In work [3] this question was solved. In the task of the flow around airfoil/profile of sonic flow the nonuniqueness appears as a result of existence at infinity of the same special feature/peculiarity and in initial flow. It is lower on the basis of the results, obtained in works [4], is proven under some assumptions the uniqueness of the solution of the problem, stated by F. I. Frankl.

1. Let us assume that there are two close solutions of equations of gas dynamics, which describe flow of gas of approximately one and the same airfoil/profile with number $M=1$ in infinity. Let the first flow have function of current $\psi(x, y)$ and of potential $\phi(x, y)$. The second flow with the function of current ψ' and in potential ϕ' let us represent in the following form:

$$\left. \begin{aligned} \psi'(x, y) &= \psi(x, y) + \varepsilon \omega^*(x, y), \\ \phi'(x, y) &= \phi(x, y) + \varepsilon \omega(x, y). \end{aligned} \right\} \quad (1)$$

The changes of functioning of current and potential, proportional to low value ε , satisfy in the variables of hodograph the small-disturbance equations for the plane adiabatic flows of gas [5]. After exception/elimination of their derivatives ω^* by crossed differentiation we will obtain for ω the equation of Chaplygin

$$K \omega_{\eta\eta} + \omega_{\xi\xi} = 0. \quad (2)$$

Page 11.

Are here accepted the designations: $K = \rho^2 (1 - M^2)$, $\sigma = - \int_{a^*}^w \rho^{-1} w^{-1} dw$, w - velocity modulus, θ - angle of the slope of velocity vector to the positive direction of X -axis, a^* - the critical speed of sound, ρ - density.

Boundary condition is assigned on the hodograph of old flow and takes the form

$$K \omega_{\eta} d\xi - \omega_{\xi} d\theta = 0. \quad (3)$$

Formula (3) means that the streamlined airfoil/profile does not change its form. Fig. 1, depicts the hodograph of flow about airfoil/profile. The origin of coordinates corresponds to the infinite point, to region $\sigma \rightarrow \infty$, is reflect/represented the vicinity of deceleration point, τ_1^0 and τ_2^0 - maximum characteristics.

In the vicinity of the origin of the coordinates of hodograph plane $\theta\sigma$, the potential ω must have the same special feature/peculiarity, as the converted potential of Legendre of the initial flow

$$\omega = \tau^{-1}[(\tau + \theta)^{1/3} + (\tau - \theta)^{1/3}], \quad \tau^2 = \theta^2 + \frac{4}{9}\sigma^3. \quad (4)$$

Task is the proof of uniqueness theorem for function $\omega(\theta, \sigma)$, that satisfies equation (2), boundary condition (3) on duct/contour L and allow/assuming at point P the special feature/peculiarity of form (4).

2. Proof of uniqueness is conducted by abc-method of Friedrichs and is based on results, obtained in works [4] in connection with question concerning flow pattern in local supersonic zone, which appears during flow around airfoil/profile of flow with high subsonic

speed at infinity.

μ - unknown solution. Let us examine the integral

$$I_\delta = \iint_{\Sigma_\delta} (B\omega_\theta + C\omega_\sigma)(K\omega_{\theta\theta} + \omega_{\sigma\sigma}) d\theta d\sigma, \quad (5)$$

where Σ_δ - subregion Σ , and B and C - function from θ and σ . Region Σ_δ has a boundary which consists of the limiting characteristics $\Gamma_{1,2}^0$, line L and arc R_δ by a radius δ , that eliminates point O . let us use to integral (5) Green's formula, as a result we will obtain the sum of two integrals on region Σ_δ and on its boundary S_δ :

$$\begin{aligned} I_\delta = & \frac{1}{2} \iint_{\Sigma_\delta} \{ \omega_\theta^2 [-KB_\theta + (KC)_\sigma] - 2\omega_\theta \omega_\sigma (B_\sigma + KC_\theta) + \omega_\sigma^2 (B_\theta - C_\sigma) \} d\theta d\sigma + \\ & + \oint \frac{B}{2} (K\omega_\theta^2 d\sigma - 2\omega_\theta \omega_\sigma d\theta - \omega_\sigma^2 d\sigma) + \\ & + \frac{C}{2} (K\omega_\theta^2 d\theta + 2K\omega_\theta \omega_\sigma d\sigma - \omega_\sigma^2 d\theta) = I_1 + I_2 = 0. \end{aligned} \quad (6)$$

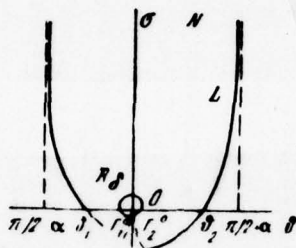


Fig. 1.

Page 12.

If we select B and C in such a way that the quadratic form, which stands under the sign of dual integral, it would be positively determined, and the value of line integral I_2 it was negative, then theorem will be demonstrated, since equality $I_2 = 0$ is fulfilled only if $\omega \equiv \text{const}$. In the first of works [4] they were found those functions B and C, for which $I_1 > 0$ for any subregion of region Σ_δ , and line integral I_2 is also positive, if it is taken on any part of boundary S_δ , which lies by pillar along one side of circumference R_δ . If in the vicinity of point O derivatives $\omega_\theta, \omega_\theta = O(\delta^{-1})$, then the limit of integral I_2 , undertaken on R_δ , vanishes during decrease δ , and uniqueness theorem is demonstrated.

We will use functions B and C from work [4] indicated. They are determined as follows:

with $\sigma \leq 0$

$$\left. \begin{aligned} B(\theta, \sigma) &= B(\theta, 0), \quad C = 0, \quad B_0 > 0, \\ B(\theta) &> 0 \text{ при } 0 < \theta \leq \theta_2, \quad B(\theta) < 0 \text{ при } \theta_1 \leq \theta < 0, \end{aligned} \right\} \quad (7)$$

Key: (1). with.

with $\sigma \geq 0$

$$\left. \begin{aligned} K^{1/2} C - iB &= \exp f(\lambda), \quad \lambda = \theta + i\mu, \\ \mu &= \int_0^{\sigma} K^{1/2} d\sigma, \quad f(\lambda) = \frac{1}{\pi} \oint_{\Lambda} \frac{f_2(t)}{t - \lambda} dt. \end{aligned} \right\} \quad (8)$$

Boundary Λ consists of the cuts of duct/contour L , arranged/located with $\sigma \geq 0$, and axis intercept θ with $\theta_1 \leq \theta \leq \theta_2$. Function $f_2(t)$ is the apparent/imaginary part analytic function $f(\lambda)$ and is assigned on Λ by the formulas

$$\left. \begin{aligned} f_2 &= \frac{\pi}{2} \text{ при } \theta_1 \leq \theta < 0, \quad \mu = 0; \\ f_2 &= -\frac{\pi}{2} \text{ при } 0 < \theta \leq \theta_2, \quad \mu = 0; \\ f_2 &= g \operatorname{arctg} \left(\frac{d\mu}{d\theta} \right)_L, \quad 0 \leq g \leq 1. \end{aligned} \right\} \quad (9)$$

Key: (1). with.

Let us use formula (6) to any subregion of region Σ_1 . From the positive certainty of dual integral I_2 , we will obtain that I_2 ,

undertaken along the boundary of the subregion in question, negative. Let us examine now in $\sigma > 0$ the field of the integral curves of the equation

$$\operatorname{Re} [(K^{1/2} C - iB)(\omega_0 - i\omega_p)^2 d\lambda] = 0. \quad (10)$$

Along them the integrand of integral I_2 turns into zero. Let us call them T-curves.

In the second of works [4] is demonstrated a series of the theorems, which characterize the behavior of T-curves. In particular, T-curves exist in each point of subregion Σ_+ of region Σ_0 , arranged/located with $\sigma > 0$, they have continuous according to Gelder tangent, are not formed loops and can begin or be terminated only on boundary of the region Σ_+ . By analogy with the second of works [4] it is possible to demonstrate which point N emerges inside region Σ_+ at least one T-curve which let us below call curve T_1 .

Page 13.

Further affirmations concern behavior of T_1 curve and are derived/concluded on the assumption that $\omega \neq \text{const}$ in Σ_+ .

The curve T_1 cannot terminate on duct/contour L [4].

For a proof let us examine integral I_2 , undertaken on T_1 and the part of duct/contour L between point of termination of T_1 curve and N . It is positive, which contradicts that demonstrated earlier.

The curve T_1 cannot terminate on line $\mu=0$ [4].

The proof of this case immediately follows from the examination of integral I_2 , undertaken T_1 , and G -characteristic, which emerges from the point of termination curved T_1 , and to the cut of duct/contour L . The obtained integral proves to be positive.

3. Given results indicate that the T_1 -curve must terminate at point O . Let us explain now the behavior of T -curves in the vicinity of point O , utilizing for this purpose a precise form of principal part of the function ω , which is assigned by equality (4). The usual methods of the study of the singular points of ordinary differential equations [6] lead to the picture, depicted in Fig. 2. Due to the symmetry of solution (4) relative to axle/axis $\theta=0$ it suffices to examine only region $\theta>0$.

Integral curve equations (10) in small vicinity of point O emerge the points of axle/axis θ , having there horizontal tangent, and then they enter in point O , concerning axle/axis μ according to the formula

$$\mu = \text{const } \theta^{3/5}.$$

(11)

Let now curve T_1 enter in point O. Let us estimate the value of integral I_2 , of the undertaken on path, which is of T_1 - curve, arc a radius δ , connecting curve with any T- curve, incoming into point D on axle/axis δ within the vicinity δ of point O, and by quite this T- curve. The contribution to integral gives only integration for arc by a radius δ :

$$I_2 = -b_1[1 + o(1)]\delta^{-\frac{1}{3}}, \quad b_1 > 0. \quad (12)$$

let us release from point D characteristic Γ_1 before intersection with hodograph L and will examine the integral I_2 , undertaken on Γ_1 and L from point D to N. Integral on L is positive according to the selection of functions B and C on formulas (7) and (8), undertaken from work [4]. Integral value on Γ_1 is estimated on the basis of formulas (4) and (7):

$$I_2 = b_2[1 + o(1)]\delta^{-1}, \quad b_2 > 0. \quad (13)$$

from formulas (12) and (13) it follows that there is that number δ , beginning with which the value of integral I_2 , undertaken on the closed duct/contour of the described form, it will be positive. This contradicts that demonstrated above. Only alternative is the nonexistence of the solution u , different from constant.

For the completeness of proof, one should examine the case of the case the dominant terms of old and new flow they coincide and $\omega(\theta, \theta)$ in the vicinity of the origin of coordinates is given not by formula (4), but by following term of expansion.

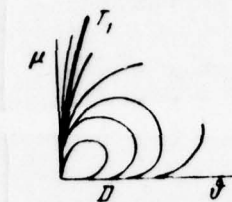


Fig. 2.

Page 14.

It takes the same form, as for Legendre's potential in flow with $M=1$ at infinity. Any expansion with dominant term (4) and following after it by the member

$$(\theta + \tau)^{1/3} + (\theta - \tau)^{1/3} \quad (14)$$

represents Legendre's potential at large distances from certain airfoil/profile in flow phase with $M_\infty=1$. Reverse/inverse affirmation not is proved. During the solution $\omega(\theta, \sigma)$ whose dominant term is given by expression (14), the value of integral I_2 , undertaken in circumference R_1 , it vanishes during decrease δ ; therefore the uniqueness of this solution is the consequence of the results, obtained in the first of works [4].

Let us note still one fact. The solution of problem in variations in the case of the flow around airfoil/profile of the

incompressible fluid exists and it is singular, if is assign/prescribed a circulation control or the condition of Zhukovskiy on new duct/contour. Equivalent from the mathematical point is the assignment of the coordinates only of tip of braking. Analogous situation occurs during the subcritical flow of airfoil/profile.

But if velocity of incident flow is equal to sonic, then, as shown above, the solution of the problem of flow in region upstream from maximum characteristics is singular without any supplementary conditions. The nonuniqueness, connected with arbitrariness in the assignment to circulation with respect to the sufficiently distant duct/contour, which covers airfoil/profile, or rear deceleration points, is transferred to the region, arranged/located downwash from shock waves. This result directly follows from the expansion of solution at large distances from airfoil/profile when [7]. First asymmetric relative to X-axis term of expansion with zero boundary conditions on shock waves exist only after them. The coefficient of it, critical for the amount of total lift, is determined either by the position of very shock waves or by the assignment to circulation.

REFERENCES

1. P. I. Frankl'. On the existence of the weak solution of direct problem of the theory of the flow around airfoil/profile of sonic flow in the first approximation. IAS USSR, Vol. 132, No. 4, 1960.
2. P. I. Frankl'. Some questions of existence and uniqueness of the theory of transonic flows. Izv. of schools of higher education. Math., No. 5, 1960.
3. Yu. B. Lifshits, G. S. Byzhov. On a variation in the gas flow in design conditions of the work of Laval nozzle. Jour. Comp. Matem. and Matem. Phys., Vol. 6, No. 2, 1966.
4. C. S. Mogawetz. On the non-existence of continuous transonic flows past profiles I, II, Comm. Pure. Appl. Math., v 9, No. 1, 1956; v 10, No. 1, 1957.
5. A. A. Nikol'skiy. Small-disturbance equations for plane adiabatic gas flows. Collection of theoretical works on aerodynamics. M., Oborongiz, 1957.
6. V. V. Nemytskiy, V. V. Stepanov. Qualitative theory of differential equations. Publ. 2, Moscow-Leningrad, the State Technical Press, 1949.

DOC = 78103901

PAGE ~~33~~ 34

7. D. Euvrard. Asymptotic study of distant flow about an obstacle moving at the speed of sound. II J Mecanique, v 7, No. 1, 1968.

Received 13/II 1970.

OPTIMUM DISTRIBUTION OF WING THICKNESS IN A SUPERSONIC FLOW.

I. I. Burakov, Yu. L. Zhilin.

Page 15.

In the work is proposed the method of the solution of variational problem for the wing of arbitrary planform, establish/installated at zero angle of attack, which possesses minimum wave impedance with the assigned/prescribed volume. Given short description of the program, comprised for ELSVM of the type M-20 the results of the calculation of delta wings.

Let us examine flow of the supersonic flow about gas of the fine/thin wing, establish/installated at zero angle of attack. Let us consider that the wing surface is symmetrical relative to planes $y=0$ and $z=0$, but its planform is assigned/prescribed (Fig. 1). The equation of suction side of wing let us write in the form $y=\delta(x, z)$. According to linear theory [1] the potential of the disturbed velocity $\phi(x, z)$ in the arbitrary point $M(x, z)$ of plane $y=0$ is equal to

$$\phi(x, z) = -\frac{U_\infty}{\pi} \iint_{\tau(x, z)} \frac{\alpha(\xi, \eta) d\xi d\eta}{\sqrt{(x-\xi)^2 - \beta^2(z-\eta)^2}},$$

where $\beta = \sqrt{M_\infty^2 - 1}$;

U_∞, M_∞ - velocity and mach number of the incident flow.

$r(x, z)$ - the part of the wing, limited by the front/leading Mach cone, carried out from point A.

$\alpha = \frac{\partial \tilde{\phi}(x, z)}{\partial x}$ - the local angle of attack of the wing surface.

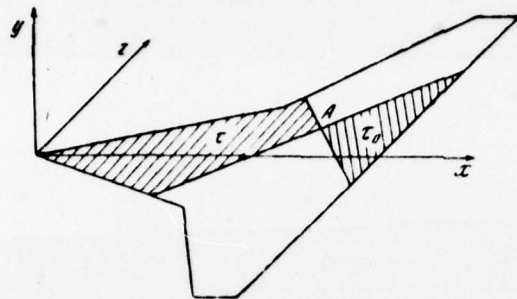


Fig. 1.

Page 16.

This relationship/ratio is the solution of the problem of the flow around the isolated/insulated wing in the setting in question.

The coefficient of wave impedance c_x can be presented in the form

$$c_x = -\frac{4}{U_\infty S} \iint_D a(x, z) \frac{\partial \varphi(x, z)}{\partial x} dx dz, \quad (1)$$

where S - a wing area.

D - part of plane $y=0$, limited by wing edges.

The complete volume of wing V is equal to

$$V = -2 \int_D \int_0^1 x \alpha(x, z) dx dz. \quad (2)$$

It is assumed that the wing thickness turns into zero on leading and trailing edges. This condition for each section $z = \text{const}$ is record/written in the form

$$\int_{a(z)}^{b(z)} \alpha dx = 0, \quad (3)$$

where $x=a(z)$ and $x=b(z)$ - equation of respectively leading and trailing wing edges.

Equation (3) means that of each section $z = \text{const}$ the sum of sources and flows is equal to zero.

Let us formulate variational problem. It is required to find the shape of surface of the wing, which possesses minimum wave impedance with the assigned/prescribed volume. It is assumed that is assign/prescribed the mach number and wing planform, wing thickness turns into zero on leading and trailing edges.

This variational problem is reduced to the determination of the minimum value of the functional Φ , equal to

$$\Phi = \iint_D \left[\alpha \frac{\partial \varphi}{\partial x} + \lambda_1 x \alpha + \lambda_2(z) \alpha \right] dx dz,$$

where λ_1 and $\lambda_2(z)$ - Lagrange's constant and alternating/variable factors.

It is possible to show that the first variation in the functional Φ turns into zero during execution in region D of the condition (see [2])

$$\frac{\partial}{\partial x} \iint_{\tau_0(x, z)} \frac{\alpha(\xi, \eta) d\xi d\eta}{V(x - \xi)^2 - \beta^2(z - \eta)^2} + \frac{\partial}{\partial x} \iint_{\tau_0(x, z)} \frac{\alpha(\xi, \eta) d\xi d\eta}{V(x - \xi)^2 - \beta^2(z - \eta)^2} + \lambda_1 x + \lambda_2(z) = 0, \quad (4)$$

in which the second term is proportional to pressure in return flow [region $\tau_0(x, z)$ it is shown on Fig. 1].

Page 17.

The physical sense of this condition consists in the fact that for the wing, which possesses minimum friction, pressure difference in direct/straight and return flows in each section $z = \text{const}$ is linear function from x with constant along spread/scope gradient λ_1 .

Relationship/ratio (4) with given ones λ_1 and λ_2 must be considered as integral equation for the local angle of attack of the surface of the wing of minimum friction.

The formulated variational problem has simple solution with deeply supersonic wing edges when interaction of its separate sections is negligibly small. In this case wing drag does not depend on planform and with the assigned/prescribed airfoil/profile is determined by the law of span distribution its thickness ratio and local chord. In this case, minimum friction possesses the wing with the parabolic airfoil/profile whose thickness ratio changes along spread/scope proportional to local chord. It is possible also to show that with any airfoil/profile a change in the wing chord ratio in this rule makes it possible to decrease the wave impedance in comparison with wing drag, which has constant thickness ratio.

For the solution of variational problem with other Mach numbers in the present work is utilized Ritz's method, who reduces it to a simpler problem of finding of the conditional minimum.

Let us introduce the new dimensionless coordinates

$$x_1 = \frac{x}{b_0}, \quad \xi_1 = \frac{\xi}{b_0}, \quad \bar{z} = \frac{2z}{l}, \quad \bar{\eta} = \frac{2\eta}{l},$$

where l and b_0 - respectively spread/scope and root wing chord.

In the new variables of relationship/ratio (1) and (2) they are record/written in the form

$$c_x = \frac{l^2}{\pi S} \iint_{D_1} \alpha dx_1 d\bar{z} \frac{\partial}{\partial x_1} \iint_{r_1} \frac{\alpha d\xi_1 d\eta}{V(x_1 - \xi_1)^2 - k^2(z - \eta)^2}; \quad (5)$$

$$V = -b_0^2 l \iint_{D_1} x_1 \alpha dx_1 d\bar{z}, \quad (6)$$

where D_1 and r_1 - regions D and r in new coordinates;

$k = \beta l / 2b_0$ - similarity parameter.

For the solution of variational problem, let us present the equation of suction side of wing in the form

$$\begin{aligned} \delta(x, z) &= \frac{V}{S b_0} [b(z) - a(z)] \bar{\delta}(\bar{x}, \bar{z}), \\ \bar{\delta}(\bar{x}, \bar{z}) &= \sum_{n=1}^{NM} a_{nm} \bar{x} (1 - \bar{x}^n) |\bar{z}|^{m-1}, \end{aligned} \quad (7)$$

where

$$\bar{x} = \frac{x - a(z)}{b(z) - a(z)};$$

a_{nm} — some constant coefficients.

Page 18.

During this assignment to surface, the condition of inversion into zero wing thicknesses on leading and trailing edges is made automatically; the shape of surface of wing is determined by assignment NM of constant coefficients. The local angle of attack of wing is equal to

$$\alpha(\bar{x}, \bar{z}) = \frac{V}{Sb_0} \sum_{n=1}^{NM} a_{nm} [1 - (n+1)\bar{x}^n] |\bar{z}|^{m-1}. \quad (8)$$

After substituting value α from equation (8) into relationship/ratios (5) and (6), we will obtain

$$\bar{c}_x = \frac{Sb_0^4}{V^2} c_x = \sum_{n=1}^{NM} \sum_{m=1}^{NM} A_{nm, pq}; \quad (9)$$

$$\sum_{n=1}^{NM} \sum_{m=1}^{NM} a_{nm} B_{nm} = -1. \quad (10)$$

Here

$$A_{nm, pq} = \frac{b_0^2 l^2}{\pi S^2} \iint_{D_1} |1 - (n+1) \bar{x}^n| |\bar{z}|^{m-1} dx_1 d\bar{z} \frac{\partial}{\partial x_1} \times \\ \times \iint_{\tau_1} \frac{|1 - (p+1) \bar{\xi}^p| |\bar{\eta}|^{q-1} d\bar{\xi}_1 d\bar{\eta}_1}{V(x_1 - \bar{\xi}_1)^2 - k^2 (z - \bar{\eta})^2}; \quad (11)$$

$$B_{nm} = \frac{b_0 l}{S} \iint_{D_1} x_1 |1 - (n+1) \bar{x}^n| |\bar{z}|^{m-1} dx_1 d\bar{z}, \quad (12)$$

where $\bar{\xi} = \frac{\xi - a(\eta)}{b(\eta) - a(\eta)}$. The formulated variational problem is reduced to finding of the conditional minima of function $\bar{c}_\lambda(a_{nm})$, whose arguments satisfy condition (10). The method of Lagrange's factors leads to the solution of following linear system of equations:

$$\sum_{\substack{n=1 \\ m=1}}^{NM} a_{nm} (A_{nm, pq} + A_{pq, nm}) + \lambda B_{pq} = 0, \quad (13) \\ 1 \leq p \leq N, \quad 1 \leq q \leq M.$$

Here λ - Lagrange's indefinite factor. The coefficient of minimum friction is determined from formula $\bar{c}_x = \frac{1}{2} \lambda$.

For the solution of variational problem, was comprised the program for computers of the type M-20. This program makes it possible to also solve direct problem for the wings whose surface can be described by expression (7). In program it is assumed that the wing planform represents by itself polygon. Wing edges can be both purely subsonic or supersonic and the mixed type. Therefore the proposed method is applicable to a broader class of wings, than the method, given in works [3] and [4].

Page 19.

During the calculation of coefficients $A_{nm, pq}$ in formula (11) it is convenient to get rid of derivative for x_1 by integration in parts, i.e., in initial relationship/ratio (1) to pass from pressure to potential. In work [5] wing drag is calculated from pressure

distribution; in this case, are utilized the analytical solutions, valid under some supplementary assumptions. Coefficients $A_{nm, pq}$ and B_{nm} are determined numerically by the consecutive application/use of Simpson's formula. For refining the calculation according to this formula, preliminarily is isolated the special feature/peculiarity in derivative of potential, that appears on leading wing edge.

After the solution of linear system and determination of coefficients a_{nm} is performed pressure distribution calculation and wing thickness of minimum friction in the assigned/prescribed sections.

According to the proposed method were carried out the calculations of delta wings. In these calculations the parameter of similarity k changed in the range from 0.2 to 2. For each value of parameter k at the assigned/prescribed values of M and N , was determined the coefficient \bar{c}_x of the wing of minimum friction, was located the distribution of wing chord ratio $\bar{\sigma}(\bar{x}, \bar{z})$ and the dimensionless coefficient of pressure $\bar{c}_p(\bar{x}, \bar{z})$, equal to

$$\bar{c}_p = \frac{\beta S b_0 \Delta p}{V q},$$

where Δp and q - a pressure increment and velocity head.

For estimating the decrease of wave impedance as initial, was undertaken the wing with the parabolic airfoil/profile, whose thickness ratio was constant along spread/scope ($M=1$, $N=1$). The coefficient of the wave impedance of this wing is designated through c_{x0} .

On Fig. 2, is represented the dependence on the parameter of similarity k of the minimum value of the coefficient of the wave impedance $\bar{c}_{x\min}$, achieved in these calculations and the coefficient of the wave impedance of initial wing. There value of the coefficient of wave impedance \bar{c}_{x00} of body of revolution, which possesses minimum friction of the assigned/prescribed length b_0 and volume V . As is known, $\bar{c}_{x00} = \frac{128}{\pi}$.

From Fig. 2, it is evident that the wings of minimum friction possess substantially smaller friction in comparison with initial wing, relative gain in friction decreases with supersonic wing edges and with $k \rightarrow \infty$ becomes equal to $\frac{c_{x0} - c_{x\min}}{c_{x0}} = \frac{1}{9}$.

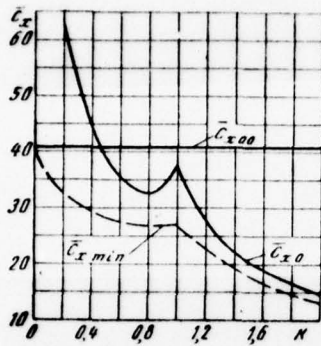


Fig. 2.

Page 20.

On Fig. 3 for the value of the parameter of similarity $k=0.8$, is shown the distribution of a difference in the coefficients of pressure $\Delta \bar{c}_p$ in direct/straight and return flows for an initial wing and the wing of minimum friction of $M=3$, $N=3$. It is evident that for the wings of minimum friction the curves of distributions $\Delta \bar{c}_p$ are close to parallel lines. Similar pattern is observed at other values of parameter k . Thus, the proposed method makes it possible to obtain approximate solutions of equation (4) both with subsonic and with supersonic wing edges.

On Fig. 4 for the different values of the similarity parameter, is shown the dependence on M and N of value $\Delta = \frac{\bar{c}_r}{c_{x0}}$, which

characterizes the decrease of wave impedance. It is evident that with near sonic and supersonic edges ($k \gg 0.8$) the friction, close to minimum, is achieved on the wings with parabolic airfoil/profile ($N=1$) whose thickness ratio decreases toward the end of the wing. With deeply subsonic edges ($k \leq 0.6$) the resistance close to minimum, it is possible to obtain on wings with constant thickness ratio ($M=1$) by the optimization of airfoil/profile ($N=4$). In these conditions/modes the essential decrease of friction is achieved also on wings with a simpler airfoil/profile ($N=1, 2$ and 3) and from variable along spread/scope by thickness ratio.

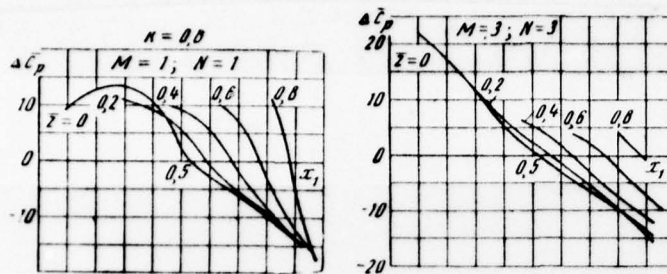


Fig. 3.

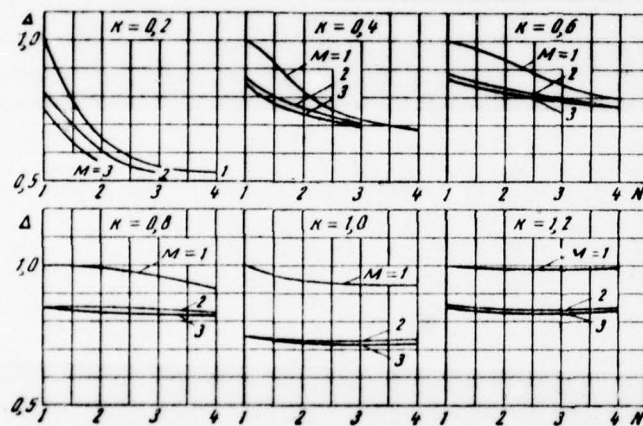


Fig. 4.

Page 21.

This position is correct for the wings of more complex planform.

On Fig. 5, is shown the form of the wing profiles minimum wave impedance with deeply subsonic leading edges with $M=1$ and $N=4$, i.e.,

with constant thickness ratio along the spread/scope (on Fig. 5a the form of airfoil/profiles is compared in identical area, on Fig. 5b - with identical maximum thickness). For these airfoil/profiles is characteristic the displacement of thickness distance forward. With an increase in the similarity parameter, decreases maximum profile thickness (see Fig. 5a), in this case the convergent part of the airfoil/profile (see Fig. 5b) it remains almost constant/invariable, and diffuser becomes more convex. The totality of these factors makes it possible to substantially decrease wave drag with deeply subsonic edges, which has the assigned/prescribed volume.

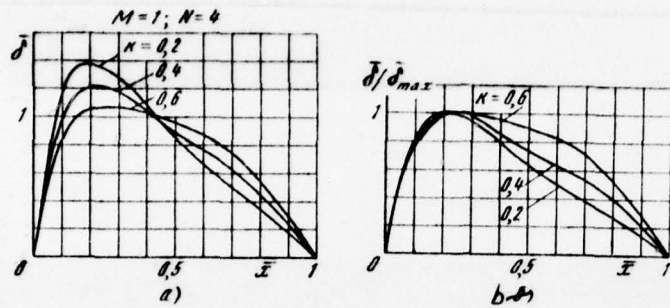


Fig. 5.

REFERENCES

1. E. A. Krasil'shchikova. Finite-span wing in compressible flow. M., Gostekhteorizdat, 1952.
2. R T Jones. The minimum drag of thin wings in frictionless flow JAS, v 18, No 2, 1951.
3. Ye. V. Bulygin. Wing of alternating/variable sweepback with the assigned/prescribed volume and minimum wave impedance. State Committee SM USSR on aviation equipment, 1960.
4. M Penain, D Vallee. Application de la theorie des ecoulements homogènes a la recherche de l'adaptation de certaines ailes en regime supersonique. ONERA, Mém Technique, 1959, No 14.

DOC = 78103902

PAGE 18 *52*

5. T Kawasaki. On favorable thickness distributions for wing
supersonic flow. AIAA Paper, No 65-716, 1965.

The manuscript entered 30/IX 1969.

DCC = 78103902

PAGE 18 *52*

5. T Kawasaki. On favorable thickness distributions for wings in
supersonic flow. AIAA Paper, No 65-716, 1965.

The manuscript entered 30/IX 1969.

Page 22.

THE SIMILARITY OF FLOWS WITH SPRAYING JETS.

V. N. Gusev, V. V. Mikhaylov.

Are examined the jet streams of viscous thermodynamically ideal gas. On the basis of dimensional theory, are establish/installated the laws of similarity for those zones of flow in which the size/dimension of initial jet cross-sectional area can be disregarded.

Let us examine the discharge of gas jet from the geometrically similar bodies, streamlined with the uniform incident flow (Fig. 1). Gases in the incident flow and in jet we assume by thermodynamically ideal. Let the distributions of the flow parameters over initial jet cross-sectional area, in reference to the appropriate characteristic values in the beginning of jet, be identical, then the solution of problem will be by pillar determined by the following set of the parameters: by pressure p_∞ , by density ρ_∞ , by the velocity u_∞ and by the coefficient of viscosity μ_∞ in the incident flow; by the linear dimension of body L by the size/dimension of initial jet cross-sectional area d ; by the characteristic flow parameters in jet p_j, ρ_j, u_j, μ_j and also by characteristic gas enthalpy on body surface H_w .

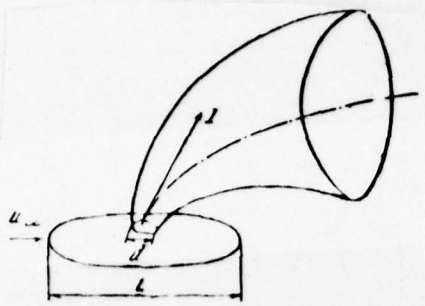


Fig. 1.

Page 23.

In this case, the constants, which determine the physical properties of gases in jet and in the external flow, for example the *ratio* of specific heat κ , the number of Prandtl σ and of so forth, we assume dimensionless and by already entering the number of criteria of similarity of problem. The remaining similarity criteria, which are the independent dimensionless combinations of the determining parameters, can be written in the form

$$\left. \begin{aligned} M_{\infty} &= \frac{u_{\infty}}{\sqrt{\kappa_{\infty} \frac{p_{\infty}}{\rho_{\infty}}}}; & Re_{\infty} &= \frac{\rho_{\infty} u_{\infty} L}{\mu_{\infty}}; & \frac{H_{\infty}}{u_{\infty}^2}; & \frac{d}{L}; \\ M_j &= \frac{u_j}{\sqrt{\kappa_j \frac{p_j}{\rho_j}}}; & \frac{u_j}{u_{\infty}}; & \frac{\mu_j}{\mu_{\infty}}; & \frac{p_j}{p_{\infty}}. \end{aligned} \right\} \quad (1)$$

Let us examine the limiting case of flows when $p_\infty \neq 0$, when parameter $dL^{-1} \rightarrow 0$, but the effect of jet on external flow is substantial, i.e., the total impulse, introduced into flow by jet during the passage to the limit indicated, let us compare with the characteristic momentum/impulse/pulse of external flow $p_\infty L^2$. Then instead of the determining parameter d into problem enters the characteristic momentum/impulse/pulse $I = d^2(p_j + \rho_j u_j^2)$, and the parameter of similarity dL^{-1} must be replaced by $p_\infty^{1/2} LI^{-1/2}$.

FOOTNOTE 1. The case of plane flow will be examined below.

ENDFOOTNOTE.

In this case, from criteria of similarity (1) it is necessary to exclude relation $p_j p_\infty^{-1}$, since when $dL^{-1} \rightarrow 0$ and finite values M_j and $p_\infty^{1/2} LI^{-1/2}$ value $p_j p_\infty^{-1} \rightarrow \infty$.

Thus, similarity criteria take the form

$$M_\infty, Re_\infty, \frac{H_w}{u_\infty^2}, L \sqrt{\frac{p_\infty}{I}}, M_j, \frac{u_j}{u_\infty}, \frac{\rho_j}{\rho_\infty} \quad (2)$$

Dimensionless dependent and independent alternating/variable problems we can be written in this case as follows:

$$\bar{u} = \frac{u}{u_j}; \quad \bar{p} = \frac{p}{p_\infty}; \quad \bar{\rho} = \frac{u_j^2}{p_\infty} \rho; \quad \bar{x} = \sqrt{\frac{p_\infty}{I}} x. \quad (3)$$

If parameter I is replaced by $p_{0j} d^2$, where p_{0j} — characteristic stagnation pressure in jet, then the similarity parameters and variables can be presented in the form

$$\left. \begin{aligned} M_\infty; \quad Re_\infty; \quad \frac{H_\infty}{u_\infty^2}; \quad K_1 = \frac{L}{d} \sqrt{\frac{p_\infty}{p_{0j}}}; \quad M_j; \quad \frac{u_j}{u_\infty}; \\ K_2 = Re_j \sqrt{\frac{p_\infty}{p_{0j}}}; \\ \bar{u} = \frac{u}{u_j}; \quad \bar{p} = \frac{p}{p_\infty}; \quad \bar{\rho} = \frac{u_j^2}{p_\infty} \rho; \quad \bar{x} = \frac{x}{d} \sqrt{\frac{p_\infty}{p_{0j}}}; \end{aligned} \right\} \quad (4)$$

where $Re_j = \frac{\rho_j u_j d}{\mu_j}$.

Page 24.

From relationship/ratios (4) it follows that with equality the obtained similarity criteria the linear dimensions of jet, in reference to the size/dimension of its initial section, increase proportional to root from relation $p_{0j} p_\infty^{-1}$, but characteristic Reynolds number jet decreases in comparison with Re_j into the same number once.

In the case of the plane flow in relationship (4) instead of parameters K_1 and K_2 they will enter $K'_1 = \frac{L}{d} \frac{p_\infty}{p_{0j}}$; $K'_2 = \text{Re}_j \frac{p_\infty}{p_{0j}}$, but independent the variable \bar{x} will take form $\bar{x} = \frac{x}{d} \frac{p_\infty}{p_{0j}}$.

Let us extract similarity criteria in some in practice interesting special cases of the flows in question:

uniform external flow ($L \rightarrow \infty$) -

$$M_\infty, K_2, M_j, \frac{u_j}{u_\infty}; \frac{\mu_j}{\mu_\infty}; \quad (5)$$

discharge into quiescent gas ($u_\infty = 0$) -

$$K_2, M_j, u_j \sqrt{\frac{\rho_\infty}{p_\infty}}, \frac{\mu_j}{\mu_\infty}; \quad (6)$$

the flow of nonviscous gas ($\mu_j = \mu_\infty = 0$) -

$$M_\infty, K_1, M_j, \frac{u_j}{u_\infty}. \quad (7)$$

If during the specific flow conditions $M_\infty \theta \gg 1$ (where θ -

characteristic angle of jet inclination), then pressure p_∞ can be disregarded, and in criterion of similarity (7) number M_∞ will not enter. In this case after replacement in (4) p_∞ by $\rho_\infty u_\infty^2$ the dimensionless dependent and independent alternating/variable problems it is possible to write in the form

$$\bar{u} = \frac{u}{u_j}; \quad \bar{p} = \frac{p}{\rho_\infty u_\infty^2}; \quad \bar{\rho} = \frac{u_j^2}{\rho_\infty u_\infty^2} \rho; \\ \bar{x} = \frac{x}{d} \sqrt{M_\infty^2 \frac{\rho_\infty}{\rho_0 j}}. \quad (8)$$

Let us note that in the examination of similarity separately inside and out of jet criterion $u_j u_\infty^{-1}$ (or replacing it when $u_\infty = 0$ parameter $u_j \rho_\infty^{1/2} p_\infty^{-1/2}$) is unessential and drops out¹.

FOOTNOTE ¹. At the examination only of geometric similarity, parameter $u_j u_\infty^{-1}$ is also unessential. This case with $K_1=0$ was examined in work [1]. ENDFOOTNOTE.

In this case, the dimensionless form of the dependent and independent variables for flow within jet remains previous, and for the external flow of value u_j , entering relationship/ratios (4) or (8), must be replaced by u_∞ .

The law of similarity for the form of jet was tested experimentally when $M_j = 1$, $u_\infty = 0$, $\kappa_j = 5/3$. The results of these investigations are given to Fig. 2, on which are plotted/applied the dimensionless coordinates of suspended shock wave in the jet

$$X = 0,5 x d^{-1} p_\infty^{1/2} p_{0j}^{-1/2}, \quad Y = 0,5 y d^{-1} p_\infty^{1/2} p_{0j}^{-1/2},$$

where x, y - cylindrical coordinates, d - a diameter of nozzle.

Page 25.

Solid line on Fig. 2 corresponds to the approximate theoretical dependence, constructed according to method of operation [2]. Let us note that the obtained previously relationship/ratio for the coordinate x , of closing shock wave [3] also it experimentally corresponds to the written above law of similarity $\frac{x}{d} \sqrt{\frac{p_\infty}{p_{0j}}} = \text{const.}$

Let us examine in conclusion the case of the outflow of gas into vacuum ($p_\infty = p_\infty = 0$), after excluding from the number of those determining the characteristic parameters of external flow. Relationship/ratios (4) are converted in this case to the form

$$M_j, \bar{u} = \frac{u}{u_j}; \quad \bar{p} = \frac{p}{p_{0j}}; \quad \bar{\rho} = \frac{u_j^2}{p_{0j}} \rho; \quad \bar{x} = \frac{x}{d} \frac{1}{Re_j}.$$

When $\mu_1 = 0$ (nonviscous gas) of the determining parameters of the problem it is not possible to comprise combination with the dimensionality of length. Consequently, in accordance with the results of work [4], far from initial jet cross-sectional area of the flow line of the flow in question are close to proceeding of one point direct/straight lines.

It should be noted that the conclusions, which relate to the case of discharge into vacuum, can be valid, also, when $p_\infty \neq 0$ for that region of the strongly expanded jet in which the effect of external flow can be disregarded.

REFERENCES

1. I. P. Moran. Similarity in high-altitude jets. AIAA J, v 5, No 7, 1967.
2. V. N. Gusev, T. V. Klinova. Flow in those escape from those underexpanded jet puffed jets. "Izv. AN of the USSR MZhG", 1968, No 4.
3. H. Ashkenas, P. S. Sherman. The structure and utilization of supersonic free jets in low density wind tunnels. Dynamics of Rarefied Gases. Forth Symp. Acad. Press, 1965.

4. M. D. Ladyzhenskiy. Analysis of the equations of hypersonic flows and the solution of the problem of Cauchy. "applied mathematics and mechanics", Vol. 26, iss. 2, 1962.

The manuscript entered 9/11 1969.

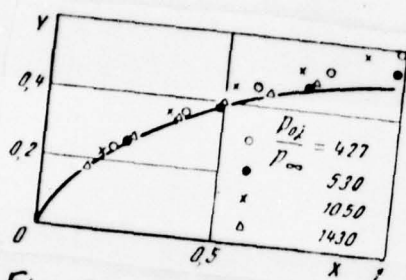


Fig. 2.

Page 26.

THE SIMULATION OF VISCOUS HYPERSONIC FLOWS IN WIND TUNNELS.

V. S. Galkin, V. S. Niklaev.

On the basis of calculation data, obtained by the method, presented in works [1] and [2], it is examined a question concerning the effect of different similarity criteria on the aerodynamic characteristic of plate, arranged/located at low angle of attack, under the conditions of interaction of laminar boundary layer with hypersonic inviscid flow. Is carried out the analysis of questions of the simulation of actual conditions in wind tunnels. Are given to recommendation regarding the recalculation of experimental aerodynamic characteristics to full-scale for the cases when dissimilarly at once to several similarity criteria.

HP
During the flow around bodies of the flow of gas of low density the aerodynamic characteristics of bodies depend not only on gas-dynamic similarity criteria, but also on a whole series of the criteria, connected with the viscosity effect and thermal conductivity on all the field of flow about body, with the conditions of cooperating the molecules of gas with the body surface, etc. Such conditions/modes of

flow, which are realized during hypersonic flights of flight vehicles at high altitudes, are extremely complex for simulation in wind tunnels.

At present because of the use of the overexpanded jets, it was possible to obtain in the low-temperature indraft wind tunnels of flow over a wide range of basic similarity criterion during hypersonic stabilization [3]

$$Re_0 = \frac{\rho_\infty u_\infty L}{\mu_0}, \quad (1)$$

where ρ_∞ , u_∞ , L , μ_0 — respectively density and velocity of incident flow, the significant dimension of body (for a plate its length) and the coefficient of viscosity, calculated of temperature of braking the incident flow T_0 . This range includes the conditions/mode of viscous hypersonic interaction (large numbers Re_0), flow conditions, close to free molecular (small numbers Re_0), and so-called transient (intermediate) flow conditions of the rarefied gas.

Page 27.

However, in the low-temperature ducts where value T_0 is close to room, is not realized/accomplished simulation on a series of other important similarity criteria. The aerodynamic characteristics we can

depend substantially on temperature factor $t_w = \frac{T_w}{T_0}$, where T_w — the temperature of body surface, and from the parameter γ , entering the law of the dependence of the coefficient of viscosity μ on temperature T (for example, $\gamma = n$, if $\mu \sim T^n$).

In connection with this arise the questions concerning the degree of the effect of different similarity criteria on the aerodynamic characteristics of bodies, concerning the recalculation of the experimental data on full-scale with the noncoincidence of similarity criteria finally on the selection of the wind tunnel, which allows in a best for this object manner to simulate conditions of natural flow. Due to the complexity of the equation of Boltzmann, to give sufficiently complete answer/response to these questions for transient conditions/mode is difficult; therefore is necessary the corresponding analysis for the limiting cases of the small and large numbers Re_0 .

A question concerning the recalculation of experimental data to full-scale for the flows, close to free molecular, is examined in monograph [4]. With the large Re_0 is logical to examine flow conditions near the limit of the applicability of the mechanics of continuous medium, i.e., the conditions/mode of the viscous hypersonic flows where the effect of decrease ρ_∞ is exhibited only in the amplification of the viscosity effect and thermal conductivity

on all the field of disturbed flow.

FOOTNOTE 1. As show the available in the published works data, under these conditions, in any case at velocities it is less or the order of the first space, the effects of imperfect gas are insignificant and air can be considered as thermodynamically ideal gas.

ENDFOOTNOTE.

In this case, maximum effect on the aerodynamic characteristics of value t_w , γ is had in the case of slender body at low angle of attack. If the effect of one or the other similarity criterion on the total aerodynamic coefficients of slender bodies is small, then it, generally speaking, will be still less in the case of "thick" bodies. For this very reason in this work is examined the case of the flow around the plate, arranged/located at low angle of attack α , under the conditions of interaction of laminar boundary layer with hypersonic inviscid flow. The utilized calculated data are obtained by the method, described in works [1] and [2], under the same assumptions of the relatively thermodynamic properties of gas, etc.

The dimensionless local and total aerodynamic characteristics of plate at the angle of attack $\alpha \neq 0$ $\left(\frac{c_x}{\alpha^3}, \frac{c_y}{\alpha^2} \right)$ and of so forth) under the conditions of the viscous hypersonic flows of the thermodynamically ideal gas are determined by criteria of similarity

$$\alpha^2 \sqrt{Re_0}, K_0 = M_\infty \alpha, t_w = \frac{T_w}{T_0}, \gamma, \kappa, Pr. \quad (2)$$

Here c_x, c_y — the drag coefficients and lift, in reference to length of plate and velocity head of the incident flow; Pr — Prandtl's number, κ — specific heat ratio, M_∞ — Mach number of the incident flow.

Page 28.

Under the conditions of hypersonic stabilization ($K_0 \gg 1$) aerodynamic characteristics do not depend on K_c . Under conditions of wind tunnel tests $t_w \leq 1$, under actual conditions $t_w \ll 1$. For helium in wide interval to temperature $\kappa = 5/3$, $Pr = 0.68$, $\mu \sim T^{0.647}$ ($n = 0.647$). For air $\kappa = 1.4$, $Pr = 0.7$, the dependence of the coefficient of viscosity on T takes the form

$$\mu \cdot 10^6 \text{ [N·s/m}^2\text{]} = 0.1755 \cdot T^{0.833} \exp - 0.167 [(\ln T - 5.403)^2 + 0.172]^{1/2}. \quad (3)$$

In this case $\gamma = T_0$. Formula (3) is obtained via approximation with error 1-20% in data on $\mu(T)$ from works [5] and [6] ¹.

FOOTNOTE 1. With $T > 2000^\circ\text{K}$ from the schedules of operation [6] were taken values μ for the high values of pressure, when the effects of imperfect gas were unessential. Let us note that the data [6] for $\mu(T)$ they will agree well with the results of work [7]. ENDFOOTNOTE.

With $T < 150^\circ\text{K}$, according to work [5], $\mu \sim T$, i.e., $n=1$, with $T > 400^\circ\text{K}$ value n is close to 0.67. Value $n=0.67$ ("large" T_0) is realized under actual conditions, case $n=1$ ("small" T_0) is nearer to experimental conditions in indraft wind tunnels without preheating of gas in precombustion chamber.

Let us note that with large T of value Pr and n for helium and air are very close and a difference in the aerodynamic coefficients of bodies is caused by a difference in the values x [with the fixed/recorded values of remaining criteria (2)].

In this work is not utilized the approximate law of similarity of Cheng [8], who correlates well (it draws together) data on γ ; however, it gives insufficient correlation on l_w [1, 2].

THE SIMULATION OF FULL-SCALE FLOW IN LOW-PRESSURE WIND TUNNELS.

Let us examine a question concerning the direct/straight simulation of actual conditions in wind tunnels under the conditions

of viscous hypersonic flows (in the case of the plate, arranged/located at small angle α). Under direct/straight simulation is implied the possibility of the direct "transfer" of experimental data to actual conditions. This is possible when all the similarity criteria in duct and nature coincide or when difference for one or even several similarity criteria leads to in effect unessential differences in aerodynamic characteristics.

During direct/straight simulation must be maintain/withstood identical criteria of similarity K_0 and α , the not connected with viscosity effect (and, of course, the value of basic criterion of similarity α^2/Re_0 or Re_0 during strong interaction). For the analysis of the role of remaining criteria of similarity γ , t_w is most characteristic the range of strong interaction ($\alpha^2/\text{Re}_0 \rightarrow 0$). It is real/actual, with an increase α^2/Re_0 , the viscosity effect on aerodynamic characteristics decreases, with respect decreases the effect of the similarity criteria, caused by the viscosity (see below). Consequently, if is realized direct/straight simulation under the conditions of strong interaction, then it, as of old, will be made under conditions of the moderate and weak interaction.

Page 29.

Therefore let us here examine only the conditions/mode of strong

interaction, moreover we will be restricted to the analysis of the basic total (taking into account both sides of plate) aerodynamic coefficients: the drag coefficient c_{x0} and of derivative of lift coefficient in angle of attack when $\alpha \rightarrow 0$ $c'_{y0} = \left(\frac{dc_y}{d\alpha} \right)_0$. Here c_{x0} is given by the theory of the strong interaction of the zero order when c_x does not depend on α , and c'_{y0} by the theory of the strong interaction of the first order, since the members of zero order for pressure on both sides of plate are identical and during the calculation of lift mutually cancel each other.

The results of calculations c_{x0} , c'_{y0} with the use of formula (3) for $\mu(T)$ are given to Figs. 1 and 2. On Fig. 1, are represented dependences $c_{x0} Re_0^{3/4}$ and $c'_{y0} Re_0^{1/4}$ on criteria t_w and $\gamma = T_0 \left(t_{eq} = \frac{T_{eq}}{T_0} \right)$, T_{eq} — the temperature of the heat-insulated plate). To Fig. 2, are given the curve/graphs, which show relative difference c_{x0} and c'_{y0} from the appropriate values with "full-scale" $m=0.67$ (in this case conditionally we take $T_0 = \infty$), depending on t_w with different T_0 . Value $\Delta_T c_{x0}$ is calculated from the formula

$$\Delta_T c_{x0} = \frac{c_{x0}(T_0) - c_{x0}(\infty)}{c_{x0}(\infty)},$$

analogously is determined $\Delta_T c'_{y0}$. Value $T_0 = 0$ conditionally corresponds to case $m=1$. Comparison is conducted with the identical number Re_0 .

It is interesting to note that the effect t_w , T_0 on c'_{y0} is substantially less than to the coefficient of pressure [2].

The analysis of dependences on Figs. 1 and 2 shows that for providing direct/straight modeling it is necessary to completely strictly maintain/withstand equality the values of criterion t_w . So, a comparatively small difference in t_w ($t_{wH} = 0,05$, $t_{wT} = 0,15$) leads to the difference in values c_x and c_y more than 10% [index of "n" is related to the conditions of hypersonic flight in the atmosphere ($T_0 = \infty$), the index of "t" to conditions in wind tunnel].

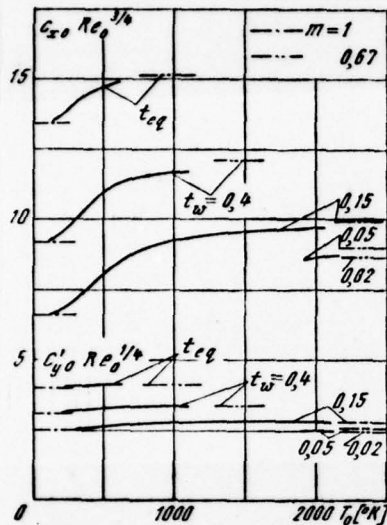


Fig. 1.

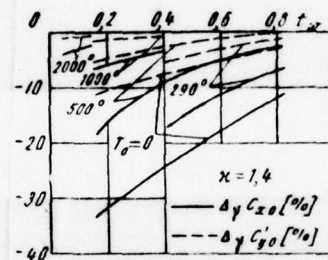


Fig. 2.

Page 30.

Essential is criterion γ . Data, presented in Figs. 1 and 2, make it possible to answer a question, to which values it is necessary to increase temperature of gas in precombustion chamber T_0 in order to ensure the simulation of actual conditions from acceptable for practical target/purposes with degree of accuracy. So, heating gas in precombustion chamber to $T_0 \approx 2000^\circ\text{K}$ provides the simulation of full-scale values c_x and c_y with error $\Delta \leq 40\%$ with $t_{wH} = t_{wT} \geq 0.05$.

RECALCULATION OF EXPERIMENTAL DATA TO FULL-SCALE.

In connection with the great difficulties of realizing the direct/straight simulation in wind tunnels, unavoidably gets up a question concerning the procedure of the recalculation of the results of experiment for actual conditions, concerning the introduction of the corresponding corrections which can be obtained from the results of the parametric analyses of the flow around the simplest bodies. Let us demonstrate in the most demonstrative form the degree of the effect of all essential criteria of similarity $(K_0, \alpha, t_w, \gamma)$ on the total aerodynamic coefficients of plate c_x, c_y in an entire interaction region from the powerful to the weak and will formulate the rules of the recalculation of experimental data to full-scale. In this case, of course, we assume that the basic criterion of similarity $\alpha^3/\sqrt{Re_0}$ under conditions of flight and aerodynamic of duct is identical. During a change in this criterion, aerodynamic coefficients can be changed on several orders and it cannot be spoken about any corrections and recalculation. At the same time incomplete similarity on criteria K_0, α, t_w, γ can lead to errors from several percentages to several tens of percentages, and recalculation can be treated as introduction of several corrections.

The analysis of the presented below graphic material makes it possible before experimentation to explain the degree of the nearness

of expected experimental and full-scale aerodynamic characteristics, and in the presence of several experimental installations to rate/estimate, which of them more approaches for a concrete/specific/actual experiment, i.e., in which case it is necessary to introduce smaller correction. For example, in the vacuum low-temperature ducts, working in air, Mach number and, therefore, K_0 are comparatively small, but in helium ducts are close to full-scale. Since corrections on K_0 can be more than corrections on experiment in helium duct can render/show more preferable experiment in low-temperature vacuum ducts.

On Figs. 3-7, are represented the results of the calculations of relative differences (corrections) in the percentages of values c_x/a^3 and c_y/a^3 from their "supporting/reference" values depending on a^2/Re_0 with different K_0 , x , l_w , γ ($m=1$ and 0.67).

On Figs. 3 and 4 supporting/reference are values c_x/a^3 and c_y/a^3 under conditions of hypersonic stabilization ($K_0=0$) when $x=1,4$:

$$\Delta_K c = \frac{c(K_0) - c(\infty)}{c(\infty)}.$$

Here below c is equal either c_x/a^3 , or c_y/a^3 .

on Figs. 5 and 6 as supporting/reference are selected values c
when $t_w = t_{eq}$:

$$\Delta_w c = \frac{c(t_w) - c(t_{eq})}{c(t_{eq})} \quad (K_0 = \infty, x = 1, 4).$$

Page 31.

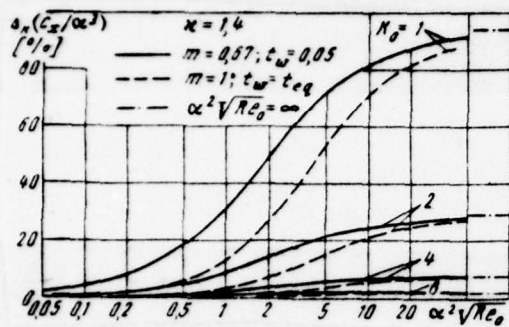


Fig. 3.

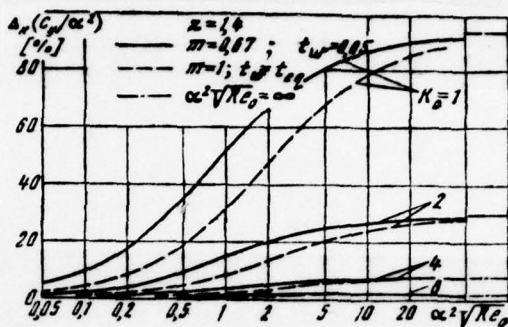


Fig. 4.

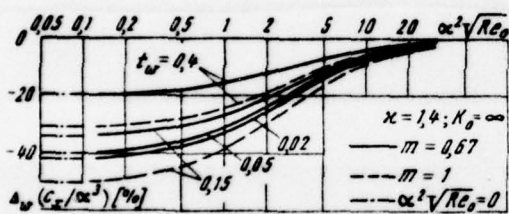


Fig. 5.

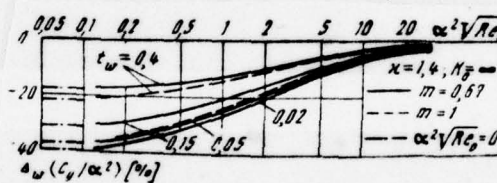


Fig. 6.

Page 32.

On Fig. 7 Reference values c with "full-scale" $m=0.67$,

$t_w=t_{eq}, K_0=\infty, x=1.4$:

$$\Delta_T c = \frac{c(m=1) - c(0,67)}{c(0,67)} ;$$

$$\Delta_x c = \frac{c\left(x = \frac{5}{3}\right) - c(1,4)}{c(1,4)} .$$

Values $\Delta_K c$, $\Delta_w c$ with are calculated at the fixed values $m=0.67$ and 1. Values $\Delta_K c$, $\Delta_w c$, $\Delta_T c$ characterize effect K_0 , l_w , m (i.e. γ) respectively. The difference for data for helium from data for air with $K_0=\infty$ is characterized by value Δ_x (here is considered the made above observation about nearness Pr and m of helium and air at high values T).

Resultant formula for the recalculation of experimental data to full-scale takes the following form:

$$c_n = \frac{c_r (1 + \Delta_K)_n (1 + \Delta_w)_n}{(1 + \Delta_K)_r (1 + \Delta_w)_r (1 + \Delta_T)_r (1 + \Delta_x)_r} (\Delta_i \equiv \Delta_i c) .$$

Here by c it is understood either c_x/a^3 , or c_y/a^2 at the identical value of criterion of similarity $a^2/\nu Re_0$ for wind tunnel and for nature. Under the actual conditions $m=0.67$, case $m=1$ in the first approximation, corresponds to test conditions in of low-temperature

vacuum ducts. For obtaining more precise value $\Delta_1 c_1$ one should $\Delta_1 c_1$ specific Fig. 7, multiply on $\frac{\Delta_1 c(T_0)}{\Delta_1 c(0)}$, undertaken Fig. 2 (strong interaction).

The degree of effect K_0 under the actual and experimental conditions (see Figs. 3 and 4) is essentially different. This is explained, in essence, by difference in values t_w ; with increase t_w sharply increases the boundary layer thickness, hypersonic stabilization sets in at smaller values K_0 . If t_w in duct or in flight considerably they differ from t_w on Figs. 3 and 4, then for refining values $(1 + \Delta_k)_u$ and $(1 + \Delta_k)_r$ it is possible to utilize linear interpolation on t_w between the values of these values (see Figs. 3 and 4) when $t_w = 0,05$ ($m = 0,67$) and $t_w = t_{eq}$ ($m = 1$). Checking in a number of examples confirmed the legitimacy of such an interpolation.

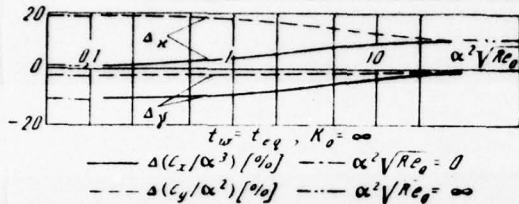


Fig. 7.

Page 33.

Primary attention in article was allotted to the analysis of corrections for c_x and c_y in connection with the fact that the lift-drag ratio and the center-of-pressure location is considerably more conservative to changes K_0, x, t_w, m [1, 2].

The formulated rules of recalculation can be utilized also for fine/thin airfoil/profiles, and also, apparently, and for the wings (during the calculation of number Re_0 for a wing as reference length it is possible to take the mean chord).

REFERENCES

1. V. S. Galkin, A. V. Zhabkova, V. S. Nikolaev. Aerodynamic characteristics of plate at angle of attack in viscous hypersonic

flow. "Bulletin AN of the USSR MZhG", 1969, No 1.

2. V. S. Galkin, A. V. Zhabkova, V. S. Nikolaev. Aerodynamic characteristics of plate at angle of attack in viscous hypersonic flow and questions of modeling in low-pressure wind tunnels.

Transactions of TsAGI [Central Institute of Aerohydrodynamics im. N. Ye Zhukovskiy, iss. 1187, 1970.

3. V. N. Gusev, M. N. Kogan, V. A. Yerepukhov. Similarity and a change of the aerodynamic characteristics in transition region at the hypersonic speeds of flow. "Scholarly notes of TsAGI", Vol. I, No 1, 1970.

4. M. N. Kogan. Dynamics of the rarefied gas. M., "Science", 1967.

5. A. W. Viore. Viscosity of air. J of Spacecraft and Rockets, v 3, No 5, 1966.

6. Yu. A. Kibardin, S. I. Kuznetsov, A. N. Liubimov, V. Ya. Shunyat'skiy. Atlas of gas-dynamic functions at high velocities and the high temperatures of air flow. M., Gosenergizdat. 1961.

7. R. M. Sevast'yanov, M. D. Zdankevich. Tables of the

thermophysical properties of air and nitrogen in the range of temperatures from 100 to 5000-15000°K. Transactions of TsAGI, iss. 922, 1964.

8. H. K. Cheng, J. G. Hall, T. C. Gclian, A. Iertzberg. Boundary-layer displacement and leading-edge effects in high-temperature hypersonic flow. J Aerospace Sci., v 28, No 5, 1961.

The manuscript entered 9/IX 1969.

Page 34.

METHOD OF CALCULATION OF THE TURBULENT JETS NEAR THE WALL WHEN THE
LONGITUDINAL GRADIENT OF PRESSURE IS PRESENT,.

A. S. Ginevskiy, A. V. Kolesnikov, I. N. Podol'nyy.

Is set forth the integral method of calculation of the turbulent jets near the wall, which are spread in the slipstream with downstream pressure gradient. On the basis of this method, it is possible to calculate the basic section of the jet near the wall for all its extent/elongation up to its degeneration into usual turbulent boundary layer or - with positive downstream pressure gradient - before the section where occurs flow breakaway.

The investigation of the semi-bounded turbulent jets, which develop along curved surface in the slipstream with downstream pressure gradient, is of interest for many areas of technology. For the approximate computation of such jets, are developed the methods,

instituted on the use of semi-empirical theories of turbulence. So, by G. N. Abramovich is proposed the method of calculation of the flat/plane semi-bounded jets in concurrent gradient-free flow [1], by N. I. Akatnov - flat/plane flooded jets [2]. Survey/coverage of foreign experiments in this field is contained in work [3], where, in particular, it is mentioned J. Harris' attempt to calculate the semi-bounded jet in the slipstream with downstream pressure gradient. The numerical method of the solution of the problem of the turbulent semi-bounded jet is described in D. E. Spaulding's work [4]. Finally, in the recently published work of Newman and Gartshore [5] is shown the empirical method of the solution of problems.

In the present work is set forth approximate integral method of the calculation of the turbulent jets near the wall in the presence of downstream pressure gradient for the case when jet velocity exceeds the velocity of the slipstream. Method is instituted on the use of the polynomial approximation of the airfoil/profiles of shearing stress in the near-wall and jet-edge parts of the semi-bounded jet, semi-empirical formulas for turbulent friction and two integral relationship/ratios.

Page 35.

In this case, in accordance with the approach/approximation of

boundary-layer theory, transverse pressure gradient is set/assumed equal to zero.

Since the jets near the wall include the cell/elements of simpler flows - boundary layer and free jet (Fig. 1), during their calculation are utilized some relationships, obtained for these flows [6, 7]. At the same time flow in the near-wall and jet-edge parts of the semi-bounded jet significantly differs from the appropriate boundary-layer flows and free jet. This difference is caused, mainly, two by facts. First, the boundary layer of the semi-bounded jet near the wall is developed under conditions of increased turbulence of "external" jet-edge flow, in consequence of which the characteristic of the boundary layer near the wall in its external part they differ somewhat from the appropriate characteristics of usual turbulent boundary layer and approach the appropriate characteristics of turbulent boundary layer with increased turbulence of external flow [8]. Furthermore, here external flow is not irrotational, and on the boundary of wall boundary layer is not made the equation of Bernoulli. In the second place, a difference in the flows in the jet-edge part of the semi-bounded jet and of usual symmetrical free jet lies in the fact that in the first case at the point of maximum speed shearing stress not is equal to zero and the line of maximum speeds is not flow line.

Within the framework of the semi-empirical theory of turbulence, the first of the differences indicated can be to some degree taken into account via the selection of the increased value of the path length of mixing in the exterior of wall boundary layer. As concerns the second difference, then the semi-empirical theories of turbulence cannot consider, since it follows the proportionality of friction stress the transverse gradient of the averaged velocity, i.e., at the point of maximum speed, friction stress is set/assumed equal to zero. It is possible, however, to expect that the noted difference for real and calculated distributions of shearing stress near the point of the maximum speed (see Fig. 1), caused by the dissymmetry of the velocity profile about this point, it will not introduce into the calculation of essential errors. In fact, the hot-wire measurements of the profiles of velocity and shearing stress in flocced semi-bounded jet [9] showed that in the cross sections of this jet the point of the maximum speed was displaced relative to the point zero value of shearing stress.

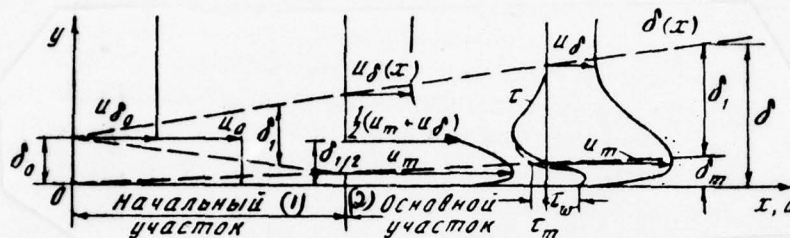


Fig. 1.

Key: (1). Initial section. (2). Basic section.

Page 36.

In this case, it proves to be that the sign of this displacement for a jet in cccurrent gradient flow depends on the sign of downstream pressure gradient [14]. It is necessary, however, to note that in all enumerated cases the displacement indicated is insignificant.

Thus, stated problem is formulated as follows. Let from tangential slot by height/altitude δ_0 it escape/ensue along surface into the slipstream whose speed $u_s = u_s(x)$ is assign/prescribed, the semi-bounded jet with the uniform initial velocity $u_0 > u_s$ (characteristic Reynolds number $Re = \frac{u_0 \delta_0}{\nu}$). Sometimes can be assign/prescribed thickness of initial boundary layer or Reynolds

number $Re^{**} = \frac{u_0 \delta_0^{**}}{\nu}$, where δ_0^{**} - a momentum thickness of boundary layer in initial section. It is required to calculate the velocity profiles in all cross sections and skin-friction distribution along flow.

During the solution of problem, the flow conditionally is divided into two sections - initial and basic. During the assigned/prescribed stepped distribution of the velocity in initial section from the place of the velocity profile, is formed the turbulent zone of mixing. The intersection of its internal boundary with boundary layer edge which builds up along wall, determines the length of the initial section (see Fig. 1). Since the turbulent zone of mixing and turbulent boundary layer within the limits of initial section are divided by the range of irrotational flow, they can be calculated independently. The method of calculation of the initial section of flat/plane free jet in cocurrent gradient flow is presented in work [7], the parameters of boundary layer within the limits of initial section are calculated from the formulas of work [6].

The transverse size/dimensions of the zone of mixing and irrotational nucleus of flow within the limits of initial section, just as the length of initial section, they depend on the initial ratio of velocities $m_0 = \frac{u_{80}}{u_0}$, initial thickness δ_0^{**} and the specified distribution of velocity $u_0(x)$. As showed the carried out calculations

and experiments, the length of initial section in the semi-bounded jets proves to be insignificant; therefore the greatest practical interest represents the calculation of the basic section of the semi-bounded jets.

During the calculation of basic section, let us consider that occurrent flow irrotational and, therefore, out of jet is correct relationship/ratio $\frac{dp}{dx} = - \frac{\rho u_0 du_0}{dx}$. Integrating equation of motion taking into account the equation of continuity across jet from surface ($y=0$) to point with the coordinate $y = \delta_m$, which corresponds to the maximum value of velocity $u = u_m$, we will obtain the integral relationship/ratio of momentum/impulse/pulses for the part of the jet near the wall.

Page 37.

The second integral relationship/ratio is obtained in the most convenient for calculations form by the multiplication of the equations of boundary layer by function $\varphi(u) = u_0 + u_m - 2u$ and the subsequent integration across the exterior of the jet from $y = \delta_m$ to $y = \delta$:

$$\left. \begin{aligned} \frac{d}{dx} \int_0^{\delta_m} u(u_m - u) dy + u'_m \int_0^{\delta_m} (u_m - u) dy &= \frac{1}{\rho} (\tau_w - \tau_m) + \delta_m (u_m u'_m - u_\delta u'_\delta); \\ \frac{d}{dx} \int_{\delta_m}^{\delta} u(u_m - u)(u - u_\delta) dy &= u'_\delta \int_{\delta_m}^{\delta} [u_\delta (u_m + u_\delta - 2u) - \\ &- u(u_m - u)] dy + u'_m \int_{\delta_m}^{\delta} u(u - u_\delta) dy - \frac{2}{\rho} \int_{\delta_m}^{\delta} u \frac{\partial \tau}{\partial y} dy. \end{aligned} \right\} (1)$$

Here τ_w and τ_m - shearing stress on wall ($y=0$) and on the outer edge of boundary layer ($y=\delta_m$), $u'_m = \frac{du_m}{dx}$, $u'_\delta = \frac{du_\delta}{dx}$. Near the wall since a quantity of unknowns in system (1) exceeds the number of equations, it must be supplemented by the dependences, which relate unknown values.

The part of the jet near the wall. As it was mentioned above, such dependences can be obtained, examining separately near-wall boundary layer and the exterior of the semi-bounded jet. Let us consider that in boundary layer communication/connection between shearing stress τ and transverse gradient of velocity is determined by Prandtl's formula

$$\tau = \rho l^2 \left(\frac{\partial u}{\partial y} \right)^2, \quad (2)$$

where l - the path length of mixing, determined by the relationship/ratio

$$\frac{l}{\delta_m} = 0,14 - 0,08(1 - \eta)^2 - 0,06(1 - \eta)^4, \quad \eta = \frac{y}{\delta_m}.$$

The airfoil/profile of shearing stress let us present in the form of polynomial according to the degrees η :

$$\tau = \tau_w \sum_{i=0}^n A_i \eta^i. \quad (3)$$

The coefficients of the polynomial can be found from boundary conditions on the wall:

$$\tau = \tau_w, \quad \frac{\partial \tau}{\partial y} = \frac{dp}{dx}, \quad \frac{\partial^2 \tau}{\partial y^2} = 0 \quad \text{with } y=0$$

or

$$\frac{\tau}{\tau_w} = 1, \quad \frac{\partial}{\partial \eta} \frac{\tau}{\tau_w} = \frac{\delta_m}{\tau_w} \frac{dp}{dx}, \quad \frac{\partial^2}{\partial \eta^2} \frac{\tau}{\tau_w} = 0 \quad \text{with } \eta=0, \quad (4a)$$

and on the outer edge of the boundary layer near the wall:

$$\tau = \tau_m = 0, \quad \frac{\partial \tau}{\partial y} = \frac{dp}{dx} + \rho u_m u'_m \quad \text{with } y = \delta_m$$

or

when

$$\frac{\tau}{\tau_w} = 0, \quad \frac{\partial}{\partial \eta} \frac{\tau}{\tau_w} = \frac{\delta_m}{\tau_w} \left(\frac{dp}{dx} + \rho u_m u'_m \right) = A + B \quad \text{with } \eta=1, \quad (4b)$$

where

$$A = \frac{\delta_m}{\tau_w} \frac{dp}{dx}, \quad B = \frac{\delta_m}{\tau_w} \rho u_m u'_m.$$

Page 38.

For determining the second and third boundary conditions on wall and the second condition when $y = \delta_m$ were used the equations of motion.

Thus, the coefficients of the polynomial (3) will be expressed as two dimensionless parameters A and B. The first of them is common for a boundary-layer theory, the second is connected with the difference for flow on the outer edge of the wall boundary layer of jet from the potential. If on boundary layer edge is made the equation of Bernoulli $dp/dx + \rho u_m u'_m = 0$, then as it is clear from equation (4b), the sum of parameters $A+B=0$.

During the use of all conditions indicated we will obtain for determination τ/τ_w the polynomial of the fourth degree from η :

$$\tau = \tau_w (1 - \eta) \{ (1 - \eta) [(1 + 2\eta)(1 + A\eta) + 3\eta^2] - (A + B)\eta^3 \}. \quad (5a)$$

If we use only two conditions (4a) and one condition (4b), let us have a polynomial, which depends only from one parameter A:

$$\tau = \tau_w (1 - \eta) [1 + (1 + A)\eta]. \quad (5b)$$

Polynomials (5a, b) are suitable for the approximation of the airfoil/profile of shearing stress only at those values of parameters A and B, when $\frac{\tau}{\tau_w} \geq 0$. In connection with this it is necessary to explain

AD-A066 206

FOREIGN TECHNOLOGY DIV WRIGHT-PATTERSON AFB OHIO
SCIENTIFIC NOTES FROM THE CENTRAL AERO-HYDRODYNAMIC INSTITUTE (--ETC(U)
AUG 78

F/G 20/4

UNCLASSIFIED

FTD-ID(RS)T-1039-78

NL

2 OF 4

AD
A066206



the range of the allowed values of these parameters. If flow on the outer edge of layer is potential, then as was mentioned above, $A+B=0$. In this case the allowed values of the parameter A must exceed its value, with which the second [for a polynomial (5a)] or the first [for (5b)] derivatives of τ/τ_w at point $\eta=1$ change sign. Hence it follows that in the case of usual boundary layer polynomials (5a) and (5b) are suitable for the approximation of the airfoil/profile of shearing stress during the measurement A within limits from -2 to infinity.

From the physical essence of the phenomenon, it follows that on the outer edge of the boundary layer $A+B \leq 0$ NEAR the WALL, i.e., $B \leq -A$. For the flooded semi-bounded jet or a jet in the slipstream with a constant velocity of $A=0$, $B \leq 0$. Another value B , which limits the range of a change in this parameter, it is possible to obtain from the condition that in case ($A=0$) in question the relation τ/τ_w must not be more than unit, or derivative of τ/τ_w must not have roots in interval $0 < \eta < 1$. From this condition it follows that with $A=0$ the allowed values of parameter B for polynomial (5a) must be more than -4 . Thus the obtained approximations of the airfoil/profile of shearing stress are valid for a comparatively narrow range of a change in parameter B .

In connection with that presented it is interesting to determine, which value is parameter B for the in practice encountered cases. The value of parameter B, designed according to the experimental characteristics of jet [10], in the case of gradient-free flow reaches values from -1 to -1.5 in the beginning of basic section and somewhat decreases with flattening of flux. This estimation confirms the applicability of the obtained approximation of the airfoil/profile of shearing stress for the calculation of the semi-bounded jets.

On the basis of formulas (2) and (5) can be designed the airfoil/profiles of the defect of the velocity in the turbulent nucleus of the boundary layer of the jet

$$\psi = \frac{u_m - u}{u_\tau} = \int_0^1 \frac{\delta_m}{l} \sqrt{\tau/\tau_w} d\eta, \quad u_\tau = \sqrt{\tau_w/\rho}, \quad (6)$$

near the wall on parameters A and B depending. Is interesting to note that the relative velocity of flow $\bar{u} = u/u_m$ equal to

$$\bar{u} = 1 - \frac{u_\tau}{u_m} \psi, \quad (7)$$

they will characterize three parameters: A, B and u_τ/u_m or A, B and local Reynolds number.

In immediate proximity of the rigid surface where the turbulent pulsations attenuate and the dominant role plays molecular friction, formula (2), and consequently also formula (6) for the velocity profile ceases to correspond to reality. In this, ranges (viscous sublayer) we utilize the formula for shearing stress, which corresponds to laminar flow $\tau = \mu \frac{\partial u}{\partial y}$. With an accuracy to a small second order, the distribution of the velocities in viscous sublayer will be expressed by the equality

$$\frac{u}{u_*} = \text{Re}_1 \eta + 0,5 A \text{Re}_1 \eta^2, \quad (8)$$

where

$$\text{Re}_1 = \frac{u_* \delta_m}{\nu}$$

As for a usual boundary layer, let us consider that the profile of velocity of viscous sublayer (8) transfer/converts into the turbulent profile of velocity (7), when Reynolds number, designed on local velocity u_l and distance from wall δ_l , reaches certain critical value α^2 :

$$\frac{u_l \delta_l}{\nu} = \text{Re}_1^2 (\eta_l^2 + 0,5 A \eta_l^3) = \alpha^2, \quad (9)$$

where $\eta_l = \frac{\delta_l}{\delta_m}$, α — constant which, on different authors's data, varies within the limits with 10-12.

After equating the velocities, determined by formulas (7) and

(8) on the boundary of viscous sublayer η_l , we will obtain communication/connection between shearing stress on wall τ_w and thickness of the boundary layer of the jet near the wall:

$$\frac{u_\tau}{u_m} = [\alpha \sqrt{1 + 0,5 A \eta_l} + \psi(A, B, \eta_l)]^{-1}. \quad (10)$$

Page 40.

Thus, being assigned by the thickness ratio of viscous sublayer, it is possible to determine for different values of A and B the value of dynamic velocity u_τ/u_m or skin friction coefficient $c_f = 2(u_\tau/u_m)^2$, but in the profiles of velocity (6) and (8) to calculate all the integral boundary layer characteristics

$$\left. \begin{aligned} \frac{\delta_m^*}{\delta_m} &= \int_0^1 (1 - \bar{u}) d\eta = \frac{u_\tau}{u_m} I_1; \\ \frac{\delta_m^{**}}{\delta_m} &= \int_0^1 \bar{u} (1 - \bar{u}) d\eta = \frac{u_\tau}{u_m} I_1 - \left(\frac{u_\tau}{u_m} \right)^2 I_2; \\ H_m &= \frac{\delta_m^*}{\delta_m^{**}} = \left(1 - \frac{I_2}{I_1} \frac{u_\tau}{u_m} \right), \end{aligned} \right\} \quad (11)$$

and also

$$Re_m^{**} = \frac{\delta_m^{**} u_m}{\nu} = \alpha \frac{I_1 - \frac{u_\tau}{u_m} I_2}{\eta_l \sqrt{1 + 0,5 A \eta_l}},$$

where

$$I_1 = \int_0^1 \psi d\eta, \quad I_2 = \int_0^1 \psi^2 d\eta.$$

For further calculations it is necessary to determine the value

of the empirical constant of α . With this target/purpose let us compare the calculated and experimental distributions of velocities near wall. From the considerations of similarity, it follows that with small downstream pressure gradients in the slipstream the velocity profile must be depicted as the dependence of form $\frac{u}{u_\tau} = f\left(\frac{yu_\tau}{\nu}\right)$, called, the "law of wall". On the other hand, on the basis of formulas (2) and (9) it is possible to write

$$\frac{u}{u_\tau} = \frac{\alpha^2}{\tau_{ll} Re_l} + \int_{\tau_{ll}}^{\eta} \frac{\delta_m}{l} V^{\tau/\tau_m} d\eta$$

or at the low values of y , when $l = 0,4y$,

$$\frac{u}{u_\tau} = \alpha - \ln \alpha + \ln \frac{yu_\tau}{\nu}.$$

Thus, for determining the constant α it is necessary to find value u/u_τ or yu_τ/ν in the point of intersection of the direct/straight $\frac{u}{u_\tau} = \frac{yu_\tau}{\nu}$ and experimental velocity profile in the turbulent part of the boundary layer near the wall, presented in the form $\frac{u}{u_\tau} = f\left(\frac{yu_\tau}{\nu}\right)$. Such constructions, made in work [6] for a usual boundary layer, showed that the constant α can be accepted equal to 10-10.5.

Page 91.

Analogous constructions for the jet near the wall with the use of experimental data of work [10] confirmed the possibility of use in the jets of the same value α near the wall that and for a usual

boundary layer. It turned out that parameter B in all range of its change does not in practice affect the distribution of the velocities in immediate proximity of wall.

On the given above formulas were carried out the calculations of the dependences, relating the local characteristics of the boundary layer near the wall, necessary for the closing/shorting of integral relationship/ratios (1). For an example Fig. 2, shows the Reynolds number effect Re_m^{**} and of parameter B on the skin friction coefficient and the parameter H_m in the case of the slipstream with zero downstream pressure gradient ($A=0$). Parameter B in all range of its change has unessential effect on boundary layer characteristics (not more than 5-60/o for c_f and 2-30/c for H_m). Taking into account the degree of approximation of the developed/prcessed calculation method, it is possible to disregard this effect and to determine all the boundary layer characteristics on the assumption that $A+B=0$.

Comparison showed that the dependences, designed with the use of polynomials of fourth degree (5a) and of square (5b), virtually coincide.

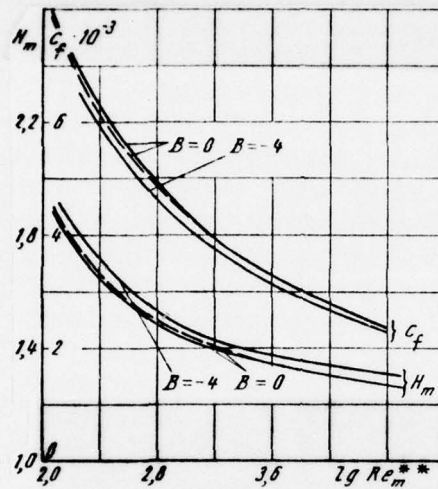


Fig. 2. — polynomial (5a), - - polynomial (5b).

Page 42.

In connection with this for the calculation of the boundary layer near the wall can be used the interpolation formulas, obtained in work [6] on the basis of approximation (5b) for the usual boundary layers:

$$\begin{aligned}
c_f &= c_{f0} [1 + b_1 f + c_1 (e^{d_1 f} - 1)], \quad c_{f0} = 2c \operatorname{Re}_m^{*-0.17}; \quad (12) \\
c &= 0,001 [6,55 - 0,0685 (\lg \operatorname{Re}_m^{**} - 4,4) + 0,2506 (\lg \operatorname{Re}_m^{**} - 4,4)^2]; \\
b_1 &= 0,2814 - 0,036 \lg \operatorname{Re}_m^{**} + 36 (\lg \operatorname{Re}_m^{**})^{-4.5}; \\
c_1 &= 0,1185 \lg \operatorname{Re}_m^{**} - 0,262; \\
d_1 &= 0,585 - 0,125 \lg \operatorname{Re}_m^{**} + 20,4 (\lg \operatorname{Re}_m^{**})^{-1.75}; \\
H_m &= H_0 (1 - kf) - 0,019 f e^f \lg \operatorname{Re}_m^{**}; \quad (13) \\
H_0 &= 1,251 - 0,0131 \lg \operatorname{Re}_m^{**} + 5,35 (\lg \operatorname{Re}_m^{**})^{-2.85}; \\
k &= 0,28 - 0,034 \lg \operatorname{Re}_m^{**} + (0,1 \lg \operatorname{Re}_m^{**})^3,
\end{aligned}$$

where

$$\begin{aligned}
\operatorname{Re}_m^{**} &= \frac{u_m \delta_m^{**}}{\nu}, \quad \delta_m^{**} = \int_0^{\delta_m} \bar{u} (1 - \bar{u}) dy, \quad \delta_m^* = \int_0^{\delta_m} (1 - \bar{u}) dy, \quad \bar{u}_m = \frac{u_m}{u_0}, \\
f &= \frac{2 \operatorname{Re}_m^{**}}{c_{f0}} \frac{1}{\operatorname{Re}} \frac{\bar{u}_\delta \bar{u}'_\delta}{\bar{u}_m^3}, \quad \operatorname{Re} = \frac{u_0 \delta_0}{\nu}, \quad \bar{u} = \frac{u}{u_m}, \quad \bar{u}_\delta = \frac{u_\delta}{u_0}, \quad H_m = \frac{\delta_m^*}{\delta_m^{**}}.
\end{aligned}$$

In work [6] it was shown, that the velocity profiles, obtained on the basis of the use of approximation (5b), were close to exponential with index $n = \frac{H_m - 1}{2}$. Therefore for determining communication/connection between δ_m and δ_m^{**} it is possible to use the relationship/ratio

$$\delta_m^{**} = \delta_m \frac{H_m - 1}{H_m (H_m + 1)}. \quad (14)$$

The exterior of the jet. For performance calculation of flow in the exterior $y > \delta_m$ of the semi-bounded jet, let us present the

airfoil/profile of shearing stress in the form of polynomial from variable $\eta_1 = \frac{y - \delta_m}{\delta - \delta_m} = \frac{y - \delta_m}{\delta_1}$ (see [7]):

$$\tau = \sum_{i=0}^n a_i \eta_1^i. \quad (15)$$

The coefficients of the polynomial let us determine from the boundary conditions

$$\tau = 0, \quad \frac{\partial \tau}{\partial y} = \rho(u_m u'_m - u_\delta u'_\delta) \text{ when } y = \delta_m (\eta_1 = 0),$$

$$\tau = 0, \quad \frac{\partial \tau}{\partial y} = 0 \text{ with } y = \delta (\eta_1 = 1).$$

As a result we will obtain

$$\tau = \rho(u_m u'_m - u_\delta u'_\delta) \delta_1 \eta_1 (1 - \eta_1)^2. \quad (16)$$

On the other hand, according to Prandtl's formula, in the exterior of the semi-bounded jet

$$\tau = \rho \delta_1 (u_m - u_\delta) \frac{\partial u}{\partial y}. \quad (17)$$

After equating the right sides of expressions (16) and (17), after integration and simple transformations, we will obtain the expression of the profile of velocity

$$u = u_\delta + (u_m - u_\delta)(1 - 6\eta_1^2 + 8\eta_1^3 - 3\eta_1^4), \quad (18)$$

and also the relationship/ratio

$$(u_m u'_m - u_\delta u'_\delta) \delta_1 = -12 \times (u_m - u_\delta)^2, \quad (19)$$

establish/installing communication/connection between u_m , δ_m and δ .

As in the case of flat/plane free turbulent jet in the slipstream with pressure gradient [7], it is constant $\alpha = 0.01$.

Page 43.

Transformation of system of equations. Thus, for performance calculation of the flat/plane semi-bounded jet we obtained three differential equations: (1) and (19). We convert these equations to the dimensionless form:

$$\left. \begin{aligned} \frac{dRe_m^*}{dx} &= \frac{1}{2} Re_m^* c_f - \frac{Re_m^* H_m + 1}{u_m^2 H_m - 1} \left[12 \times \frac{(\bar{u}_m - \bar{u}_\delta)^2}{\bar{\delta}_1} + (H_m - 1) \bar{u}_\delta \bar{u}'_\delta \right]; \\ \frac{du_m}{dx} &= \frac{\bar{u}_\delta \bar{u}'_\delta}{u_m} - 12 \times \frac{(\bar{u}_m - \bar{u}_\delta)^2}{u_m \bar{\delta}_1} \left(\bar{x} = \frac{x}{\bar{\delta}_0}, \bar{u}_m = \frac{u_m}{u_0}, \bar{u}_\delta = \frac{u_\delta}{u_0}, \bar{\delta}_1 = \frac{\delta_1}{\bar{\delta}_0} \right); \\ \frac{d\bar{\delta}_1}{dx} &= 12 \times \frac{\bar{u}_m - \bar{u}_\delta}{u_m} \Phi_1 - \bar{\delta}_1 \frac{\bar{u}'_\delta}{u_m} \Phi_2, \end{aligned} \right\} \quad (20)$$

where

$$\Phi_1 = \frac{0.1034 \bar{u}_m - 0.0426 \bar{u}_\delta}{0.0535 \bar{u}_m + 0.0608 \bar{u}_\delta}, \quad \Phi_2 = \frac{0.0680 \bar{u}_m + 0.0462 \bar{u}_\delta}{0.0535 \bar{u}_m + 0.0608 \bar{u}_\delta}.$$

Thus, the problem of the calculation of the flat/plane semi-bounded jet is reduced to the solution of the system of three

differential equations (20), solved relative to derivatives of three unknown functions. Those entering the system of equations of value c_f and H_m are expressed as the unknown functions with the aid of formulas (12) and (13). In the general case the system of equations (20) can be solved numerically ~~by~~ ^{on the} computer. In this case, they must be assign/prescribed Reynolds number $Re = \frac{u_0 \delta_0}{\nu}$, the dependence of the velocity of external flow u_0 on the longitudinal coordinate x and the characteristic of jet in initial section with $\bar{x} = \bar{x}_0$:

$$\bar{u}_m = \bar{u}_{m0}, \quad \bar{\delta}_1 = \bar{\delta}_{10}, \quad Re_m^* = Re_{m0}^*.$$

The distinctive special feature/peculiarity of the system of differential equations (20) is that that the parameters of the exterior of the jet δ_1 and u_m can be found independent of the parameters of its part near the wall. This fact is caused by the special selection of second integral relationship/ratio (1). Thus, for the calculation of the exterior of the semi-bounded jet on its basic section may be used the known solutions of the problem of the propagation of free turbulent jet in the slipstream with downstream pressure gradient. This conclusion does not contradict the available experimental data.

Comparison of the results of calculation and experiment. The comparison of the data of calculation and experiment for the semi-bounded jet hinder/hampered by the ambiguity of flow conditions in the boundary layer near the wall - here with comparatively small

Reynolds numbers flow can be laminar not only within the limits of viscous sublayer, but also in an entire part of jet [11] near the wall. Let us give the results of this comparison for the flooded jets near the wall and the jets near the wall in cocurrent gradient-free (Fig. 3) and gradient (Fig. 4 and 5) flows. In all cases the results of the calculation of velocity u_m and of the transverse size/dimensions of jet $\delta_{1/2}$ and δ_m sufficiently satisfactorily will agree with experimental data.

As concerns the comparison of the calculated and experimental values of local skin friction coefficient, it is here necessary to note following. The experimental values c_f at the fixed values of Reynolds number for the gradient-free jets near the wall, according to different investigations, it is dismantled approximately to 20-25%, the high values c_f corresponding to the flooded jets less - to jets in slipstream [10].

Page 44.

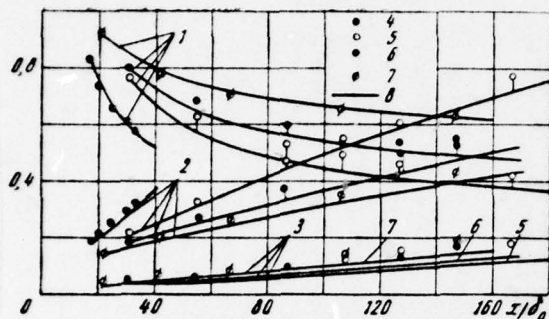


Fig. 3.

1 - u_m/u_0 ; 2 - $0.1 (\delta_{1/2}/\delta_0)$; 3 - $0.1 (\delta_m/\delta_0)$; 4 - $u_\delta/u_0 = 0$, $Re = 5 \cdot 10^4$ [12]; 5 - $u_\delta/u_0 = 0.197$, $Re = 2.02 \cdot 10^4$ [5]; 6 - $u_\delta/u_0 = 0.333$, $Re = 2.02 \cdot 10^4$ [5]; 7 - $u_\delta/u_0 = 0.487$, $Re = 1.745 \cdot 10^4$ [5]; 8 - расчет (1)

Key: (1). calculation.

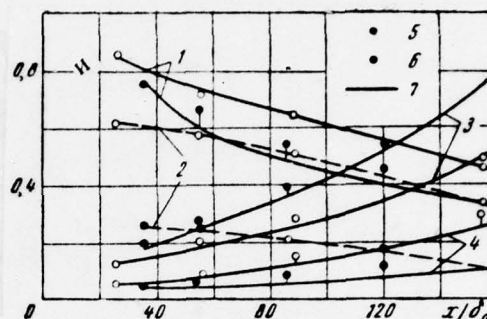


Fig. 4.

1 - u_m/u_0 ; 2 - u_δ/u_0 ; 3 - $0.1 (\delta_{1/2}/\delta_0)$; 4 - $0.1 (\delta_m/\delta_0)$; 5 - $Re = 3 \cdot 10^4$ [5]; 6 - $Re = 2.3 \cdot 10^4$ [5]; 7 - расчет (1)

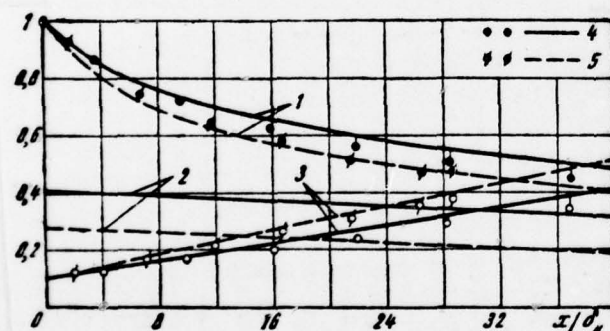


Fig. 5.

1 - u_m/u_{mH} ; 2 - u_δ/u_{mH} ; 3 - δ/δ_m ; 4 - $Re_{mH} = \delta_H u_{mH}/\nu = 1.93 \cdot 10^4$ [13]; 5 - $Re_{mH} = 3.55 \cdot 10^4$ [13].

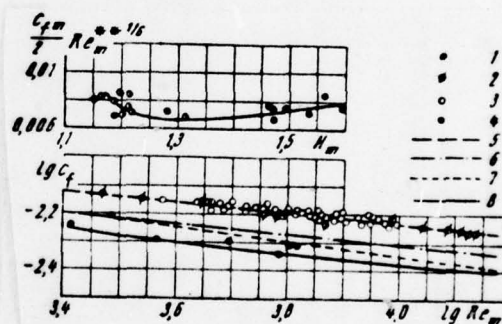


Fig. 6.

Fig. 6. 1 - $m_0 \neq 0$ [5]; 2 - $m_0 = 0$, Preston's tube [10]; 3 - $m_0 = 0$, weight measurements [8]; 4 - $m_0 = 0$, experiments of authors and K. A. Pochkinoy; 5 - $m_0 = 0$, empirical formula [10]; 6 - $m_0 \neq 0$, empirical

formula [10]; 7 - $\alpha_0=0$, calculation of Glauert [10]; 8 - calculation according to proposed method.

Page 45.

Fig. 6, gives calculated dependence $\frac{1}{2} c_f (Re_m^*)^{1/6} = \varphi(H_m)$, to the law of friction for a flat/plane plate, and experimental data for the flooded jet (experiences in the authors of present article and K. A. Pochkinoy) near the wall and the jet in the slipstream (experiences in Nicol [5]). Here convergence should consider satisfactory.

On the lower curve/graph Fig. 6, are compared calculated and experimental dependences $c_f(Re_m)$ for flooded jets $\left(Re_m = \frac{u_m \delta_m}{\nu} \right)$. Near the wall Here is detected disagreement indicated above. In this case, experiences in the authors and K. A. Pochkinoy satisfactorily will agree with the results of calculation.

Thus, the method presented makes it possible to calculate the flat/plane turbulent semi-bounded jet for all its extent/elongation from nozzle exit section to its degeneration into the usual boundary layer when $\frac{u_m}{u_b} \rightarrow 1$, or, in the case of diffuser slipstream, before the section where occurs flow breakaway, i.e., $c_f=0$. This method easily is spread to the case of the axisymmetric jet near the wall on body of

revolution or in the walls of axisymmetric channel, and also to the case of the radial jet near the wall.

REFERENCES.

1. G. N. Abramovich. Theory of turbulent jets. M., Fizmatgiz, 1960.

2. N. I. Akatnov. the propagation of flat/plane turbulent jet along solid, smooth and rough surface. "Proceedings of the AS USSR, CTN, mechanics and machine-building", 1960, No 1.

3. R. Ville, G. Ferngol'ts. Report/communication about first European colloquium of the mechanics, dedicated to effect Coanda. Coll. of translation/conversions "mechanics", 1966, NO 5 (99).

4. D. B. Spaulding. Some application/appendices of the new method of calculation of turbulent boundary layer. Coll. "heat- and mass transfer", T. 1. M., "energy", 1968.

5. I. S. Gartshore, E. G. Newman. The turbulent wall jet in an arbitrary pressure gradient. The Aeronautical Quarterly, v XX, p 1, February, 1969.

6. K. K. Fedyaevskiy, A. V. Wheelwrights, A. N. Smol'yaninova. On the calculation of turbulent boundary layer with downstream pressure gradient the transactions of TsAGI, iss. 1088, 1967.
7. A. S. Ginevskiy. Theory of turbulent jets and traces. M., "machine-building", 1969.
8. J. Mathieu. Ecoulement parletaux. J de Mecanique, v 8, No 1, 1969.
9. A. Tailland, J. Mathieu. Jet parletal. J de Mecanique, v 6, No 1, 1967.
10. P. Bradshaw, M. T. Gee. Turbulent wall jet with and without an external strim. ARC r and M, 1962, No 3252.
11. L. A. Bulis, V. E. Kashkarov. Theory of the jets of viscous fluid. M., "science", 1965.
12. E. Portman. Uber turbulente Strahlatsbreitung. Ingenieur-Archiv, 1934, B 5.
13. K. Weinhold. Untersuchung von Wandstrahlen bet ruhender und bewegter Aubenstromung chne und mit Druckanstieg. Mecanique

DOC = 78103903

PAGE 2 /07

appliquee, t 12, No 1, 1967.

14. Fadel F Erian. Influence of pressure gradient on turbulent flows with asymmetric mean velocity. Trans. ASME, E 36, No 4, 1969.

The manuscript entered 11/11 1969.

Page 46.

CALCULATION BY THE METHOD MONTE-CARLO OF HEAT FLOW BETWEEN PARALLEL PLATES IN THE RAREFIED GAS.

V. I. Vlasov.

With the aid of computers is designed the heat flow in the relations of the temperatures of plates $\theta=1.5; 4; 16; 100$ and Knudsen's numbers $Kn=0.2; 0.5; 2; 10$. The model of molecules - elastic spheres whose section is inversely proportional to relative velocity before the collision. For such molecules, as for Maxwellian, the viscosity of gas is proportional to temperature. Method consists in the performing of the random wanderings of one test molecule among field molecules, minimally necessary quantity of which it render/showed equal to approximately $100/Kn$. In each small geometric cell was memorized the field molecular velocity which was changed according to the specific rule, which provided the representation of an entire distribution function. Are given the density profiles and temperature.

The proposed in article method is the development of the method

of Monte-Carlo, described in works [1] and [2]. During the use of this method, is outlined the motion of one molecule during the function of distribution memorized from the preceding/previous iteration. The essential deficiency/lack, which limits its application/use, is the large capacity of necessary machine storage, since distribution function depends on several variables. In the work of author [3] is suggested the improvement, which allows in each geometric cell instead of distribution function to memorize the velocity of one molecule. This method was illustrated by the flow construction of heat between plates with the relation of the temperatures of plates $\frac{T_1}{T_2} = 4$ and Knudsen's number $Kn=0.5$. However, as a result of insufficient correct method of the selection of the memorized velocities in practical calculation it was necessary in each geometric cell to memorize as the minimum of 7 velocities. In this article is examined the method, by which this incorrectness of the selection of molecules is removed and in each geometric cell (layer) is memorized in accuracy/precision one molecular velocity. Method of applying the temperatures of plates (from 1.5 to 100) and of Knudsen's numbers (from 0.2 to 10).

Page 47.

Essence of method.

Let us assume that the monatomic gas, included between parallel planes, consists of the molecules, which interact in such a way that

a) the complete effective collision cross-section of two molecules with speeds $\vec{\xi}$ and $\vec{\xi}_1$ is equal

$$\sigma = \frac{\sigma_0}{g}, \quad (1)$$

where $\sigma_0 = \text{const}$ and $g = |\vec{\xi} - \vec{\xi}_1|$ - relative velocity of the molecules before the collision;

b) the velocities of molecules after collision can be defined what velocities of the elastic spheres:

$$\vec{\xi}' = 0,5(\vec{\xi} + \vec{\xi}_1 + g\vec{e}), \quad \vec{\xi}'_1 = 0,5(\vec{\xi} + \vec{\xi}_1 - g\vec{e}), \quad (2)$$

where \vec{e} - the random vector, evenly distributed on the surface of single sphere.

In order to explain the physical content of this model of intermolecular interaction, let us give the coefficient of the viscosity of this gas, obtained according to Chapman-Enskog's method:

$$\mu = \frac{2kT}{\sigma_0}, \quad (3)$$

where k - Boltzmann constant, T - temperature of gas. Since the coefficient of viscosity is proportional to temperature, then the

proposed model of molecules is analogous Maxwellian and it is possible to call/name the model of Maxwellian spheres.

Let us designate the temperature of the hot and cold plates through T_1 and T_2 , the numerical density of the gas through n , average density - n_0 , the velocity distribution function of molecules - $f(x, \vec{\xi})$, the distance between plates - d . Let us assume that axis x is perpendicular to plates. Space between planes let us break into N of narrow layers with a thickness of $h=d/N$. The parameters of gas within layer let us consider constants. With the aid of computers we design the motion of one test molecule against the background of field molecules. The collision rate of molecule $\vec{\xi}$ is equal to

$$N_{cr} = \int \sigma g f(\vec{\xi}_1) d\vec{\xi}_1 = \sigma_0 n, \quad (4)$$

i.e. for the model of molecules accepted it does not depend on distribution function.

Page 48.

The probability of colliding the molecule within layer is equal to $\frac{\sigma_0 nh}{|\vec{\xi}_x|}$. Let us assume that the test molecule must clash in this layer with some field molecule $\vec{\xi}_1$. Then velocity $\vec{\xi}_1$ must be selected in accordance with probability density

$$\frac{\sigma g f(\vec{\xi}_1)}{N_{cr}} = \frac{f(\vec{\xi}_1)}{n}. \quad (5)$$

In order to manage without itself the memorization of the function of distribution $f(\vec{\xi})$, let us note following. Probability that the molecule, entering the layer, has velocity $\vec{\xi}$, is proportional to value $|\xi_x| f(\vec{\xi})$. Probability that the molecule, which collides in layer, has velocity $\vec{\xi}$, is proportional to value

$$\frac{|\xi_x| f(\vec{\xi}) \sigma_0 n h}{|\xi_x|} \sim f(\vec{\xi}). \quad (6)$$

Comparing expressions (5) and (6) we see that it is possible to enter as follows: during each collision of test molecule $\vec{\xi}$ to memorize its velocity in the appropriate layer, and as velocity $\vec{\xi}$ for formula (2) to take the velocity, memorized during the preceding/previous collision in this layer. Thus, in each geometric cell instead of distribution function it is necessary to memorize the density of gas and the velocity of the clashing molecule.

Density field is previously unknown; therefore calculation we conduct according to iterations. As initial approach/approximation we take free molecular state of the gas. Reflection of molecules from wall diffuse with the temperature of wall. Knudsen's number

$$Kn = \frac{3 \left(\frac{p_0}{2m} \right)^{1/2}}{\sigma_0 n_0^{3/2} d},$$

where m - molecular mass, $p_0 = n_0 k \sqrt{T_1 T_2}$ - pressure gas in free

molecular state.

Results of calculation.

To the relation of the temperatures of plates $\theta = T_1/T_2$ during the variation of the parameters were given values by 1.5; 4; 16 and 100, but to Knudsen's number value 0.2; 0.5; 2 and 10. Table gives the flow values of the heat q , in reference to value q_0 in free molecular state of the gas:

$$q_0 = 2kn_0 \left(\frac{2kT_1T_2}{\pi m} \right)^{1/2} (\sqrt{T_1} - \sqrt{T_2}).$$

through q_1 is designated the heat flow, designed with the description of 2000 velocities of field molecules, q_2 - with the description of 500 velocities, q_3 - a precise value of heat flow for model kinetic equation [4, 5], q_4 - heat flow in the approach/approximation of Navier-Stokes with temperature jump on wall [4]. For q_1 and q_2 are shown the error bounds.

Page 49.

As can be seen from table, numerical results will agree well with the data of the exact solution of model equation, and for the moderate values θ and Kn and with results in the approach/approximation of Navier-Stokes.

Fig. 1 and 2, compare the density profiles and temperature of gas for the calculation conducted and for the equations of Nav'ye - Stokes with $\theta=1.5$ and $Kn=0.2$ and 0.5 .

Fig. 3-8, gives the density profiles and temperature for the remaining calculated cases. It was revealed/detected that for this problem of iteration they converge very rapidly. With $\theta=1.5$ all iterations, beginning with the first, they differed only in terms of random fluctuations. With $\theta=4$ and 16 virtually coincided the iterations, beginning with the second, and for $\theta=100$ - with the third.

η	(1) Принятые обозначения потока тепла	(2) Величины потока тепла			
		$Kn=0,2$	$Kn=0,5$	$Kn=2$	$Kn=10$
1,5	q_1	$0,44 \pm 0,01$	$0,63 \pm 0,01$	—	—
	q_4	0,44	0,62	—	—
4	q_1	$0,48 \pm 0,01$	$0,66 \pm 0,01$	$0,86 \pm 0,01$	$0,96 \pm 0,01$
	q_2	$0,47 \pm 0,01$	$0,67 \pm 0,01$	$0,86 \pm 0,02$	$0,96 \pm 0,02$
	q_3	0,50	0,70	0,87	0,97
	q_4	0,53	0,73	—	—
16	q_1	$0,66 \pm 0,01$	$0,80 \pm 0,01$	$0,93 \pm 0,01$	$0,99 \pm 0,01$
	q_2	$0,66 \pm 0,01$	$0,79 \pm 0,01$	$0,95 \pm 0,01$	$0,99 \pm 0,02$
	q_3	0,68	0,82	0,94	0,99
100	q_1	$1,24 \pm 0,03$	$1,14 \pm 0,02$	$1,05 \pm 0,01$	$1,02 \pm 0,01$
	q_2	$1,20 \pm 0,03$	$1,14 \pm 0,02$	$1,05 \pm 0,01$	$1,02 \pm 0,02$
	q_3	1,25	1,18	1,07	1,02

Key: (1). Adopted designations of heat flow. (2). Flow values of heat.

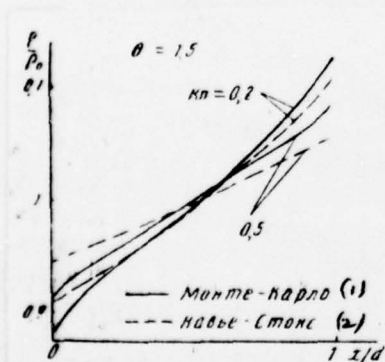


Fig. 1.

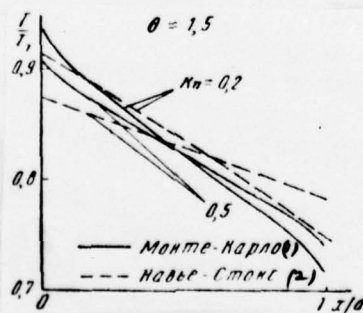


Fig. 2.

Key: (1). Monte-Carlo. (2). Navier-Stokes.

Page 50.

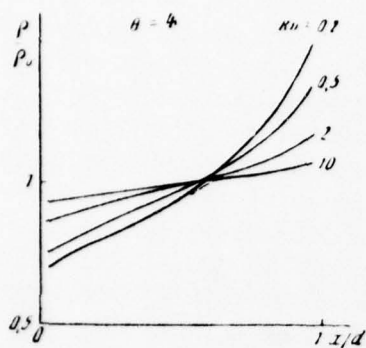


Fig. 3.

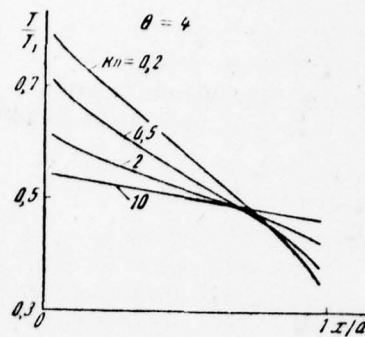


Fig. 4.

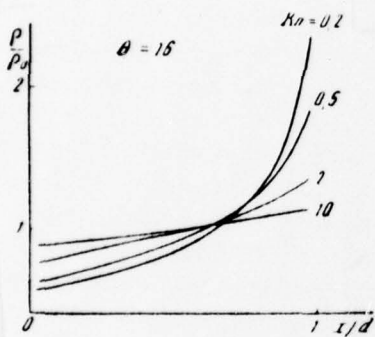


Fig. 5.

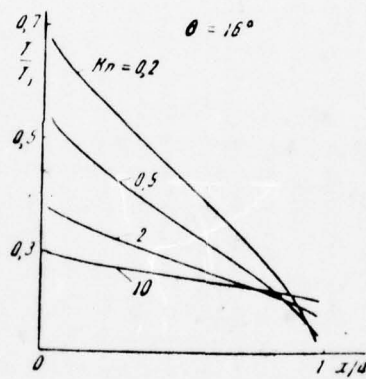


Fig. 6.

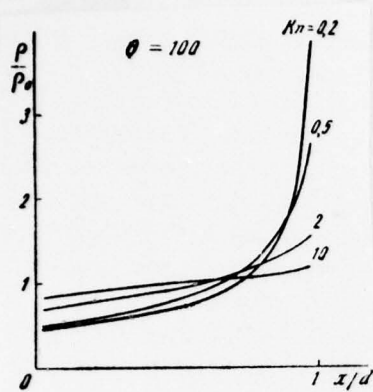


Fig. 7.

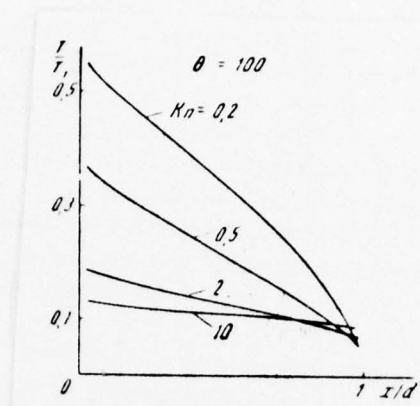


Fig. 8.

Page 51.

With $\theta=10^4$ attempts at the calculation by this method failed. Gradual deterioration in the convergence with an increase in the relation of the temperatures of plates is connected with the increase of the role of the rare molecules, which fly off from hot plate at small angles to it. The minimum quantity of memorized molecular velocities, necessary for accuracy/precision 2-3%, rendered/showed equal to approximately $100/Kn$.

REFERENCES

1. J. K. Naviland, M. L. Lavin. Application of the Monte Carlo method to heat transfer in a rarefied gas. The Phys. of Fluids, v 5,

№ 11, 1962.

2. J. K. Naviland. The solution of two molecular flow problems by the Monte Carlo method. Methods in computational physics, New York, 1965.

3. V. I. Vlasov. Improvement in the method of statistical testings (Monte Carlo) for the calculation of flows of rarefied gas. Reports of the PAS of the USSR, Vol. 167, № 5, 1966.

4. M. N. Kogan. Dynamics of the rarefied gas. M., "science", 1967.

5. D. R. Willis. Heat transfer in a rarefied gas between parallel plates at large temperature ratios. Rarefied Gas Dynamics. Third Symp., v 1, Acad. Press. New York - London, 1963.

The manuscript entered 11/VII 1969.

Page 52.

INTERACTION OF FAST PARTICLES WITH SOLID SURFACE.

A. I. Yerofeyev.

Is examined interaction of the atom of gas with linear harmonic oscillator and interaction of the atom of gas with solid surface, been simulated by the semi-infinite lattice of the elastic connected atoms. Assuming that the time of interaction is small in comparison with the period of oscillation of oscillator or in comparison with the characteristic time of the fluctuation of atom in lattice, for the solution of problem, is used the method of the asymptotic spliced expansions. The obtained results for the accommodation coefficient of energy are compared with the results of the numerical solution of problems. Is obtained the asymptotic estimation of the applicability of assumption about the single collision of the atom of gas with oscillator and with surface atom.

Is examined interaction of the atom of gas with the atom,

elastic that connected with its position of equilibrium (linear harmonic oscillator), and interaction of the atom of gas with solid surface, been simulated by the semi-infinite lattice of the elastic connected atoms. By the force of assumption about the fact that the characteristic time of interaction is small in comparison with the characteristic time of the fluctuation of oscillator or surface atom, for the solution of problem, is used the method of the asymptotic spliced expansions. Analogous method was applied in work [1] for the solution of the problem of cooperating the atom of gas with the linear array of the elastic connected atoms. The methods of perturbation theory were applied also in works [2], [3]. However, method of operation [3] in the case high velocities of the atom of gas, is valid, when the ratio of the masses of the atom of gas and atom of lattice $\mu \rightarrow 0$, in works [1] [2] strict estimation of the applicability of methods given.

In the present work is obtained the asymptotic estimation of the applicability of assumption about the single collision of the atom of gas with oscillator or with surface atom. The obtained results for the accommodation coefficient of energy are compared with the results of the numerical solution of problems.

§1. Interaction with harmonic oscillator.

Let us examine interaction of the atom of gas of mass m with the atom of solid body of mass M . The atom of body is represented by harmonic oscillator. The force of interaction between atoms let us describe by the potential of the repulsion

$$U(r) = De^{-ar}, \quad (1.1)$$

where r - distance between particles a , D - parameters.

Equations of motion take the form (Fig. 1):

$$m \ddot{\tilde{x}}_1 = aDe^{-a(\tilde{x}_1 - \tilde{x}_2)}; \quad M \ddot{\tilde{x}}_2 + k\tilde{x}_2 = -aDe^{-a(\tilde{x}_1 - \tilde{x}_2)}; \quad (1.2)$$

the initial conditions:

$$\dot{\tilde{x}}_1(-\infty) = -V_0; \quad \tilde{x}_2(-\infty) = \dot{\tilde{x}}_2(-\infty) = 0.$$

Time $\tilde{t} = -\infty$ corresponds to the state of system before interaction, $\tilde{t} = +\infty$ - to a state at the termination of interaction. Let us introduce the characteristic linear dimension $l = 1/a$ and characteristic time $\tau = 1/aV_0$. Utilizing these values for making dimensionless of system, we obtain $t = aV_0\tilde{t}$, $x = a\tilde{x}$,

$$\begin{cases} \ddot{x}_1 = \varepsilon e^{-(x_1 - x_2)}; & \ddot{x}_2 + k^2 x_2 = -\mu \varepsilon e^{-(x_1 - x_2)}; & \dot{x}_1(-\infty) = -1; \\ x_2(-\infty) = \dot{x}_2(-\infty) = 0. \end{cases} \quad (1.2')$$

In equations (1.2')

$$\mu = \frac{m}{M}, \quad \varepsilon = \frac{D}{m V_0^2}, \quad k^2 = \frac{\omega_0^2}{a^2 V_0^2}, \quad \omega_0^2 = \frac{\kappa}{M} \quad (1.3)$$

ω_0 - natural frequency of oscillator.

Let us examine the case when $k^2 \ll 1$. Physically this means that the characteristic time of interaction $\tau \approx 1/aV_0$ is small in comparison with the period of oscillation of atom $M(T=2\pi/\omega_0)$. Let us search for the solution of system (1.2') in the form

$$x_1 = x_0 + k^2 x_{11} + k^4 x_{12} + \dots; \quad x_2 = x_{20} + k^2 x_{21} + k^4 x_{22} + \dots \quad (1.4)$$

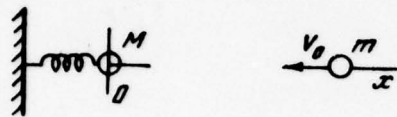


Fig. 1.

Page 54.

Substituting (1.4) and (1.2') and equating the coefficients of the identical degrees of k , we have:

in the first approximation,

$$\ddot{x}_{10} = \varepsilon e^{-(x_{10}-x_{20})}, \quad \ddot{x}_{20} = -\mu \varepsilon e^{-(x_{10}-x_{20})}; \quad (1.5)$$

In the second approach/approximation

$$\begin{aligned} \ddot{x}_{11} &= -\varepsilon e^{-(x_{10}-x_{20})} (x_{11}-x_{21}), \quad \ddot{x}_{21} + x_{20} = \\ &= \mu \varepsilon e^{-(x_{10}-x_{20})} (x_{11}-x_{21}). \end{aligned} \quad (1.5')$$

and so forth. Initial conditions let us write in the form

$$\begin{aligned} x_{10}(-\infty) &= -1; \quad x_{1j}(-\infty) = 0; \quad x_{2j}(-\infty) = x_{20}(-\infty) = 0; \\ (j &= 1, 2, \dots, \quad j=0, 1, 2, \dots). \end{aligned} \quad (1.6)$$

As it will be shown further, the selection of initial conditions in the form (1.6) provides the unique that obtained from (1.5) solution with solution on other time/temporary scale (connected with u_0).

It is not difficult to see that the system of equations (1.5') describes interaction of free particles. Utilizing initial conditions from (1.6) we obtain:

$$\left. \begin{aligned} \dot{x}_{10}(t) &= \frac{2}{1+\mu} \frac{1}{1+e^{-t}} - 1; \\ \dot{x}_{20}(t) &= -\frac{2\mu}{1+\mu} \frac{1}{1+e^{-t}}; \\ x_{20}(t) &= -\frac{2\mu}{1+\mu} \ln(1+e^t); \\ x_{10}(t) &= \frac{2}{1+\mu} \ln(1+e^t) - t + \ln \frac{\varepsilon(1+\mu)}{2}; \\ \varepsilon e^{-(x_{10}-x_{20})} &= \frac{1}{2(1+\mu)} \operatorname{sch}^2\left(\frac{t}{2}\right). \end{aligned} \right\} \quad (1.7)$$

With $t \rightarrow x_{10} = 1 - \mu/1 + \mu$, $x_{20} = -2\mu/1 + \mu$. Substituting solution (1.7) in (1.5''), we obtain with $t \rightarrow$:

$$\left. \begin{aligned} \dot{x}_{11}(t) &= \frac{2\mu}{(1+\mu)^2} \frac{\pi^2}{3}; \\ \dot{x}_{21}(t) &= \frac{2\mu}{1+\mu} \left(\frac{1-\mu}{1+\mu} \frac{\pi^2}{6} + \frac{t^2}{2} \right); \\ x_{21}(t) &= \frac{2\mu}{1+\mu} \left(\frac{1-\mu}{1+\mu} \frac{\pi^2}{6} + t + \frac{t^3}{6} + \frac{2\mu}{1+\mu} C \right); \\ x_{11}(t) &= \frac{2\mu}{(1+\mu)^2} \left(\frac{\pi^2}{3} t - 2C \right), \end{aligned} \right\} \quad (1.8)$$

where

$$C = \frac{\pi^2}{3} + \sum_{n=1}^{\infty} (-1)^{n+1} \frac{1}{n^3} + 2 \sum_{n=1}^{\infty} (-1)^{n+1} \frac{1}{(n+1)^3} \sum_{l=1}^n \frac{1}{l}. \quad (1.9)$$

Solution $x_{11}(t)$, $x_{21}(t)$, $\dot{x}_{11}(t)$, $\dot{x}_{21}(t)$ for any moment of time we do not extract due to their unwieldiness. Let us note just in the second approach/approximation of coordinate and velocity they vanish exponentially with $t \rightarrow \infty$.

Page 55.

Let us show that the particle speed in the third approach/approximation with $t \rightarrow \infty$ can be obtained that without solving equation (1.5) for this approach/approximation. Let us examine the law of conservation of the energy:

$$\frac{m \tilde{x}_1^2}{2} + \frac{M}{2} (\tilde{x}_2^2 + \omega_0^2 \tilde{x}_2^2) + D e^{-a(\tilde{x}_1 - \tilde{x}_2)} = \frac{m V_0^2}{2} \quad (1.10)$$

or in a dimensionless form

$$\dot{x}_1^2 + \frac{1}{\mu} (\dot{x}_2^2 + k^2 x_2^2) + 2\epsilon e^{-(x_1 - x_2)} = 1. \quad (1.10')$$

Substituting here expansion (1.4) and equalizing the coefficients of the identical degrees of k , we will obtain:

for the first approximation

$$\dot{x}_{10}^2 + \frac{1}{\mu} \dot{x}_{20}^2 + 2\epsilon e^{-(x_{10} - x_{20})} = 1; \quad (1.11)$$

for the second approach/approximation

$$2\dot{x}_{11}\dot{x}_{10} + \frac{1}{\mu} (2\dot{x}_{21}\dot{x}_{20} + \dot{x}_{20}^2) - 2\epsilon e^{-(x_{10} - x_{20})} (x_{11} - x_{21}) = 0 \quad (1.11')$$

and so forth. But with $t \rightarrow \infty$ from (1.7) we have $\varepsilon \exp - (x_{10} - x_{20}) \rightarrow 0$ as e^{-t} . Then in relationship/ratios (1.11) for the n -th approach/approximation remain only terms \dot{x}_{1n} and \dot{x}_{2n} . The second equation, which relates \dot{x}_{1n} and \dot{x}_{2n} , can be obtained by the integration of equations of motion (1.5), and this equation also is not included values x_{1n} and x_{2n} . This makes it possible to determine \dot{x}_{1n} and \dot{x}_{2n} with $t \rightarrow \infty$, without solving system (1.5) in the n approach/approximation, using results $(n-1)$ -th of approach/approximation.

Utilizing the described procedure for obtaining the third approach/approximation, we obtain finally for velocities \dot{x}_1, \dot{x}_2 with $t \rightarrow \infty$:

$$\left. \begin{aligned} \dot{x}_1(t) &= \frac{1-\mu}{1+\mu} + k^2 \frac{2\mu}{(1+\mu)^2} \frac{\pi^2}{3} - k^4 \left[\frac{4\mu}{(1+\mu)^3} \frac{7\pi^4}{360} + \right. \\ &\quad \left. + \frac{16\mu^2}{(1+\mu)^3} C_1 + \frac{4\mu}{(1+\mu)^2} \frac{\pi^4}{72} \right] + \dots; \\ \dot{x}_2(t) &= -\frac{2\mu}{1+\mu} + k^2 \frac{2\mu}{1+\mu} \left(\frac{1-\mu}{1+\mu} \frac{\pi^2}{6} + \frac{t^2}{2} \right) + \\ &\quad + k^4 \left[\frac{4\mu^2}{(1+\mu)^3} \frac{7\pi^4}{360} - \frac{8\mu^2(1-\mu)}{(1+\mu)^3} C_1 - \right. \\ &\quad \left. - \frac{4\mu^3}{(1+\mu)^2} C_1 - \frac{2\mu(1-\mu)}{(1+\mu)^2} \frac{\pi^2}{12} t^2 - \frac{2\mu}{1+\mu} \frac{t^4}{24} \right] + \dots \end{aligned} \right\} \quad (1.12)$$

where C by specific relationship (1.9), and

$$C_1 = 4.84387 \pm 0.00023. \quad (1.12')$$

Let us examine now the solutions of equations (1.2) on other scale of time, connected with ω_0 (exterior). Let us introduce

$t^* = \omega_0 \tilde{t} = kt$, $x^* = k^2 x$. Then (1.2') it is rewritten in the form

$$\left. \begin{aligned} \ddot{x}_1^* &= \mu e^{-\frac{x_1^* - x_2^*}{k^2}}; \\ \ddot{x}_2^* + x_2^* &= -\mu e^{-\frac{x_1^* - x_2^*}{k^2}}. \end{aligned} \right\} \quad (1.13)$$

Page 56.

With $k^2 \rightarrow 0$, we obtain:

$$\ddot{x}_1^* = 0; \quad \ddot{x}_2^* + x_2^* = 0, \quad (1.14)$$

whence

$$\dot{x}_1^* = \text{const}; \quad x_2^* = A^* \sin t^* + B^* \cos t^*. \quad (1.15)$$

Solution (1.15) is correct with an accuracy to any degree of parameter k , and this fact simplifies the search of solutions for internal and exteriors.

During description by equations (1.14) of particle motion before interaction we have following initial conditions for the oscillator:

$x_2(-\infty) = x_2(+\infty) = 0$. Then $A = B = 0$, and solution (1.15) is spliced with the solution of problem for interior (in alternating variable x , t) which follows from (1.7) and tendency toward zero coordinates and velocities in the second approach/approximation with $t \rightarrow -\infty$. For determining the coefficients of A and B in the termination of interaction, let us rewrite (1.15) in the variables x , t :

$$x_1 = \text{const}; \quad x_2 = A \sin(kt) + B \cos(kt). \quad (1.15')$$

With fixed/recorded t and $k > 0$ we have for second equation (1.15*):

$$x_2 = A \left[kt - \frac{(kt)^3}{6} + \dots \right] + B \left[1 - \frac{(kt)^2}{2} + \dots \right]. \quad (1.16)$$

Comparing now (1.16) with (1.7) and (1.8) (with $t \rightarrow -\infty$ for interior), we will obtain

$$\left. \begin{aligned} A_k &= -\frac{2\mu}{1+\mu} \left[1 - k^2 \frac{1-\mu}{1+\mu} \frac{\pi^2}{6} + \dots \right]; \\ B &= k^2 \frac{4u^2}{(1+\mu)^2} C + \dots \end{aligned} \right\} \quad (1.17)$$

Thus, the method of united asymptotic expansions makes it possible to describe the motion of the interacting particles both in the zone of interaction and before and after interaction. From (1.15) it follows also that the solution of internal problem for incident particles is correct in exterior.

The described calculation procedure is used when the impinging

atom experience/tests only one collision with oscillator. This means that at the termination of the first collision the interatomic distance of gas and the oscillator must be sufficiently great so that interacting strength would be negligible. The criterion of smallness can be selected from following considerations. Kinetic energy of the emitted atom with $t \rightarrow \infty$ in the first approximation, is equal to $E_r = \left(\frac{1-\mu}{1+\mu} \right)^2 E_0$; potential interaction energy $U = De^{-a(\tilde{x}_1 - \tilde{x}_2)}$. Let us require so that in the exterior value $\frac{U}{E_r}$ would be order δ , where δ - low value. The obtained above solution is correct with $k \rightarrow 0$. If we in the solution are restricted to the first term of expansion, i.e., to disregard terms $\sim k^2$, then also the parameter δ must be value $\sim k^2$. Generally speaking, the parameter δ must be of the order of the value of the reject/thrown terms.

Page 57.

For the first approximation we have:

$$\frac{U}{E_r} = \left(\frac{1+\mu}{1-\mu} \right)^2 2e^{-a(\tilde{x}_1 - \tilde{x}_2)} \sim k^2, \quad (1.18)$$

whence

$$\tilde{x}_1 - \tilde{x}_2 \approx \frac{1}{a} \ln \left[\frac{2e}{k^2} \left(\frac{1+\mu}{1-\mu} \right)^2 \right].$$

From solution for an exterior, we have:

$$\tilde{x}_1 - \tilde{x}_2 = \frac{1}{a} \ln \frac{e(1+\mu)}{2} + \frac{1-\mu}{1+\mu} \tilde{t} V_0 + \frac{2\mu}{1+\mu} \frac{V_0}{\omega_0} \sin \omega_0 \tilde{t}. \quad (1.19)$$

Time \tilde{t} which the distance between particles is minimal, let us find, equalizing zero derivative (1.19) on \tilde{t} :

$$\frac{1-\mu}{1+\mu} + \frac{2\mu}{1+\mu} \cos \omega_0 \tilde{t} = 0. \quad (1.20)$$

From (1.18) and (1.19) we obtain:

$$\frac{1-\mu}{1+\mu} \frac{\omega_0 \tilde{t}}{k} + \frac{2\mu}{1+\mu} \frac{\sin \omega_0 \tilde{t}}{k} = \ln \frac{4(1+\mu)}{k^2(1-\mu)^2}. \quad (1.21)$$

After introducing designations $\omega_0 \tilde{t} = \phi$, instead of (1.20) and (1.21) we will obtain the following equations:

$$-k \frac{1+\mu}{1-\mu} \ln \frac{4(1+\mu)}{k^2(1-\mu)^2} + \phi = \operatorname{tg} \varphi; \quad \frac{1-\mu}{2\mu} = -\cos \varphi. \quad (1.22)$$

Since appears itself the first minimum of function $\tilde{x}_1 - \tilde{x}_2$, then ϕ lie/rests within limits $\pi < \phi < 3/2\pi$. With $k > 0$ we have:

$$\varphi = \operatorname{tg} \varphi, \quad \frac{1-\mu}{2\mu} = -\cos \varphi. \quad (1.23)$$

It is logical that equations (1.23) coincide with the equations, obtained in supposition, that interaction between particles is described by the model of solid sphere. From (1.23) we obtain, that the assumption about single collision is correct when $\mu \leq 0.697^1$.

FOOTNOTE ¹. This result and relationship/ratics (1.23) are obtained also in work [7]. ENDFOOTNOTE.

Taking into account (1.22) or holding in (1.19) the members of higher order on k , we will obtain that supposition about single collision is correct with $\mu \leq 0.697 + \delta_1$, moreover $\delta_1 \rightarrow 0$ with $k \rightarrow 0$. Then inequality $\mu < 0.697$ gives strict asymptotic estimation of the applicability of method presented above.

Let us use the now obtained results to the calculation of the accommodation coefficient of energy, which let us determine in the following manner.

$$\alpha_e = \frac{E_i - E_r}{E_i}, \quad (1.24)$$

where E_i, E_r - energy of the atom of gas on and after interaction with oscillator, or

$$\alpha_e = 1 - \dot{x}_1^2. \quad (1.24')$$

Page 58.

Substituting here (1.12), we obtain:

$$\alpha_e = \frac{4\mu}{(1+\mu)^2} \left\{ 1 - \frac{1-\mu}{1+\mu} k^2 \frac{\pi^2}{3} + k^4 \left[\frac{1-\mu}{(1+\mu)^3} \frac{7\pi^4}{180} + \frac{8\mu(1-\mu)}{(1+\mu)^3} C_1 + \frac{1-\mu}{1+\mu} \frac{\pi^4}{36} - \frac{4\mu}{(1+\mu)^2} \frac{\pi^4}{36} \right] + \dots \right\}. \quad (1.25)$$

With $\mu \rightarrow 0$ we have:

$$\alpha_1 \approx 4\mu \left(1 - k^2 \frac{\pi^2}{3} + k^4 \frac{\pi^4}{15} + \dots \right). \quad (1.26)$$

Fig. 2, depicts the results of calculations α_1 according to formula (1.25) and the results of numerical calculations for $\mu=0.11$ and 0.5 [1 - first approximation, the first term (1.25); 2 - second approach/approximation, yes the first of term (1.25); 3 - third approach/approximation; 4 - numerical calculation]. Instead of k^2 is here introduced another parameter:

$$\epsilon_2 = \frac{m V_0^2}{2\pi l^2} = \frac{\mu}{2\bar{a}^2 k^2}, \quad (1.27)$$

where l - certain characteristic linear dimension ($l=10^{-6}$ cm),
 $\bar{a}=al=2.6$.

Comparison shows that with $\mu=0.11$ formula (1.25) will agree well with numerical results when $\epsilon_2 \geq 0.1$ (that it corresponds $k^2 \leq 0.1$), with $\mu=0.5$ the agreement somewhat is worse, what, apparently, is connected, on one hand, with the insufficient number of approach/approximations, and on the other hand - with the disturbance/breakdown of assumption about single collision. The realization of the second possibility, indicates the tendency toward a change of the limit of the applicability of assumption about single collision to the side of the smaller values μ with increase in k during estimation according to the first approximation of expansion (1.4), see (1.22).

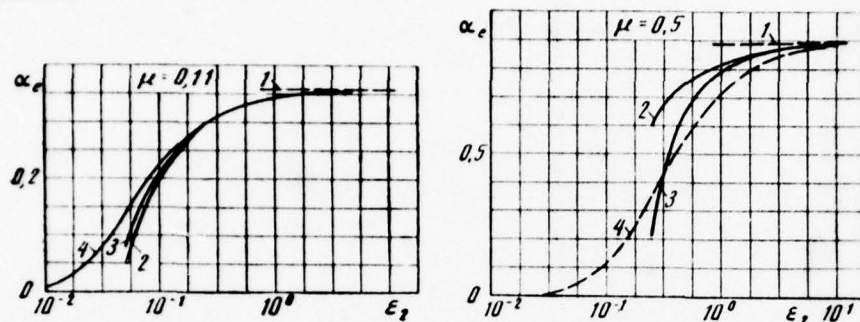


Fig. 2.

Page 59.

§2. Interaction of the atom of gas with solid surface.

Let us examine now interaction of the atom of gas with solid surface in setting [4], i.e., on the assumption that solid body is simulated by the simple cubic lattice atoms in which are connected by elastic central and noncentral forces with constant elasticity κ and $\lambda\kappa$ respectively, but the atom of gas moves along the normal to surface and it interacts only with one atom of surface, with impact parameter $\rho=0$ (Fig. 3). Interacting strength between the surface atom and the atom of gas let us describe by potential (1.1). We have following equations of motion for the interacting system (in a dimensionless form):

$$\begin{aligned}
 \ddot{z} &= \epsilon e^{-(z-z_{0,0,0})}; \\
 \ddot{z}_{i,0,l} &= k^2 [z_{i,1,l} - z_{i,0,l} + \lambda(z_{i-1,0,l} + \\
 &\quad + z_{i+1,0,l} - 2z_{i,0,l}) + \lambda(z_{i,0,l-1} + \\
 &\quad + z_{i,0,l+1} - 2z_{i,0,l})] - \mu \epsilon e^{-(z-z_{0,0,0})} \delta_{(i,0,l;0,0,0)}; \\
 \ddot{z}_{i,j,l} &= k^2 [z_{i,j+1,l} + z_{i,j-1,l} - 2z_{i,j,l} + \\
 &\quad + \lambda(z_{i-1,j,l} + z_{i+1,j,l} - 2z_{i,j,l}) + \\
 &\quad + \lambda(z_{i,j,l-1} + z_{i,j,l+1} - 2z_{i,j,l})] \\
 &\quad (-\infty < i, l < \infty, j = 1, 2, \dots).
 \end{aligned} \tag{2.1}$$

First equation (2.1) describes the motion of the atom of gas, the second - motion of surface atoms, the third - motion of the atoms of interior layers of the lattice

$$k^2 = \frac{x}{Ma^2 V_0^2},$$

where M - mass of the atom of lattice;

$$\delta_{(i,0,l;0,0,0)} = \begin{cases} 1 & \text{при } i=0, l=0, \\ 0 & \text{во всех остальных случаях.} \end{cases}$$

Key: (1). with. (2). In all remaining cases.

Initial conditions for (2.1):

$$\left. \begin{aligned}
 z(-\infty) &= -1; \\
 z_{i,j,l}(-\infty) &= \dot{z}_{i,j,l}(-\infty) = 0 \\
 (-\infty < l, l < \infty, j = 0, 1, 2, \dots).
 \end{aligned} \right\} \tag{2.2}$$

Again as it will interest case $k_2 \ll 1$. We search for solution in the form

$$\left. \begin{aligned}
 z &= z^{(0)} + k^2 z^{(1)} + k^4 z^{(2)} + \dots; \\
 z_{i,j,l} &= z_{i,j,l}^{(0)} + k^2 z_{i,j,l}^{(1)} + k^4 z_{i,j,l}^{(2)} + \dots
 \end{aligned} \right\} \tag{2.3}$$

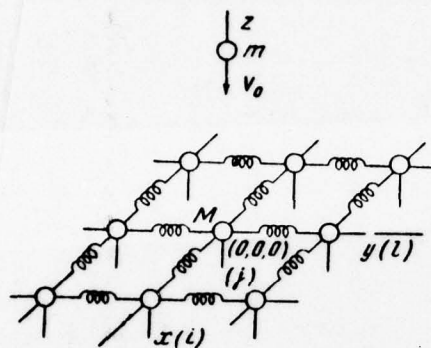


Fig. 8.

Page 60.

Let us substitute (2.3) and (2.1) let us extract the equations whose solutions are not equal identical to zero. We will obtain:

the first approximation

$$\left. \begin{aligned} \ddot{z}(0) &= se^{-\left(z^{(0)} - z_{0,0,0}^{(0)}\right)}; \\ \ddot{z}_{0,0,0}^{(0)} &= -\mu se^{-\left(z^{(0)} - z_{0,0,0}^{(0)}\right)}; \\ \ddot{z}^{(0)}(-\infty) &= -1; \\ z_{0,0,0}^{(0)}(-\infty) &= \ddot{z}_{0,0,0}^{(0)}(-\infty) = 0; \end{aligned} \right\} \quad (2.4')$$

the second approach/approximation

$$\left. \begin{aligned} \ddot{z}^{(1)} &= -se^{-\left(z^{(0)} - z_{0,0,0}^{(0)}\right)} \left(z^{(1)} - z_{0,0,0}^{(1)}\right); \\ \ddot{z}_{0,0,0}^{(1)} &= -(1 + 4\lambda) \ddot{z}_{0,0,0}^{(0)} + \mu se^{-\left(z^{(0)} - z_{0,0,0}^{(0)}\right)} \left(z^{(1)} - z_{0,0,0}^{(1)}\right); \\ \ddot{z}_{1,0,0}^{(1)} &= \ddot{z}_{1,0,0}^{(1)} = \ddot{z}_{0,0,1}^{(1)} = \ddot{z}_{0,0,-1}^{(1)} = \lambda \ddot{z}_{0,1,0}^{(1)} = \lambda \ddot{z}_{0,0,0}^{(0)}. \end{aligned} \right\} \quad (2.4'')$$

Initial conditions - zero for all functions systems (2.4").

The analysis of system of equations (2.4) shows that in the first approximation, surface atom (0, 0, 0), with which it interacts the atom of gas, it moves ^{like} with ~~it~~ free, i.e., communication/connections in lattice are not exhibited. In the second approach/approximation into motion, are involved the nearest to atom (0, 0, 0) adjacent atoms of lattice, but their motion does not affect the motion of atom (0, 0, 0). Atom (0, 0, 0) moves in the manner that if its nearest neighbor rested, i.e., with each following approach/approximation into motion, are drawn in all the new layers of the atoms of lattice.

The solution of system (2.4) is analogous solution described above of problem with harmonic oscillator. For velocity \dot{z} with $t \rightarrow \infty$, we have:

$$\dot{z} = \frac{1-\mu}{1+\mu} + k^2 \frac{2\mu}{(1+\mu)^3} \frac{\pi^2}{3} (1+4\lambda) - \left. \begin{aligned} &- k^4 \left\{ (1+4\lambda)^2 \left[\frac{4\mu}{(1+\mu)^3} \frac{7\pi^4}{360} + \frac{16\mu^2}{(1+\mu)^3} C_1 + \right. \right. \\ &\left. \left. + \frac{4\mu}{(1+\mu)^2} \frac{\pi^4}{72} \right] + (1+4\lambda^2) \frac{4\mu}{(1+\mu)^3} \frac{\pi^4}{30} \right\} + \dots \end{aligned} \right\} \quad (2.5)$$

Accommodation coefficient of the energy

$$\begin{aligned}
 \alpha_e = \frac{4\mu}{(1+\mu)^2} \left\{ 1 - \frac{1-\mu}{1+\mu} k^2 \frac{\pi^2}{3} (1+4\lambda) + \right. \\
 + k^4 2 \frac{1-\mu}{1+\mu} \left((1+4\lambda)^2 \left[\frac{\pi^4}{72} + \frac{1}{1+\mu} \frac{7\pi^4}{360} + \right. \right. \\
 \left. \left. + \frac{4\mu}{1+\mu} C_1 \right] + (1+4\lambda)^2 \frac{\pi^4}{30} \right) - \\
 \left. - k^4 \frac{\mu}{(1+\mu)^2} (1+4\lambda)^2 \frac{\pi^4}{q} + \dots \right\}.
 \end{aligned} \quad (2.6)$$

Here C_1 to determination by formula (1.12').

With $\mu \rightarrow 0$ we have

$$\begin{aligned}
 \alpha_e \approx 4\mu \left\{ 1 - k^2 \frac{\pi^2}{3} (1+4\lambda) + 2k^4 \frac{\pi^4}{15} (1+4\lambda) + \right. \\
 \left. + 10\lambda^2 + \dots \right\}.
 \end{aligned} \quad (2.7)$$

Page 61.

Result (2.7) coincides with the result of Gudmen [3], by the obtained method of perturbation theory at high velocities and valid with $\mu \rightarrow 0$. From (2.6) it is evident that the accommodation coefficient of energy during interaction with three-dimensional lattice differs from α , during interaction of the atom of gas with oscillator only in the coefficient of k^4 , if the natural frequency of oscillator is accepted equal to $\omega^2_0 = \chi/H(1+4\lambda)$.

Let us now determine the limit of the applicability of method for the problem of cooperating the atom of gas with lattice. For this, we will use the obtained in §1 position that with $k \rightarrow 0$ the limit of the applicability is determined from the model of interaction of solid spheres. For the model of solid spheres, it is easy to find the action of surface atom [4]:

$$\tilde{z}_{0,0,0}(\tilde{t}) = - \frac{2\mu}{1+\mu} V_0 I(\tilde{t}), \quad (2.8)$$

where $I(\tilde{t})$ - the function of the reaction of lattice,

$$\left. \begin{aligned} I(\tilde{t}) &= \left(\frac{1}{2\pi} \right)^3 \int_{-\pi}^{\pi} \int_{-\pi}^{\pi} \int_{-\pi}^{\pi} (1 + \cos \theta_z) \frac{\sin \omega_z \tilde{t}}{\omega_z} d\theta_x d\theta_y d\theta_z; \\ \omega_z^2 &= \frac{4\pi}{M} \left[\sin^2 \frac{\theta_z}{2} + \lambda \left(\sin^2 \frac{\theta_x}{2} + \sin^2 \frac{\theta_y}{2} \right) \right]. \end{aligned} \right\} \quad (2.9)$$

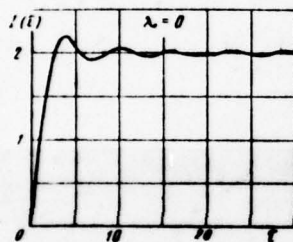
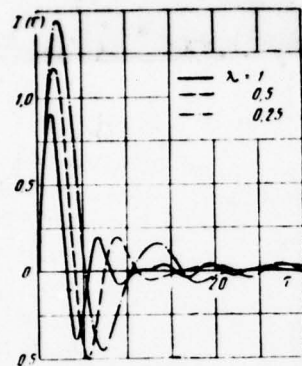


Fig. 4.

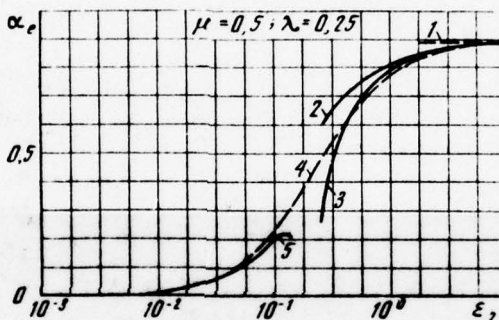
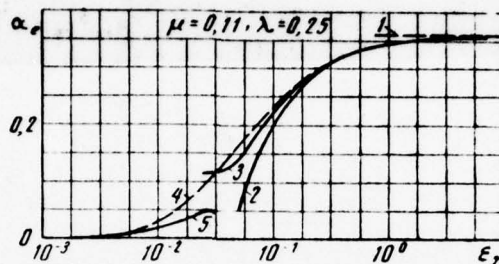


Fig. 5.

Page 52.

The boundary of the single collision of the atom of gas with surface atom let us find from the conditions

$$\left. \begin{aligned} \tilde{z}(\tilde{t}) - \tilde{z}_{0,0,0}(\tilde{t}) &= \frac{1-\mu}{1+\mu} \tilde{t} V_0 + \frac{2\mu}{1+\mu} V_0 I(\tilde{t}) - 0; \\ \tilde{z}(\tilde{t}) - \tilde{z}_{0,0,0}(\tilde{t}) &= \frac{1-\mu}{1+\mu} V_0 + \frac{2\mu}{1+\mu} V_0 I(t) = 0. \end{aligned} \right\} \quad (2.10)$$

Fig. 4, depicts the function of reaction for different values λ , calculated on formula (2.9); the graph/diagram of dependence $I(\tilde{t})$ for

$\lambda=1.0$ is given in work [4], in work [5] it is represented to dependence $I(t)$ for $\lambda=0.3$. Utilizing conditions (2.10), graphically let us find μ_{rp} , the determining upper boundary of single collision from μ with $k \rightarrow 0$.

$$\begin{array}{l} \lambda = 1; \quad 0.5; \quad 0.25; \quad 0; \\ \mu_{rp} = 0.84; \quad 0.846; \quad 0.885; \quad 1. \end{array}$$

Result for $\lambda=1$ is contained in [4].

Fig. 5, depicts the results of the calculation of the accommodation coefficient of energy α_e in formula (2.6) and results of numerical calculations, carried out by the author according to method of operation [6], for $\mu=0.11$ and 0.5 (1 - first approximation, 2 - second approach/approximation, 3 - third approach/approximation, 4 - numerical calculation). As in Fig. 2, is here instead of k^2 introduced parameter ϵ_2 , determined by formula (1.29). The comparison of the given results shows that formula (2.6) gives good results with $k^2 \leq 0.1$, moreover for $\mu=0.5$, the agreement of results is better/best than in problem for an harmonic oscillator, which is understandable in view of the expansion of the limit of the applicability of supposition about single collision in the problem of interaction of the atom of gas with lattice. Fig. 5, gives also the results of work [3] for another limiting case $k^2 \gg 1$ (curve 5).

The author expresses appreciation to M. N. Kogan and V. V.

Mikhaylov for the discussion of this work and G. Ye. Tsar'kova and A. V. Zhbakova for aid in conducting necessary of calculations by ETsVM.

REFERENCES.

1. Szaniawski A. Collision of a fast particle with a one — dimensional cold lattice. Oddziaływanie. Gazu ze sciankami stalymi. Praca zbiorowa, 6/1969, Warszawa.
2. Logan R. M., Keck J. C. Classical theory for the interactions of gas atoms with solid surfaces. J. Chem. Phys., 49, № 2, 1968.
3. Goodman F. O. Classical perturbation theory of the thermal accommodation coefficient in the dimensions. Surface Science, 11, № 2, 1968.
4. Goodman F. O. The dynamics of simple cubic lattices I. J. Phys. Chem. Solids, 23, 1269, 1962.
5. Goodman F. O. Response function and thermal motions of a simple n-dimensional lattice model. Surface Science, 3, № 4, 1965.
6. Goodman F. O. On the theory of accommodation coefficients V. Classical theory of thermal accommodation and trapping. Rarefied Gas Dynamics, 1967, p. 366—395.
7. Secrest D. Linear collision of a classical harmonic oscillator with a particle at high energies. J. Chem. Phys., 51, № 1, 1969.

The manuscript entered 11/VII 1969.

Page 63.

CRITERIA OF THE LONGITUDINAL STABILITY OF AERODYNAMIC AIR-CUSHION
VEHICLE.

E. D. Irodov.

Are examined some questions of the longitudinal stability of aerodynamic air-cushion vehicle, direct-connected with the selection of its aerodynamic layout.

Aerodynamic air-cushion vehicle - flight vehicle, which uses an effect of an essential increase in the lift effectiveness and lift-drag ratio of wing in flight rear surface (screen). The favorable effect of screen is exhibited the greater, the lesser the height/altitude of location above it of trailing wing edge, expressed in chord. With the assigned/prescribed wing area and the assigned/prescribed absolute distance from screen to trailing wing edge, determined by the possible height of the irregularities of screen, the effect of screen will be the greater, the lesser wing aspect ratio. This fact defines the layout of aerodynamic air-cushion vehicle as flight vehicle with low-aspect-ratio wing [1]. Some special feature/peculiarities of the aerodynamic characteristics of

aerodynamic air-cushion vehicle lead to the need for the introduction of new stability criteria and to the appearance in connection with this of supplementary requirements to its aerodynamic layout.

Page 64.

1. Equations of axial motion of aerodynamic air-cushion vehicle do not differ in form from analogous equations for aircraft and are recorded/written in the form [2]

$$\left. \begin{aligned} \frac{dV}{dt} &= g(n_x - \sin \theta), \\ \frac{d\theta}{dt} &= \frac{g}{V}(n_y - \cos \theta), \\ \frac{d^2 \theta}{dt^2} &= \frac{M_x}{I_x}, \\ \frac{dH}{dt} &= V \sin \theta, \end{aligned} \right\} \quad (1)$$

where g - acceleration of gravity [m/s^2], n_x and n_y - relation to weight of aircraft of sum of projections of thrust of engines and aerodynamic forces on horizontal and vertical axes of high-speed/velocity coordinate system, t - time [s], v - flight speed [m/s], θ - flight path angle [rad], θ - pitch angle [rad], of H - flight altitude (distance from center of gravity of aerodynamic air-cushion vehicle to surface of screen [m], M_x - pitching moment [$kgf \cdot m$].

The weight of aerodynamic air-cushion vehicle G and its moment of inertia I_z during the analysis of motion during small time intervals can be considered constants. The effect of aerodynamic forces on aerodynamic air-cushion vehicle is assigned by dependences n_x , n_y and M_z on the parameters, which determine flight conditions, taking into account obvious equations of communication/connection $\beta = \theta + \alpha$, where α - an angle of attack.

During the evaluation of the stability of aircraft the dominant role plays the examination of motion with constant velocity (short-period motion). Let us write the equations of the short-period motion of aerodynamic air-cushion vehicle in increases, being based on these not assumptions that and in the case of aircraft [2]:

$$\begin{aligned} V &= \text{const}; \theta = \theta_{\text{ncx}} + \Delta\theta; \\ n_y &= n_{y\text{ncx}} + \Delta n_y; H = H_{\text{ncx}} + \Delta H; \dot{\theta} = \dot{\theta}_{\text{ncx}} + \dot{\Delta\theta}; M_z = M_{z\text{ncx}} + \Delta M_z. \end{aligned}$$

Initial conditions, mode - level steady flight:

$$\theta_{\text{ncx}} = 0; M_{z\text{ncx}} = 0; n_{y\text{ncx}} = 1.$$

As a result of these assumptions, the first equation of system (1) becomes identical ($n_x = 0$), remaining three are record/written in the form

$$\left. \begin{aligned} \Delta\dot{\theta} &= -\frac{g}{V} \Delta n_y, \\ \Delta\ddot{\alpha} + \Delta\dot{\theta} &= \frac{1}{I_z} \Delta M_z, \\ \Delta\dot{H} &= V\Delta\dot{\theta}. \end{aligned} \right\} \quad (2)$$

(by point markedly differentiation with respect to time).

Proposing further that the angles of attack α and of the deviation of stabilizer ϕ and flight altitude H in the process of the disturbed motion change within such limits, that increase in aerodynamic coefficients Δc_y and Δm_z ($\Delta n_y = \frac{\rho V^2}{2G} S \Delta c_y$; $\Delta M_z = \frac{\rho V^2}{2} S b_A \Delta m_z$, where ρ - air density [$\text{kg} \cdot \text{s}^2 / \text{m}^3$]; b_A - the mean aerodynamic chord of wing [m]; S - wing area [m^2]) it is possible to consider as the linearly depending on them, let us write

$$\Delta c_y = c_y^\alpha \Delta \alpha + c_y^H \Delta H;$$

$$\Delta m_z = m_z^\alpha \Delta \alpha + m_z^\phi \Delta \phi + m_z^{\omega_z} \omega_z + m_z^H \Delta H.$$

Here $\omega_z = \frac{d\phi}{dt}$ - the angular rate of rotation of aerodynamic air-cushion vehicle, ϕ - angle of deflection of stabilizer.

Page 55.

After substituting expressions for Δc_y and Δm_z into system and after excluding an increase in the flight path angle $\Delta \theta$, we will obtain the system of two linear differential second order equations with constant coefficients.

Transfer/converting in this system to new time unit τ_m that depends on the parameters of aerodynamic air-cushion vehicle and

flight conditions $\tau = \frac{t}{\tau_m}$, $\tau_m = \frac{2G/S}{\rho g V}$ [s], introducing the operator of differentiation the dimensionless time $D = d/d\tau$ and after designating for the brevity

$$2\xi = c_y^a - \frac{m_z^{\omega} + m_z^{\alpha}}{i_z};$$

$$\omega_0^2 = -\frac{\mu}{i_z} c_y^a \sigma_n; \quad \omega_z = \omega_z \frac{b_A}{V};$$

$$\alpha = \frac{d\alpha}{dt} \frac{b_A}{V};$$

$$\bar{H} = \frac{H}{b_A};$$

$\mu = \frac{2G/S}{\rho g b_A}$ - relative density of aerodynamic air-cushion vehicle;

$i_z = \frac{g}{G} \frac{I_z}{b_A^2}$ - dimensionless moment of inertia; $\bar{x}_r - \bar{x}_{Fa} = \frac{m_z^a}{c_y^a}$ - supply

of longitudinal static angle of attack stability - distance in

portions MAC from the center of gravity of aerodynamic air-cushion

vehicle (\bar{x}_r) to the point of the application/appendix of lift

increment because of a change in the angle of attack \bar{x}_{Fa} ;

$\bar{x}_r - \bar{x}_{FH} = \frac{m_z^H}{c_y^H}$ - the supply of longitudinal static stability with

respect to the height/altitude above the screen - distance in

portions MAC from the center of gravity of aerodynamic air-cushion

vehicle \bar{x}_r to the point of the application/appendix of lift

increment because of change in altitude of flight (\bar{x}_{FH}) ;

$\sigma_n = \bar{x}_r - \bar{x}_{Fa} + \frac{m_z^{\omega}}{\mu}$ - the supply of longitudinal static stability with

respect to overload $(\bar{x}_r, \bar{x}_{Fa})$ and \bar{x}_{FH} regarding are positive with the

location of the center of gravity and foci behind the leading edge

MAC of wing), let us write the system of equations of the disturbed motion of aerodynamic air-cushion vehicle (2) in the following convenient for analysis form:

$$(D^2 + 2\xi D + \omega_0^2) \Delta \alpha + \left[c_y^H D - \frac{\mu}{l_z} c_y^H \left(\bar{x}_r - \bar{x}_{FH} + \frac{m_z^{\omega_z}}{\mu} \right) \right] \Delta \bar{H} - \frac{\mu}{l_z} m_z^{\varphi} \Delta \varphi(\tau);$$

$$\mu c_y^a \Delta \alpha - (D^2 - \mu c_y^H) \Delta \bar{H} = 0.$$

Page 66.

In the absence of the effect of screen, i.e., the altitude effect of flight or aerodynamic coefficients ($c_y^H = m_z^H = 0$) this system decomposes into two independent equations: the equation of the short-period motion

$$(D^2 + 2\xi D + \omega_0^2) \Delta \alpha = \frac{\mu}{l_z} m_z^{\varphi} \Delta \varphi(\tau)$$

and the equation, which describes change in altitude depending on a change in the angle of attack,

$$D^2 \Delta \bar{H} = \mu c_y^a \Delta \alpha(\tau), \text{ i. e. } \Delta \bar{H} = \mu c_y^a \int_0^{\tau} \left(\int_0^{\tau} \Delta \alpha(\tau) d\tau \right) d\tau,$$

or the equations, which describe a change of the angle of attack and flight altitude in short-period motion,

$$(D^2 + 2\xi D + \omega_0^2) \Delta \alpha = \frac{\mu}{l_z} m_z^{\varphi} \Delta \varphi(\tau),$$

$$(D^2 + 2\xi D + \omega_0^2) D^2 \Delta \bar{H} = \frac{\mu^2}{l_z} c_y^a m_z^{\varphi} \Delta \varphi(\tau).$$

With $2\xi > 0$ and $\omega_0^2 > 0$ in the isotropic atmosphere at constant

velocity the aircraft is stable on angle of attack and it is neutral on flight altitude. Consequently, for a precise constant altitude control of flight is necessary either pilot's virtually continuous interference in the aircraft control or the introduction to stabilization of aircraft on height/altitude by means automatic control.

In flight near the screen (i.e. the earth's surface or water) of force and the torque/moments, which act on aircraft, substantially depend not only on angle of attack, but also on height/altitude. Therefore the system, which describes the motion of aerodynamic air-cushion vehicle with constant velocity, does not decompose into two independent second order equations. eliminating from system an increase in the angle of attack, it is possible to write one the equation of the fourth order, describing change in altitude of the flight of aerodynamic air-cushion vehicle in the brief periodic motion

$$\left[D^4 + 2\zeta D^3 + (\omega_0^2 - \mu c_y^H) D^2 - \mu c_y^H (2\zeta - c_y^a) D + \frac{\mu^2}{I_z} c_y^a c_y^H (\bar{x}_{FH} - \bar{x}_{Fa}) \right] \Delta H = \frac{\mu^2}{I_z} c_y^a m_z^* \Delta \varphi(\tau).$$

Analogously it is possible to write the equation, which describes a change in the angle of attack of the aerodynamic air-cushion vehicle:

$$\left[D^4 + 2\xi D^3 + (\omega_0^2 - \mu c_y^H) D^2 - \mu c_y^H (2\xi - c_y^2) D + \frac{\mu^2}{i_z} c_y^a c_y^H (\bar{x}_{FH} - \bar{x}_{Fa}) \right] \Delta x =$$

$$= \frac{\mu}{i_z} (D^3 - \mu c_y^H) m_z^2 \Delta \varphi(z).$$

Page 67.

2. Let us write characteristic equation of system in standard form:

$$D^4 + A_1 D^3 + A_2 D^2 + A_3 D + A_4 = 0,$$

where

$$A_1 = 2\xi = c_y^a - \frac{m_z^2 + m_z^2}{i_z};$$

$$A_2 = \omega_0^2 - \mu c_y^H = -\frac{\mu}{i_z} c_y^a \left(\sigma_n + i_z \frac{c_y^H}{c_y^a} \right);$$

$$A_3 = -\mu c_y^H (2\xi - c_y^2) = \frac{\mu}{i_z} c_y^H (m_z^2 + m_z^2);$$

$$A_4 = \frac{\mu^2}{i_z} c_y^H c_y^a (\bar{x}_{FH} - \bar{x}_{Fa}) = -\frac{\mu^2 D(c_y, m_z)}{i_z D(z, H)},$$

where $\frac{D(c_y, m_z)}{D(z, H)}$ - Jacobian functions $c_y(\alpha, \bar{H})$ and $m_z(z, H)$.

Stability of motion in the case of equation of the fourth order will be provided with

$$A_1, A_2, A_3, A_4 > 0 \text{ and } A_1 A_2 A_3 - A_1^2 A_4 - A_3^2 > 0.$$

For all aircraft layouts in the range of flight angles of

attack, is made inequality $c_y^* > 0$. By condition of the stabilization of aerodynamic air-cushion vehicle out of the effect of the screen is execution of inequality $\sigma_n < 0$.

From testings of airfoil/profiles, wings and layouts of aircraft near screen, it is known that usually the lift coefficient of the assigned/prescribed angle of attack increases with approach/approximation to screen (Fig. 1), i.e., $c_y^H < 0$.

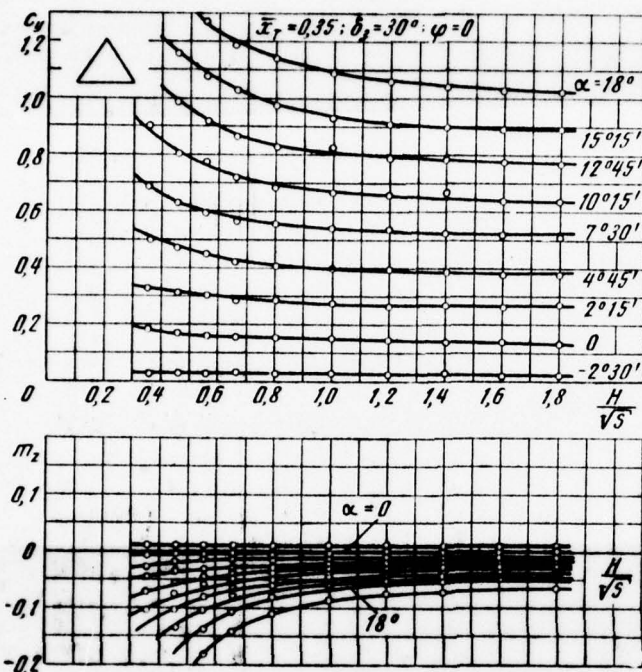


Fig. 1.

Page 68.

From formulas for the calculation of coefficients A_i it is evident that under these assumptions of condition $A_1 > 0$, $A_2 > 0$, $A_3 > 0$ they are satisfied always. Consequently, the stability conditions of the short-period motion of aerodynamic air-cushion vehicle in flight near screen are reduced to two inequalities: $A_4 > 0$ and $A_1 A_2 A_3 - A^2 A_4 - A_1^2 > 0$.

The satisfaction of the first condition provides the dead-beat stability of aerodynamic air-cushion vehicle (i.e. the absence of the nonnegative real roots of characteristic equation), the satisfaction of the second condition - its oscillatory stability (i.e. the absence of the nonnegative real parts of the complex roots of characteristic equation).

After substituting the expressions, which determine the coefficients through the aerodynamic derivatives, it is possible to write the criteria of stability of aerodynamic air-cushion vehicle in short-period motion in the following form:

dead-beat stability -

$$\bar{x}_{FH} - \bar{x}_{Fa} < 0 \quad (3)$$

or, with any sign of derivative \bar{c}_y^H ,

$$\frac{D(c_y; m_z)}{D(x; H)} < 0; \quad (3a)$$

oscillatory stability -

$$\bar{x}_1 - \frac{1 - \frac{\bar{c}_y^a}{2\xi} \frac{\bar{x}_{Fa}}{\bar{x}_{FH}}}{1 - \frac{\bar{c}_y^a}{2\xi}} \bar{x}_{FH} + \left(\frac{\bar{c}_y^H}{2\xi} i_z + \frac{\bar{m}_z^u}{\mu} \right) < 0, \quad (4)$$

Thus, for ensuring of the dead-beat stability of aerodynamic

air-cushion vehicle, it is necessary with the selection of aerodynamic layout to ensure the position of focus on the height/altitude above screen (x_{FH}) in front of focus on angle of attack (x_{Fa}). For providing the oscillatory stability, it is necessary to select correspondingly centering \bar{x}_T .

Consequently, unlike the aircraft whose longitudinal static stability in the absence of the compressibility effect of air always, with any aerodynamic layout, can be provided by the selection of centering, the longitudinal aperiodic (static) stability of aerodynamic air-cushion vehicle under these conditions can be provided only with in a specific manner to the selected aerodynamic layout. If the aerodynamic layout of aerodynamic air-cushion vehicle is such, that the focus on the height/altitude above the screen is arranged/located behind focus on angle of attack, then with the selection of the center-of-gravity location the dead-beat stability of aerodynamic air-cushion vehicle it is not possible to ensure.

During model tests with screen in wind tunnels under the height/altitude of the model above the screen, usually is understood the distance from screen to trailing wing edge in the point of its intersection with the mean aerodynamic chord.

4

Under conditions of the essential dependence of the aerodynamic characteristics of aerodynamic air-cushion vehicle on flight altitude, the derivatives c_y^a, m_z^a and focus for angle of attack \bar{x}_{Fa} prove to be dependent from the point, relative to which occurs the rotation of aerodynamic air-cushion vehicle during a change in the angle of attack. Focus on height/altitude \bar{x}_{FH} from position on MAC of this point does not depend. If values c_y^a, m_z^a and \bar{x}_{Fa} determined during the rotation of aerodynamic air-cushion vehicle of relatively trailing wing edge, are assigned/prescribed, then their values during the rotation of aerodynamic air-cushion vehicle relative to the center of gravity can be designed on the formulas

$$\begin{aligned} (c_y^a)_1 &= (c_y^a)_{3.K} - c_y^H (1 - \bar{x}_1); \\ m_{z_1}^a &= m_{z_{3.K}}^a - m_z^H (1 - \bar{x}_1); \\ \bar{x}_{Fa_1} &= \bar{x}_{Fa_{3.K}} \frac{1 - \frac{c_y^H}{c_{y_{3.K}}^a} (1 - \bar{x}_1) \frac{\bar{x}_{FH}}{\bar{x}_{Fa_{3.K}}}}{1 - \frac{c_y^H}{c_{y_{3.K}}^a} (1 - \bar{x}_1)} \end{aligned}$$

(during the calculation of derivatives $m_{z_{3.K}}^a$ and m_z^H torque/moment is measured relative to the center of gravity of aerodynamic air-cushion vehicle \bar{x}_1 , therefore both derivatives depend on centering).

It is obvious that during the center-of-gravity disturbance of aerodynamic air-cushion vehicle forward along chord its focus on angle of attack is displaced to the side of focus on the height/altitude above the screen and within limit coincides with it when $x_1 \rightarrow -\infty$. Thus, use for the evaluation of the static longitudinal stability of the aerodynamic air-cushion vehicle of the materials of model tests in the wind tunnels in which the angle of attack changed with the rotation of model of relatively trailing wing edge, cannot lead to inaccurate qualitative evaluation - the order of the location of foci on MAC of wing it does not depend on the center of rotation of wing during a change in the angle of attack, i.e., on centering of aerodynamic air-cushion vehicle.

The account of velocity change in the examination of disturbed movement of aerodynamic air-cushion vehicle does not virtually change the condition of dead-beat stability - the aft limit, determined without the account of a change in the flight speed, is somewhat placed back/ago in comparison with actual, but with sufficiently low heaviness aerodynamic air-cushion vehicle again loses oscillatory stability.

3. Let us examine for example longitudinal static (aperiodic)

stability in flight near screen of delta-wing airplane and arranged/located on fuselage horizontal tail assembly whose aerodynamic characteristics were given to Fig. 1. Fig. 2, gives these characteristics, changed dependence $m_z(c_y)$ with $\bar{H}=\text{const}$ and $\alpha=\text{const}$ (H - a distance from center of gravity of model to screen). The slope tangents of these curves are respectively the supplies of angle of attack stability $m_z^{c_y^{(a)}} = \bar{x}_r - \bar{x}_{F\alpha}$ and with respect to flight altitude above screen $m_z^{c_y^{(H)}} = \bar{x}_r - \bar{x}_{FH}$ with centering $\bar{x}_r = 0,35$.

Page 70.

It is evident that at all height/altitudes within the limits of the effect of screen and on all angles of attack the negative slope/inclination curved $\alpha=\text{const}$ is greater than slope/inclination curved $\bar{H}=\text{const}$; this means that the focus on the angle of attack of aircraft is arranged/located in front of focus on height/altitude, which indicates the dead-beat instability of aircraft in flight near screen.

Taking into account that the focus on the angle of attack of low-aspect-ratio wings with approach/approximation to screen only completely insignificantly is displaced back/sgc, so that the isolated/insulated wing can be considered neutral on the height/altitude above the screen or weakly unstable, the considerable

instability of the aircraft of normal diagram with the low arranged/located horizontal tail assembly can be explained by the fact that during the setting up of horizontal tail assembly in lower position the focus on the height/altitude above the screen is shift/sheared back/ago more than focus on angle of attack.

The setting up of tail assembly on fuselage in front of wing (schematic of "weft"), obviously, will lead to the shift of focus on angle of attack forward and virtually will not change the position of focus on the height/altitude above the screen, since the tail assembly will undergo considerably smaller ground effect, since it lies/rests above wing at positive angles of attack and its area considerably lesser than the wing area. Hence it follows that the aircraft, arranged according to the schematic of "weft", will also be aperiodically unstable in flight near screen.

Thus, aerodynamic air-cushion vehicle for providing the longitudinal static stability in flight near screen must have the special aerodynamic layout, different from the layouts, characteristic for aircraft with low-aspect-ratio wing.

One of the possible aerodynamic layouts of aerodynamic air-cushion vehicle, proposed Lippish [1], has highly arranged/located horizontal tail assembly. This tail assembly

shift/shears focus on angle of attack considerably more than focus on the height/altitude above the screen, since it is located in the zone of the sufficiently weak effect of screen (at least at sufficiently low angles of attack). This schematic provides the position of focus on angle of attack of behind focus on the height/altitude above the screen under conditions of maximum lift-drag ratio.

Another schematic can be "bobtailed aircraft" with overflow in rect (cf aircraft type "dragon" J-35).

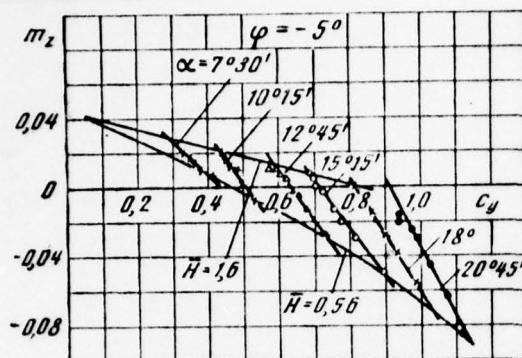


Fig. 2.

Page 71.

With approach/approximation to screen, the overflow insignificantly changes the position of focus on angle of attack (\bar{x}_{Fa}) , on is noticeably shift/sheared forward the focus on flight altitude (\bar{x}_{FH}) because of the decrease of relative distance from the screen of wing center section with overflow in front.

8. For practical problems of evaluation of static stability of aerodynamic air-cushion vehicle based on materials of testings of its model in wind tunnel, it proves to be possible to write condition of aerodynamic longitudinal stability of aerodynamic air-cushion vehicle (3a) in other form which makes it possible to estimate according to one only derived, defined as slope/inclination of experimental

curved, virtually without supplementary reorganization of curved, obtained as a result model tests.

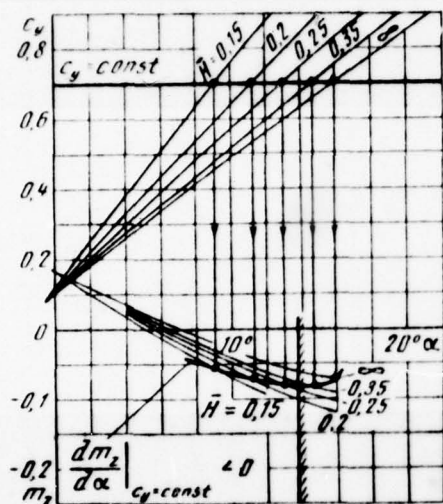


Fig. 3.

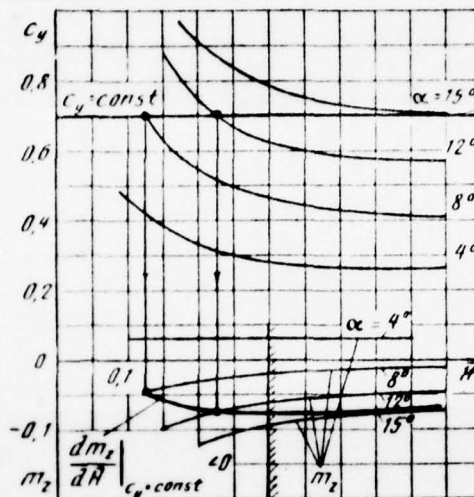


Fig. 4.

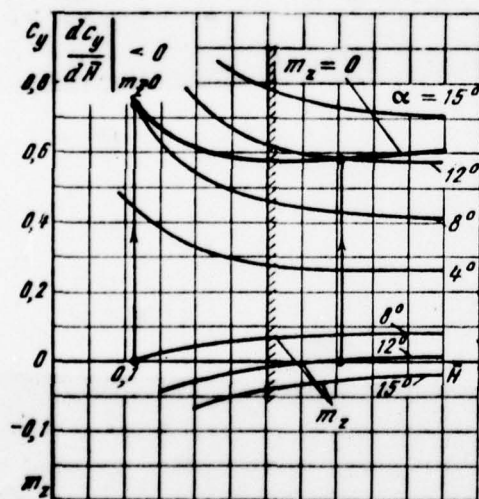


Fig. 5.

Page 72.

The basic inequality

$$\frac{D(c_y, m_z)}{D(\alpha, H)} < 0$$

can be written in any of the following four forms:

$$\begin{aligned} \frac{dc_y}{d\alpha} \Big|_{m_z=0} m_z'' < 0; & \quad \frac{dc_y}{dH} \Big|_{m_z=0} m_z'' > 0; \\ \frac{dm_z}{d\alpha} \Big|_{c_y=c_{y \text{ r. n}}} c_y'' > 0; & \quad \frac{dm_z}{dH} \Big|_{c_y=c_{y \text{ r. n}}} c_y'' < 0 \end{aligned}$$

(here $c_{y \text{ r. n}}$ - a lift coefficient in the level steady flight). It is most convenient to utilize one of two last/latter inequalities. Since under cruising conditions of flight $c_y'' < 0$, $c_y'' > 0$, stability criterion they can be written in the form

$$\frac{dm_z}{d\alpha} \Big|_{c_y=c_{y \text{ r. n}}} < 0; \quad \frac{dm_z}{dH} \Big|_{c_y=c_{y \text{ r. n}}} < 0.$$

When $m_z'' < 0$ can be used criterion $\frac{dc_y}{dH} \Big|_{m_z=0} < 0$. Derivatives can be found as slope/inclinations of curves $m_z(\alpha)$ when $c_y = \text{const}$, $m_z(H)$ when $c_y = \text{const}$ or $c_y(H)$ when $m_z = 0$, as this is shown on Fig. 3-5.

Since the stability of aerodynamic air-cushion vehicle is estimated under the conditions of the steady flight, the examination of stability, strictly speaking, has sense only when $m_z = 0$, at the points of balance.

During the analysis of the stability of aircraft, usually is made the assumption that the control-surface deflection does not change the position of focus on angle of attack, or, in other words, the slope/inclination of curves $m_z(\alpha)$. Accepting this assumption and for an aerodynamic air-cushion vehicle and assuming additionally that the control displacement does not change and the position of focus on the height/altitude above the screen, we obtain possibility to judge the stability with respect to slope/inclination appropriate curve $m_z(\alpha)$ or $m_z(H)$ with $C_y = C_{y0}$ and the arbitrary value of pitching moment.

REFERENCES.

1. N. I. Belavin. Aerodynamic air-cushion vehicles. L., "ship-building", 1968.
2. I. V. Ostoslavskiy, G. S. Kalachev. Longitudinal stability and aircraft handling. P., Oborongiz, 1951.

The manuscript entered 6/XI 1969.

During the determination of the maneuverability capabilities of apparatus [1] appears situation, when local buoyancy effect on overload proves to be exhausted. This case in work [2] is named irregular. In this same work is demonstrated the principle of maximum for the limitations of class $g(x, u) \leq 0$ in the case when

optimum trajectory contains the finite or denumerable number of irregular points, moreover the principle of maximum [2] in the regular case it is equivalent to the classical principle of Pontryagin's maximum.

Let us examine the task of the selection of the angle of attack control of the braked in the atmosphere machine in flight to minimum range taking into account limitation to the value of complete overload in the case of the local ineffectiveness of control.

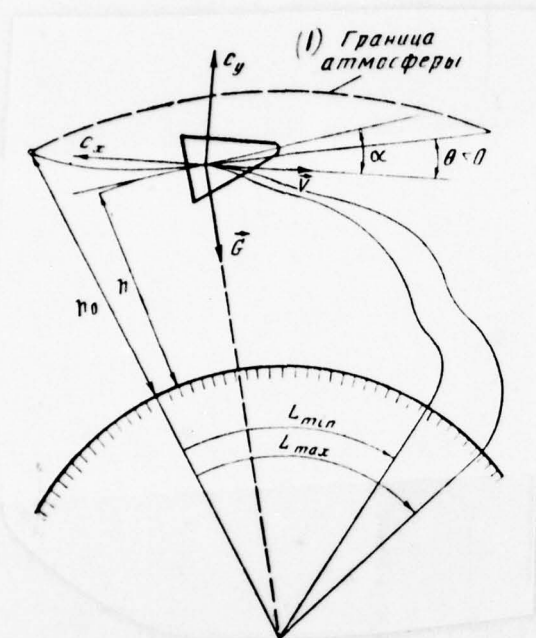


Fig. 1.

Key: (1). Boundary of the atmosphere.

Page 74.

Expression for flying range takes the form

$$L = \int_{t_0}^{t_1} \frac{RV \cos \theta}{R + h} dt, \quad (1)$$

where h , v - height/altitude and flight speed; θ - flight path angle to the horizon; R - radius of the Earth; t_0 , t_1 - time of motion (Fig. 1).

It is required to find the program of control of lift $F_y = c_y(t)qS$, that gives the minimum to functional $A(t_1)$ under the conditions:

$$\left. \begin{aligned} 1. \quad n_2 - N &= \sqrt{c_x^2 + c_y^2} \frac{qS}{G} - N \leq 0; \\ 2. \quad c_{y \min} &\leq c_y \leq c_{y \max}; \quad c_x = c_{x0} + \alpha c_y^2; \\ 3. \quad V &= -c_x q \frac{S}{m} - g(h) \sin \theta; \quad g(h) = g_0 \left(\frac{R}{R+h} \right)^2; \\ \dot{\theta} &= c_y \frac{qS}{mV} - \left(\frac{V}{R+h} - \frac{g}{V} \right) \cos \theta; \\ \dot{h} &= V \sin \theta; \quad q = \rho \frac{V^2}{2}; \quad \rho = \rho_0 e^{-\beta h}; \\ 4. \quad h(t_0) &= h^{(0)}; \quad V(t_0) = V^{(0)}; \quad \theta(t_0) = \theta^{(0)}; \quad h(t_1) = h^{(1)}. \end{aligned} \right\} (2)$$

Necessary conditions of extremum in irregular case.

The points of the set, determined by equations $\frac{\partial n_2}{\partial c_y} = 0$ and $n_2 = N$, following [2], let us call/name irregular points. In stated problem $\frac{\partial n_2}{\partial c_y} = 0$ when $c_y = 0$ and many irregular points consist of the finite number of isolated points, since ballistic trajectory with $c_x = c_{x0} = \text{const}$ cannot be uniform overloading. For the solution of problem, we will use the principle of maximum, formulated in work [2]. Designating the conjugated/combined variables of variational problem P_1, P_2, P_3, P_4 , let us extract the Hamiltonian of the expanded system:

$$\begin{aligned} H = P_1 \left[c_y \rho \frac{VS}{2m} + \left(\frac{V}{R+h} - \frac{g}{V} \right) \cos \theta \right] + P_2 V \sin \theta - \\ - P_3 \left(c_x \rho \frac{V^2 S}{2m} + g \sin \theta \right) + \frac{P_4 R V \cos \theta}{R+h}. \end{aligned} \quad (3)$$

accordingly [2], the system of the adjoint equations in the presence of irregular points takes the form

$$\dot{P}_i = -\frac{\partial H}{\partial x_i} + \lambda(t) \frac{\partial n_x}{\partial x_i} + \mu \delta(t-t^*) \frac{\partial n_x}{\partial x_i},$$

where $\lambda(t)$ - Lagrange's factor, not equal to zero when $n_x = N$; $\lambda(t)$ it is set/assumed equal to zero when $n_x \neq N$ and

$$\lambda(t) = \frac{g_0 \left(\frac{P_1}{2} - x P_3 c_y V \right)}{V c_y [1 + 2 x c_x]} \sqrt{c_x^2 + c_y^2},$$

μ - constant; $\delta(t)$ - a delta function, and it is known that $\left. \frac{\partial n_x}{\partial c_y} \right|_{t=t^*} = 0$.

Page 75.

Thus, the system of the adjoint equations can be extracted completely:

$$\begin{aligned} \dot{P}_1 &= P_1 \left(\frac{V}{R+h} - \frac{g}{V} \right) \sin \theta - P_2 V \cos \theta + P_3 g \cos \theta + P_4 \frac{RV \sin \theta}{R+h}; \\ \dot{P}_2 &= P_1 \left[\frac{\beta c_y \rho V S}{2m} + \frac{V \cos \theta}{(R+h)^2} - \frac{2g \cos \theta}{V(R+h)} \right] - \\ &- P_3 \left(\frac{\beta c_x \rho V^2 S}{2m} + \frac{2g \sin \theta}{R+h} \right) + P_4 \frac{RV \cos \theta}{(R+h)^2} + \\ &+ \lambda(t) \frac{\partial n_x}{\partial h} + \mu \delta(t-t^*) \frac{\partial n_x}{\partial h}; \\ \dot{P}_3 &= -P_1 \left(\frac{c_y \rho S}{2m} + \frac{\cos \theta}{R+h} - \frac{g \cos \theta}{V^2} \right) - P_2 \sin \theta + P_3 \frac{c_x \rho V S}{m} - \\ &- P_4 \frac{R \cos \theta}{R+h} + \lambda(t) \frac{\partial n_x}{\partial V} + \mu \delta(t-t^*) \frac{\partial n_x}{\partial V}; \\ P_4 &= 0, \end{aligned} \quad (4)$$

where

$$\frac{\partial n_z}{\partial h} = -\frac{\beta \rho V^2 S}{2 m g_0} \sqrt{c_x^2 + c_y^2},$$

$$\frac{\partial n_z}{\partial V} = \frac{\rho V S}{m g_0} \sqrt{c_x^2 + c_y^2}.$$

from condition $P_4^{(1)} = -1$ and (4) follows $P_4 = -1$ in an entire trajectory. Since at the right end/lead of trajectory t, v, θ are free and system (2) autonomous, $H=0$ and

$$P_1^{(1)} = P_3^{(1)} = 0. \quad (5)$$

Conditions (5) are boundary for system (4):

The solution of two-point boundary-value problem (just as in the regular case [1]) is convenient to reduce to the solution of the problem of Cauchy. It is necessary to assign $P_1^{(0)}$ and $P_3^{(0)}$ also, from condition $H(t_0)=0$ to determine value $P_2^{(0)}$ in accordance with requirements $P_1^{(1)} = P_3^{(1)} = 0$, satisfying simultaneously condition $H(t) \rightarrow \max_{c_y}$ for a problem $L^{(1)} \rightarrow \min$.

However, at irregular point it is required to satisfy supplementary conditions for phase coordinates and the conjugated/combined variables.

From (4) it follows that at irregular point with $t^* < t_1$ $c_y(t^*)=0$, and momentum/impulse/pulses P_2 and P_3 will experience/test jump for value $\mu \frac{\partial n_z}{\partial n}$ and $\mu \frac{\partial n_z}{\partial V}$ respectively (μ - positive constant). Of this,

consists the essential difference for the irregular case from the regular, where all momentum/impulse/pulses are continuous functions in an entire trajectory for limiting the class $g(x, u) \leq 0$.

Page 76.

Work [2] shows, that in optimum trajectory must be carried out the following requirements:

$$\int_{t_0}^{t_1} \lambda(t) dt < +\infty, \quad (6)$$

$$-P_1 + \int_{t_0}^{t_1} \lambda(t) dt = C > 0, \quad (7)$$

where C - a constant value for this family of optimum trajectories.

Requirement (6) leads to the fact that at irregular point in the optimum trajectory where $c_y = 0$ and $n_x = N$, must be $P_1 = 0$. Let us extract the condition of integrability (6):

$$\begin{aligned} \int_{t_0}^{t_1} \lambda(t) dt &= \int_{t_0}^{t_1} \frac{g_0 \left(\frac{P_1}{2} - x P_3 c_y V \right)}{V c_y [1 + 2 x c_x]} V \sqrt{c_x^2 + c_y^2} dt = \\ &= \int_{t_0}^{t_1} \frac{g_0 P_1 V \sqrt{c_x^2 + c_y^2}}{2 c_y [1 + 2 x c_x]} dt - \int_{t_0}^{t_1} \frac{x P_3 g_0 V \sqrt{c_x^2 + c_y^2}}{[1 + 2 x c_x]} dt < \infty. \end{aligned} \quad (8)$$

Using the fact that, as a rule (see below), $\left. \frac{dc_y}{dt} \right|_{c_y=0} \neq 0$, let us examine certain low time interval t , which contains point $c_y = 0$. The

integral, calculated on this range from second term, is limited when $|P_3| < +\infty$. Integral $\int_{t_0}^{t_1} \frac{P_1 g_0 \sqrt{c_x^2 + c_y^2}}{c_y V[1 + 2xc_x]} dt$ will be limited, if when $c_y(t) \rightarrow 0$ and $\frac{dc_y}{dt} \rightarrow \text{const}$ function $P_1(t)$ decreases at least as $P_1(t) \sim c_y^n$ where $n > 0$. Consequently, in the irregular case in the optimum trajectory of zero functions P_1 it must coincide with the point of irregularity.

Condition (7) is the condition of the standardization of momentum/impulse/pulses [$\lambda(t) > 0$, $-P_4 > 0$], essential only in the extreme case when $P_4 \rightarrow 0$.

Let us examine now conditions, which must satisfy phase coordinates at irregular point.

In certain interval $n_x = N$, then there $\frac{d}{dt} n_x = 0$,

$$n_x = \dot{q}(c_x^2 + c_y^2) + c_y \dot{c}_y [1 + 2xc_x] q = 0.$$

At point t^* , where $c_y = 0$, if $|c_y| < \infty$, then value $\dot{q} = 0$.

Thus, in the optimum trajectory, which satisfies all limitations, in point $t^* \in t_1$, $c_y(t^*) = 0$ must be carried out the conditions

$$q = q(N, c_{x0}); \quad \dot{q}(t^*) = 0; \quad P_1(t^*) = 0.$$

Hence it follows that for obtaining the optimum trajectory in the irregular case it is necessary to simultaneously satisfy boundary conditions (4) and conditions (9) at irregular point. But on the cut $[t_0, t^*]$ is formulated the two-point boundary-value problem of the second order; therefore by conditions (9) optimum trajectory for $t_0 < t < t^*$ is determined unambiguously. As a result in the irregular case, the search of optimum trajectory as a whole is reduced to the consecutive search of the cuts of optimum trajectory (two cuts in the presence of one irregular point and $n+1$, if a quantity of points it is equal to n).

Let us examine now the cut of trajectory, which lies to the right of irregular point. In equations (4) value $\dot{P}_1(t^{*+0})$ is determined unambiguously, if with the aid of μ are determined $P_2(t^{*+0})$, $P_3(t^{*+0})$:

$$P_1(t^{*+0}) = P_1(t^{*-0}) + \mu \frac{\partial n_1}{\partial h}; \quad P_2(t^{*+0}) = P_2(t^{*-0}) + \mu \frac{\partial n_2}{\partial V};$$

In expressions $\dot{P}_2(t^{*+0})$ and $\dot{P}_3(t^{*+0})$ we should to set/assume $\delta(t^{*+0})=0$, and the value $\lambda(t^{*+0})$ assign. This does not contradict the conditions of integrability, since discontinuity/interruption $\lambda(t)$ with $t=t^*$ let us allow. Moreover, only because of new free constant it is possible with $t > t^*$ to obtain the family of trajectories with the parameters μ and $\lambda(t^{*+0})$ and to find the extremal, which satisfies conditions (5) or (9), if irregular point is not only.

On the basis of the comparison of the regular and irregular cases, it is possible to call/name conditions (9) the conditions the continuation of extremal, since with their nonperformance occurs the disturbance of limitation $n_2 = N$ and $P_{2,3} \rightarrow \infty$.

During the numerical solution it is important that the assignment μ is equivalent to assignment $P_3(t^*+0)$, and assignment $\lambda(t^*+0)$ - to assignment $P_3(t^*+0)$ (E_2 and P_3 are connected); value $E_2(t^*+0)$ it is determined with the use of relationship/ratio $E_1(t^*+0)=0$ from the equivalent with $t=t^*$ conditions $H=0$ or

$$P_2(t^*+0) - P_2(t^*-0) = \frac{\partial n_2}{\partial n} [P_3(t^*+0) - P_3(t^*-0)] \left(\frac{\partial n_2}{\partial V} \right)^{-1}$$

Since point t^* is the removed singular point for system (4), during the integration of the latter it is necessary point t^* to select for initial, which will simplify the solution of boundary-value problem.

1. Let us assign values of h^* , from conditions (9) let us find V^* , θ^* with known N ; let us assign $P_3(t^*-0)$ and, utilizing $P_1(t^*-0)=0$ and $H(t^*-0)=0$, let us determine $P_2(t^*-0)$ and $E_1(t^*-0)$. However, for integration it is necessary to determine $\lambda(t^*-0)$. Let us show that h^* and $P_3(t^*-0)$ determine value $\lambda(t^*-0)$, connected with limit $\lim_{t \rightarrow t^*-0} \frac{P_1(t)}{c_y(t)} =$
 $= \lim_{t \rightarrow t^*-0} \frac{P_1(t)}{c_y(t)}$. From expression $n_2 = N$ it follows that $n_2 = 0$, i.e.,
 $V \sqrt{c_x^2 + c_y^2} q = N$ and $N^2 \frac{q}{q^3} + c_y c_y (1 + 2\kappa c_1) = 0$, where $q = q(v, h, \theta, c_1)$. Hence when $c_y = 0$ it is possible to obtain

$$\bar{N}^2 \frac{\ddot{q}}{q^3} + \ddot{c}_y^2 (1 + 2xc_x) + \ddot{c}_y c_y |_{c_y \rightarrow 0} (1 + 2xc_x) = 0,$$

where $\ddot{q} = \ddot{q}(c_y, \dot{c}_y, V, h, \theta, c_y, c_x)$.

Page 78.

Considering that with $t < t^* - 0$ the value $|\dot{c}_y| < \infty$, we will obtain expression for $c_y(t^* - 0)$ in the form of function v^*, h^*, θ^* let us determine $\lambda(t^* - 0)$. Relationship/ratio $n_y = 0$ shows that the function $\dot{c}_y(t)$ can be disruptive. Thus, from the family of trajectories, determined by parameter $h^*, P_3(t^* - 0)$, it is possible to select the trajectory, which satisfies conditions $V(h^{(0)}) = V^{(0)}$ and $\theta(h^{(0)}) = \theta^{(0)}$.

Virtually, in view of the instability of the solution of system (2), are convenient to enter somewhat otherwise.

2. Let us assign value of \hat{h} (or \hat{t}), that satisfies condition $h^{(0)} < \hat{h} < h^*$. Then the cuttings off of trajectory in the band $[\hat{h}, h^*]$ it is possible to obtain by integration to the left from irregular point, and cut $[h^{(0)}, h]$ - by integration on right. At point \hat{t} , all variables must be the continuous functions:

$$\hat{t}^+ = \hat{t}^-; \hat{V}^+ = \hat{V}^-; \hat{P}_1^+ = \hat{P}_1^-; \hat{P}_3^+ = \hat{P}_3^- \quad (10)$$

[from condition $H(\hat{t}) = 0$ follows that $\hat{P}_2^+ = \hat{P}_2^-$].

Let us note that the expanded system is autonomous and time assign/prescribed, but coordinate 1 cyclic; therefore conditions $\hat{L}^+ = \hat{L}^-$ and $\hat{t}^+ = \hat{t}^-$ can satisfied separately from (10).

During appropriate selection $P_1^{(0)}, P_3^{(0)}, (F_3(t^*-0), h^*,$ it is possible to satisfy the condition (10) by the numerical solution of four-parameter boundary-value problem.

Some special cases of the principle of maximum (minimum).

Let us examine the system of adjoint equations (4).

1. If optimum trajectory is regular, then $\mu\delta(t-t^*)=0$.

If we in this trajectory assume $P_4 \equiv 0$, then on the basis of boundary conditions (5), of equality $H \equiv 0$ and of equations (4) we will obtain $P_1 = P_2 = P_3 = P_4 \equiv 0$ in an entire trajectory (i.e. during this standardization the principle of maximum (minimum) it is satisfied trivially). Consequently, in the regular case in optimum trajectory for problems $L^{(0)} \rightarrow \min$ and $L^{(0)} \rightarrow \max$. are functions $P_4 \neq 0$ [1].

2. Let optimum trajectory in question in problem $L^{(0)} \rightarrow \min$ be irregular and $P_4 \equiv 0$. Of irregular point can be determined to the left the conjugated/combined vector $(P_1, F_2, P_3, 0)$, to which is

superimposed a series of the limitations, following from boundary conditions.

With $t > t^*$, there are two possibilities: 1. motion without output into new irregular point; 2. Movement by output into irregular point.

In the case of 1, must be $P_1^{(1)} = P_3^{(1)} = 0$, $H = 0$, i.e., $P_2^{(1)} = 0$ and, thus, $\dot{P} = 0$ with $t > t^*$. As a result the selection of control with $t > t^*$ with the use of principle of maximum (i.e. the first variation in the functional) is impossible. Further, since $P_1(t^*+0) = P_3(t^*+0) = 0$ by said force, for a problem $L^{(1)} \rightarrow \min$ we will obtain:

$$P_3(t^* - 0) = -\mu \frac{\partial n_2}{\partial V}; \quad P_2(t^* - 0) = -\mu \frac{\partial n_2}{\partial h} \quad (\text{r.e. } \mu > 0).$$

Page 79.

Hence and from (4) follows $P_1(t^*-0) < 0$, and consequently, $P_1(t^*-\varepsilon) > 0$ when $\varepsilon > 0$. Therefore during the solution of problem on $L^{(1)} \rightarrow \min$ $c_y(t^*-\varepsilon) > 0$. Conditions $q = GN / c_{y0} S$, $q = 0$ at irregular point uniquely determine $V(t^*0)$, $\theta(t^*-0)$ and relation $\frac{P_2(t^*-0)}{P_3(t^*-0)}$ with assigned/prescribed h^* and N . Selecting correspondingly h^* and N for the left segment of trajectory, it is possible to satisfy conditions $V(h^{(0)}) = V^{(0)}$ and $\theta(h^{(0)}) = \theta^{(0)}$, where $h^{(0)}$ — initial height/altitude of machine. [Analogous examination is obtained for a problem on $L^{(1)} \rightarrow \max$. [1] taking into account condition $P_3(t^*-0) = \mu \frac{\partial n_2}{\partial V}$ and $P_2(t^*-0) = \mu \frac{\partial n_2}{\partial h}$].

Let us designate value N , obtained as a result of the solution of boundary-value problem for the left cut of trajectory, through N_0 . In this case, it is obvious that with $N=N_0$ the cut of trajectory, which lies to the left of irregular point, will be identical for problems to the minimum and to the maximum of distance and represents by itself the solution of the problem of the minimum of maximum overload with given ones $V^{(0)}, \theta^{(0)}$ [2]. The stability of trajectory in this case is determined not by functional L , but by limitation $n_z \leq N_0$.

Problem to the minimum of maximum overload can be solved and in another manner. Let us be in the process of the solution of problem on $L^{(1)} \rightarrow \min$ (or $L^{(1)} \rightarrow \max$. [1]) monotonically change N to the side of decrease with given ones $V^{(0)}, \theta^{(0)}$. In this case, the initial values $P_1^{(0)}, P_3^{(0)}$ will grow in absolute value. Based on (7) value P_4 will decrease with increase $\int_{t_0}^{t_1} \lambda(t) dt$. It is clear that there is lower bound N , which depends on $V^{(0)}, \theta^{(0)}, c_x, c_y$ and determines those, that the problems in question have solution, i.e., $\inf N = N_0$ [2].

The second possibility (case 2) lies in the fact that there is several irregular points. Conditions at the irregular point, nearest toward the end of the trajectory, are described above; let us note that in this case when assign/prescribed $V^{(0)}, \theta^{(0)}$ value N_0 is determined by last/latter irregular point. It is real/actual, if at

penultimate irregular point momentum/impulse/pulses P_2 and P_3 abruptly turn into zero (i.e. N_0 is defined by penultimate point $N_0 = N_0^{(n-1)}$), then for the selection of the continuation of optimum trajectory there remains only one parameter $\lambda(t_{n-1}^* + 0)$, while for satisfaction of conditions (9) in t_n^* taking into account limitation $N_0^{(n-1)}$ are required two parameters. Hence it follows that only by selecting by special form $V^{(0)}$ or $\theta^{(0)}$ it is possible in principle to ensure conditions (9) at two irregular points in a row (it is not more than in three, selecting and $V^{(0)}$, and $\theta^{(0)}$). The number of outputs into the irregular points, placed is more left than the last/latter point, at which is assigned value $N=N_0$, it is in practice determined with the use of conditions $V(h^{(0)}) = f_1(h_n^*, N) = V^{(0)}$, $\theta(h^{(0)}) = f_2(h_n^*, N) = \theta^{(0)}$.

It is obvious, there are initial values $V^{(0)}$, $\theta^{(0)}$ such, that with $N=N_0$, $h^*=h^{(1)}$. In this case in an entire trajectory, is determined the nonzero conjugated/combined vector, since the irregular point coincides with the end/lead of the trajectory.

Page 80.

Procedure and the results of the numerical determination of optimum trajectories in the irregular case.

During obtaining of the left cut of trajectory in problem on

$L^{(1)} \rightarrow \min$ was solved the four-parameter boundary-value problem of the selection of values $P_1^{(0)}, P_3^{(0)}, h^*, P_3(t^*-0)$ for the satisfaction of conditions (10) at point \hat{h} . As the function of discrepancy, was examined value

$$\varphi(\hat{h}) = \left[(\hat{\theta}^+ - \hat{\theta}^-)^2 + \left(\frac{\hat{V}^+ - \hat{V}^-}{V^{(0)}} \right)^2 + (\hat{P}_1^+ - \hat{P}_1^-)^2 + (\hat{P}_3^+ - \hat{P}_3^-)^2 \right]^{\frac{1}{2}}.$$

From the continuity condition of the variables indicated at point \hat{h} , it follows that $\varphi(\hat{h}) = 0$. Virtually during the solution of the problem of zero functions $\varphi(\hat{h})$ it was checked with an accuracy to 10^{-5} . Since the derivative $\frac{d\varphi(\hat{h})}{dt}$ contains clearly control, surface $\varphi[\hat{h}, P_1^{(0)}, h^*, P_3(t^*-0)]$ has complex structure. The analysis of the structure of this surface was carried out by the method of gradient. In this case, it turned out that $\varphi[\hat{h}]$ has several local minimums. After the selection of the smallest minimum with the use of Newton's method [3] was satisfied condition $\varphi(\hat{h}) \leq 10^{-5}$. The search of solution $P_{1,3}^{(0)}(N_i), h^*(N_i), P_3(t^*-0, N_i)$ during known solutions $P_{1,3}^{(0)}(N_i), h^*(N_i), P_3(t^*-0, N_i)$ ($i=1, 2, 3$) was fulfilled with the use of gradient method [1] and of quadratic extrapolation. Further this solution was more precisely formulated according to Newton's method [3]. On the right cut of trajectory, was solved the biparametric boundary-value problem of the search of the initial conditions $P_3(t^*+0)$ and $\lambda(t^*+0)$ for satisfaction of conditions (5). Fig. 2, gives the results of trajectory calculation $L^{(1)} \rightarrow \min$ for $N=10$, $\theta^{(0)} = -3^\circ, 8$, $V^{(0)} = 7900$ m/s. It is evident that there is a time interval t , where $c_v(t) > 0$. Limitation to overload leads to the redistribution of the

resource/lifetimes of control. During decrease of N time interval where $c_y(t) > 0$, grow/rises. In this case, the flying range increases.

Overload N_0 , which corresponds $\min \max_{c_y(t) t} n_z$, is obtained by the method of solution of the four-parameter boundary-value problem of the selection of values $P_{1,3}^{(0)}$, $h(h^*)$, h^* . As a result of the solution of this problem, is obtained $N_0 = 3.334$ with $V^{(0)} = 7900$ m/s and $\theta^{(0)} = -3^\circ$, 8 (Fig. 3).

As has already been indicated that with $N = N_0$ optimum control is determined only on the part of the trajectory to the left of irregular point, and the to the right conjugated/combined vector is identically equal to zero. On the right cut of trajectory, the functional can be any. In Fig. 3, solution of the problem of search $N_0 = 3.334$ is conjugate/combined with the solution of problem $L^{(1)} \rightarrow \min$ with $h < h^* = 0.0399R$; it was assumed that $P_A = -1$ for $t > t^*$. Let us note that with $\theta < -\pi/2$ the functional begins to decrease, in this case, the lift acts against the gravitational force of machine.

Pages 81-82.

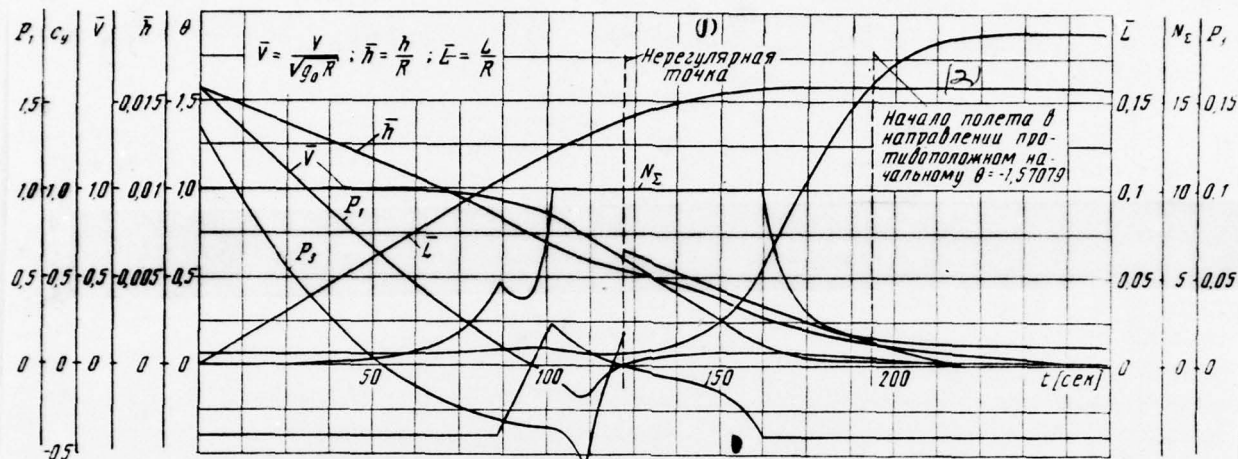


Fig. 2.

Key: (1). Irregular point. (2). Beginning of flight in direction opposite initial $\theta = -1.57079$.

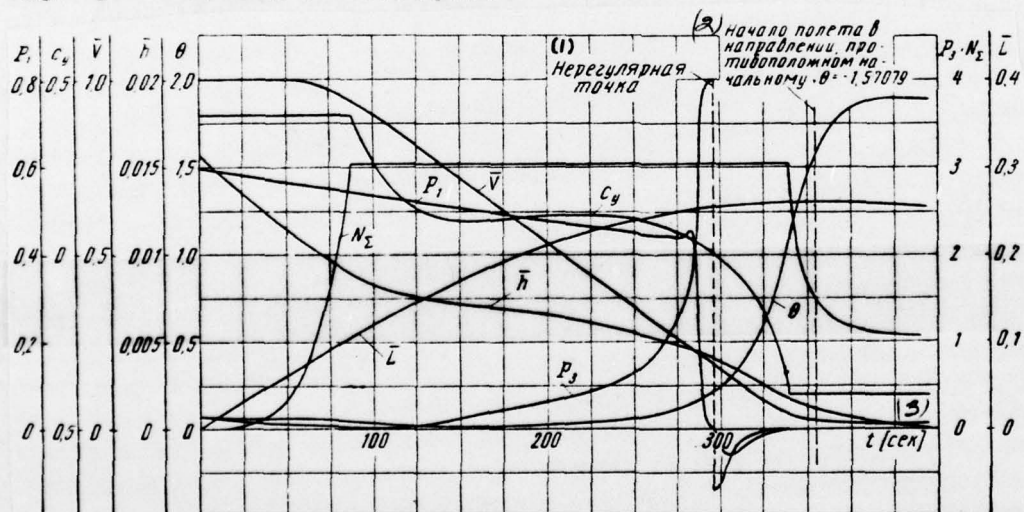


Fig. 3.

Key: (1). Irregular point. (2). Beginning of flight in direction, opposite to initial, $\theta = -1.57079$. (3) s.

Page 83.

The final part of the trajectory represents by itself gliding/planning with constant angle $\theta = -\arctg k$.

Fig. 4, gives the results of the calculation of the maneuverability capabilities of machine with $V^{(0)} = 7900$ m/s and $\theta^{(0)} = -3^\circ$, & according to the data of the calculation of regular and irregular optimum trajectories [1].

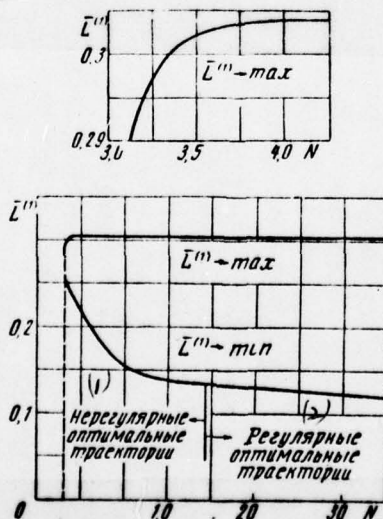


Fig. 4.

Key: (1). Irregular optimum trajectories; (2). Regular optimum trajectories.

The authors thank A. A. Milyutina for numerous conversations and a series of valuable indications for this work.

REFERENCES

1. V. V. Dikumar, A. A. Shilov. Optimization of the flying range of vehicle in the atmosphere taking into account limitations to complete overload. "Scientific notes of TsAGI [- Central Institute of Aerohydrodynamics in. N. Ye Zhukovskiy", Vol. 1, No 2, 1970.

2. A. Ya. Dubovitskiy, A. A. Milyutin. Necessary conditions of weak extremum in the problems of optimum control with special limitations of the type of inequality. ZhVM and MF No 4, 1968.

3. V. K. Isaev, V. V. Sonin. On one modification of Newton's method of the numerical solution of boundary-value problems. ZhVM and MF, Vol. 3, No 6, Pages 1114-1116, 1961.

Received 28 April 1969.

Page 84.

EQUATIONS OF ROLLING OF AN ELASTIC TIRE.

V. S. Gozdek.

Is examined communication/connection between the motion of the wheeling wheel with elastic busbar/tire and reaction to it from the side of the earth/ground under the assumption about the absence of the slippage of the surface of busbar/tire relative to the earth/ground. It is shown, that this problem mathematically is formulated without the enlistment of supplementary hypotheses about the mechanism of the rolling of busbar/tire. Is presented the method of the composition of the equations, which approximately characterize the process of the rolling of wheel.

The study of the character of the motion of auto or aircraft with its landing run along the earth/ground, the shimmy of the wheels of an auto or aircraft and series of other phenomena is inseparable from the investigation of the forces, which act from the side of the earth/ground to the busbar/tires of the wheeling wheels. Let us pause at the explanation of communication/connections between the motion of the housing of the wheeling wheel and the reaction to elastic

busbar/tire from the side of the earth/ground in the case when this reaction contains the comprising, located in plane earth/ground.

During the composition of the equations of the rolling of busbar/tire, usually it is assumed that the material of busbar/tire is ideally elastic. This assumption makes it possible to express effect on the wheel through the shift of its relatively housing of the section of the surface of busbar/tire, adjacent at this torque/moment to the earth/ground. Furthermore, they accept, that the rolling of busbar/tire occurs without the slippage of its surface relative to the earth/ground. With this assumption between the motion of the housing of wheel by the shift relative to it lying/horizontal on the earth/ground points of the surface of busbar/tire there is definite dependence, which, however, does not form the closed system of equations. For obtaining the closed system of equations of the rolling of elastic busbar/tire, are accepted different hypotheses about the existence of the additional constraint between as those composing the strains of the wheeling busbar/tire. Widest use received the hypothesis of rolling, introduced by M. V. Keldysh [1], and the hypothesis of lateral tilt [2].

Page 85.

Let us show that the process of the rolling of elastic

busbar/tire can be represented in the solution of boundary-value problem for the equations of the stressed state of busbar/tire without the introduction of the additional constraints between the components of its strain. To the same question is dedicated work [3]; however, in it the results presented are used only in the case of the rougher schematization of busbar/tire.

Let the wheel, which consists of undeformable housing and elastic busbar/tire, rectilinearly to roll along flat/plane undeformable surface with a constant velocity of v , being found under constant external load. Let us call/name this action of wheel that not disturbed. Let us introduce the rectangular coordinate system $Oxyz$ whose axle/axis Ox is parallel to the earth/ground and lie/rests at the center-line plane of the housing of wheel on constant distance from its center, but axle/axis Oy it passes through the center of wheel (Fig. 1). Furthermore, let us introduce driving/moving at a rate of v rectangular coordinate system $O'x'y'z'$, after arranging axle/axes $O'x'$ and $O'z'$ on the earth's surface and after directing axle/axis $O'x'$ in the direction, opposite to the velocity vector of the undisturbed motion. Let during the undisturbed motion the corresponding axle/axes of both coordinate systems coincide, the housing of wheel rotates with angular velocity ω_0 , and the reduction of busbar/tire is equal f_0 .

Let us describe the disturbed motion of the housing of wheel by the following values: the rate $V_x(t)$ of point C along os $O' x'$, where t - time, by the rate $V_z(t)$ of the same point along axle/axis $O' z'$, by shift $f(t)$ of the center of wheel along axle/axis $O' y'$, by an increase $\omega_z(t)$ in the angular velocity ω_0 , by angle $\theta(t)$ between the axle/axes $O' x'$ and Ox , and also the angle $\psi(t)$ between axle/axes $O' y'$ and Oy . The components of the disturbed motion of the housing of wheel together with the derivatives $\dot{f}(t)$, $\dot{\theta}(t)$ and $\dot{\psi}(t)$ let us consider the small first-order quantities.

Let during the undisturbed motion to us be known the motion of each point of busbar/tire relative to the housing of wheel in the form of the function of angle γ between the axle/axis Oy and the connected with the housing of wheel vector \vec{E} , which lie at plane xOy (see Fig. 1). It is expressed shift relative to the housing of the wheel of the points of the turned to the earth/ground part of the surface of busbar/tire during the disturbed motion through shift $u(x, z, t)$ of these points along axle/axis Ox , shift $v(x, z, t)$ along axle/axis Oy and shift $w(x, z, t)$ along axle/axis Oz from the position which they occupied at the same value of angle γ in the process of the undisturbed motion.

Let us assume that with the rolling of the busbar/tire of point of its surface, being located in the contact zone with the

AD-A066 206

FOREIGN TECHNOLOGY DIV WRIGHT-PATTERSON AFB OHIO
SCIENTIFIC NOTES FROM THE CENTRAL AERO-HYDRODYNAMIC INSTITUTE (--ETC(U)
AUG 78

F/G 20/4

UNCLASSIFIED

FTD-ID(RS)T-1039-78

NL

3 of 4

AD
A066206



earth/ground, they do not slip relative to the earth/ground. Let us select certain point of busbar/tire, which lies at torque/moment t_0 on the earth's surface and having in system $O' x' y' z'$ coordinates x'_0, z'_0 . After time interval Δt , the same point of busbar/tire, without moving relative to the earth/ground, will have coordinates $x'_0 + V\Delta t, z'_0$.

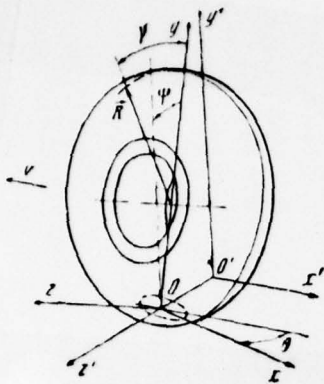


Fig. 1.

Page 86.

Considering interval Δt small, it is expressed the shift of this point through the components of the disturbed motion of the housing of wheel and the comprising shifts of bush/tire $u(x, z, t)$ and $w(x, z, t)$:

$$\left. \begin{aligned} V_x \Delta t + (\omega_0 + \omega_z) \frac{V}{\omega_0} \Delta t - z_0 \dot{\theta} \Delta t + \frac{\partial u}{\partial x} \Delta x_0 + \frac{\partial u}{\partial t} \Delta t + O(\delta^3) &= V \Delta t; \\ V_z \Delta t + x_0 \dot{\theta} \Delta t + \theta \Delta x_0 + \frac{\partial w}{\partial x} \Delta x_0 + \frac{\partial w}{\partial t} \Delta t + O(\delta^3) &= 0, \end{aligned} \right\} \quad (1)$$

where x_0 , z_0 and Δx_0 - respectively the coordinate of the selected point at torque/moment t_0 and to change in value x_0 in system $Oxyz$, and δ - low value.

Transfer/converting in system (1) to limit with tendency toward zero time interval Δt and of the components of the disturbed motion

of wheel, we will obtain the differential equations of the form:

$$V \frac{\partial u}{\partial x} + \frac{\partial u}{\partial t} + V_x + \frac{V}{\omega_0} \omega_z - z\dot{\theta} = 0; \quad (2)$$

$$V \frac{\partial w}{\partial x} + \frac{\partial w}{\partial t} + V_z + V\theta + x\dot{\theta} = 0. \quad (3)$$

The unknown function $v(x, z, t)$ in the zone of contact of busbar/tire with the earth/ground is expressed as functions $f(t)$ and $\psi(t)$:

$$v(x, z, t) + f(t) + z\psi(t) = 0. \quad (4)$$

Thus, the shift of the points of the surface of the wheeling without slippage busbar/tire in the zone of its contact with the earth/ground is subordinated to relationship/ratios (2)-(4). It is not difficult to be convinced of the fact that these relationship/ratios are not still determined completely the process of the rolling of elastic busbar/tire.

Considering busbar/tire consisting of ideally elastic and the which does not possess inertia material, let us pause at the special feature/peculiarities of its strair in the case when wheel is not rolled, but its busbar/tire is pressed to the earth/ground by certain force. Let at first the location of all points of busbar/tire relative to the housing of wheel coincide with their location at certain moment of the undisturbed motion. let us displace the housing of wheel from this position. Let in this case the concerning earth/ground of the point of the surface of busbar/tire remain

actionless. As a result the busbar/tire will occupy new position of equilibrium, while in the zone of contact of busbar/tire with the earth/ground, will occur a change in external normal and tangential load. The components $u(x, z)$ and $w(x, z)$ the shift of busbar/tire together with their first-order derivatives in x and z will be continuous everywhere, with the exception/elimination of the line, which limits the zone of contact of busbar/tire with the earth/ground where the derivatives $\frac{\partial u}{\partial x}$, $\frac{\partial u}{\partial z}$, $\frac{\partial w}{\partial x}$ and $\frac{\partial w}{\partial z}$ can have a first-order discontinuity.

The form of the equilibrium of busbar/tire and the law of load distribution on it from the side of the earth/ground under assigned/prescribed displacement law relative to the housing of the wheel of the points of the part of its surface in principle can be always determined by the method of the theory of elasticity. We will not concern here this problem, set/assuming known the components of reaction to wheel from the side of the earth/ground and strain components in all points of busbar/tire, if is known shift relative to the housing of the wheel of all tangents to the earth/ground of the points of its surface.

Page 87.

Let us turn to the special feature/peculiarities of the strain

of the wheeling busbar/tire near the line, which limits the zone of its contact with the earth/ground. On interface in this case, occur two processes. On the part of the boundary, the material of the wheeling busbar/tire fits closely to the earth/ground. Let us call it leading edge of contact. On the remaining part of the boundary, called subsequently trailing edge of contact, the surface of busbar/tire will move away from the earth/ground.

Let us show that with the introduced by us assumptions the derivatives $\frac{\partial u}{\partial x}$, $\frac{\partial u}{\partial z}$, $\frac{\partial w}{\partial x}$ and $\frac{\partial w}{\partial z}$ will be continuous at the leading edge of contact. Let us isolate infinitesimal cell/element of busbar/tire, one of faces of which it is formed by the points of its surface (Fig. 2). Let fin/edge AB at torque/moment t_0 coincide with the leading edge of contact and further, being located in the contact zone, it is not moved relative to the earth/ground, but fin/edge CD becomes motionless from the torque/moment of time $t_0 + \Delta t$. Let us visualize that derivatives indicated above have a first-order discontinuity at the leading edge of contact. Let, for example, at moment t_0 of the value of derivative $\frac{\partial u}{\partial x}$ in the vicinity of point A to the left and to the right of fin/edge AB, i.e., inside and out of the zone of contact of busbar/tire with the earth/ground, they differ to the first-order degree of smallness. Let us conduct on the earth's surface axle/axis \widetilde{Ax} , which coincides in the direction with axle/axis Ox at torque/moment t_0 . In this case point D during time interval Δt

must move along axle/axis $\tilde{A\tilde{x}}$ up to the distance of the second order of smallness. Let us note that for the same time the shift of point D along axle/axis $\tilde{A\tilde{x}}$, caused by a change in the strain of the free from external surface load of busbar/tire, is expressed by the small third-order quantity. Consequently, before cohesion/coupling of the surface of busbar/tire with the earth/ground to this surface must act the external load, directed along axle/axis $\tilde{A\tilde{x}}$ and calling the local slippage of busbar/tire relative to the earth/ground. However, this process would contradict the law of friction, since the direction of the slippage of busbar/tire in this case proves to be coinciding with the direction of the action of external load. Hence it follows that at the leading edge of the contact of the wheeling without slippage elastic busbar/tire the derivatives $\frac{\partial u}{\partial x}$, $\frac{\partial u}{\partial z}$, $\frac{\partial w}{\partial x}$ and $\frac{\partial w}{\partial z}$ must remain continuous.

The existence of the first-order discontinuity of these derivatives at trailing edge of contact, the giving rise to slippage of the surface of the busbar/tire before its departure/withdrawal from the earth/ground, is located in accordance with the law of friction. Under the actual conditions when functions u and w , take some finite values, trailing edge of contact represents by itself not line, but the band, in which the surface of busbar/tire slips relative to the earth/ground, but the external tangential load is gradually decreased to zero. Nevertheless we will disregard the

influence of the slippage of the surface of the busbar/tire before the departure/withdrawal from the earth/ground and will consider conditions (2) and (3) carried out in an entire contact zone.

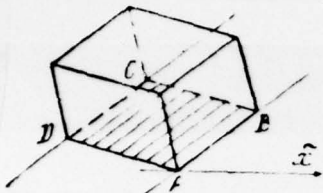


Fig. 2.

Page 88.

Thus, with the introduced assumptions the increase in the reaction to the wheeling busbar/tire, given rise to the disturbed motion of the housing of wheel, is determined by the solution of the equations of the stressed state of the quiescent busbar/tire, which has with the earth/ground the constant/invariable contact zone, if are satisfied the following boundary conditions:

1. The displacement of the points of busbar/tire, which lie on the housing of wheel, is equal to zero.
2. To surface of busbar/tire, which is located beyond limits of zone of its contact with earth/ground and clear housing of wheel, does not act external load.
3. Displacement of points of surface of busbar/tire within

contact zone with earth/ground is subordinated to relationship/ratios (2)-(4).

4. On part of interface, which corresponds to leading edge in process of rolling of busbar/tires, derivatives $\frac{\partial u}{\partial x}$, $\frac{\partial u}{\partial z}$, $\frac{\partial w}{\partial x}$ and $\frac{\partial w}{\partial z}$ remain continuous.

The formulated problem is represented by very complex; therefore let us point out to one of the methods of the composition of the closed system of ordinary differential equations, which approximately characterizes the process of the rolling of elastic busbar/tire. Let us present function u and w on the section of the surface of busbar/tire within the contact zone in the form of the polynomials:

$$\left. \begin{aligned} u &= \sum x_{ij}(t) x^i z^j; \\ w &= \sum \beta_{kl}(t) x^k z^l; \end{aligned} \right\} \quad (5)$$

$$i = 0, 1, 2, \dots, m; j = 0, 1, 2, \dots, n;$$

$$k = 0, 1, 2, \dots, p; l = 0, 1, 2, \dots, q,$$

where $x_{ij}(t)$ and $\beta_{kl}(t)$ - the unknown functions of time.

Let us designate through $u_{ij}(x, z)$, $w_{ij}(x, z)$ and $u_{kl}(x, z)$, $w_{kl}(x, z)$ the components of the shift of the points of the floating surface of the busbar/tire when within the zone of contact of the point of busbar/tire are displaced respectively according to the laws: $u = x^i z^j$, $w = 0$ and $u = 0$, $w = x^k z^l$.

Let us present function u and w on the section of the surface of busbar/tire out of the zone of its contact with the earth/ground in the following form:

$$\left. \begin{aligned} u &= \sum_{ij} \alpha_{ij}(t) u_{ij}(x, z) + \sum_{kl} \beta_{kl}(t) u_{kl}(x, z) + f(t) u_f(x, z) + \\ &\quad + \psi(t) u_\psi(x, z); \\ w &= \sum_{ij} \gamma_{ij}(t) w_{ij}(x, z) + \sum_{kl} \delta_{kl}(t) w_{kl}(x, z) + f(t) w_f(x, z) + \\ &\quad + \psi(t) w_\psi(x, z); \\ i &= 0, 1, 2, \dots, m; \quad j = 0, 1, 2, \dots, n; \\ k &= 0, 1, 2, \dots, p; \quad l = 0, 1, 2, \dots, q. \end{aligned} \right\} \quad (6)$$

Here u_f , u_ψ , w_f and w_ψ - comprising shifts, given rise to the shift of the housing of wheel along axle/axis $O^* y^*$ up to single distance and its rotation relative to axle/axis $O^* x^*$ to the unit angle (see Fig. 1). Given ones in the form (5) and (6) of function u and w satisfy the equations of the stressed state of busbar/tire with the observance of the first and the second of the boundary conditions indicated. Let us subordinate approximately to function u and w to remaining boundary conditions.

Page 89.

Let us isolate in the zone of contact of busbar/tire with lines $n+1$ earth/ground, parallel to line $z=0$. Let us note on each line on $m+1$ points, after arranging on one of them on the leading edge of contact. Let us require continuity the derived $\frac{\partial u}{\partial x}$ and $\frac{\partial u}{\partial z}$ in $n+1$ selected points of the leading edge of contact and satisfaction of the conditions, dictated by equation (2) in the others $m(n+1)$ the

selected points.

First-order derivatives on x and z of assigned/prescribed in the form expressions (5) and (6) of functions u and w have on the band edge of the contact of busbar/tire with the earth/ground as in the examined above load case of motionless busbar/tire, a first-order discontinuity. A difference in the values of these indicated derivatives of both sides of interface in each of its points is expressed by linear function of variables $\sigma_{ij}(t)$, $\beta_{kl}(t)$, by $f(t)$ and $\psi(t)$. That means that the continuity of derivatives $\frac{\partial u}{\partial x}$ and $\frac{\partial u}{\partial z}$ at $n+1$ points of interface can be reached by introduction $n+1$ of the linear dependences between these variables, since in the direction of tangent to interface derivative of function u remains of the continuous because of the continuity function itself u .

As a result we will obtain $n+1$ algebraic $n(n+1)$ of differential linear equations, containing $(n+1)$ $(n+1)$ functions $\sigma_{ij}(t)$ and $(p+1)$ $(q+1)$ functions $\beta_{kl}(t)$. Entering thus with respect to composing shifts w , it is possible to obtain $(p+1)$ $(q+1)$ the equations, which contain the same variables.

Using the method presented, let us comprise the more precise equations of the rolling of busbar/tire in comparison with those obtained in work [1].

Because of the symmetry of busbar/tire, the processes of its longitudinal and transverse disturbed motion are not connected, if the parameters of the disturbed motion are low. The transverse motion of the housing of wheel is characterized by variables $V_z(t)$, $\theta(t)$ and $\psi(t)$.

Function u in this case must be skew-symmetric, and function w - symmetrical relative to axle/axis Cx . Assuming that in expressions (5) $m=1$, $n=1$, $p=2$, $q=0$, let us assign function u and w within the contact zone in the following form:

$$\begin{aligned} u &= z [\sigma(t) - \varphi(t)] + xz [\chi(t) - \varepsilon(t)]; \\ w &= \lambda(t) + x [\sigma(t) + \varphi(t)] + \frac{x^2}{2} [\chi(t) + \varepsilon(t)]. \end{aligned} \quad (7)$$

The unknown functions of time $\lambda(t)$ and $\sigma(t)$ here express the action of contact surface as rigid body, and functions $\sigma(t)$, $\varepsilon(t)$ and $\chi(t)$ - strain of busbar/tire in the contact zone. Let us require so that functions (7) would satisfy equations (2) and (3) in the vicinity of point with coordinates $x=0$, $z=0$ with an accuracy to small order x^2+z^2 . This gives rise to following communication/connections between variables, entering relationship/ratios (7), (2) and (3):

$$\begin{aligned} V(\varphi + \sigma) + \dot{\lambda} + V_z + V\theta &= 0; \\ V\varepsilon + \dot{\varphi} + \dot{\theta} &= 0; \\ V\chi + \dot{\sigma} &= 0. \end{aligned} \quad (8)$$

Page 90.

Representing function u and w beyond the limits of the zone of contact of busbar/tire with the earth/ground, just as in expressions (6), let us draw nearer at the leading edge of contact derivatives

$\frac{\partial u}{\partial x}$, $\frac{\partial u}{\partial z}$, $\frac{\partial w}{\partial x}$ and $\frac{\partial w}{\partial z}$ the continuous, retaining equal to zero value of their discontinuity/interruption at the point of intersection of leading front with line $z=0$ with an accuracy to small order z^2 . The last/latter requirement, equivalent to the equality of derivatives $\frac{\partial^2 u}{\partial x \partial z}$ and $\frac{\partial w}{\partial x}$ from two sides of interface in the vicinity of the point indicated, leads to the appearance of two presented below linear dependences between variables, entering expression (7), and with function $\psi(t)$:

$$\left. \begin{aligned} \varepsilon &= a_1 \lambda + a_2 \varphi + a_3 \sigma + a_4 \psi, \\ \chi &= a_5 \lambda + a_6 \varphi + a_7 \sigma + a_8 \psi, \end{aligned} \right\} \quad (9)$$

where a_1 - a_8 - constant, determined by strain busbar/tires during the shift of its points in the contact zone according to the assigned/prescribed laws. Relationship/ratios (8) and (9) form the closed system of equations, which relate the parameters of the transverse disturbed motion of the housing of wheel with the components of the shift of the points of busbar/tire in the zone of its contact with the earth/ground. The components of reaction to wheel from the side of the earth/ground in this case are expressed by the linear functions of variables, that participate in equations (9).

The system of equations, which approximately characterizes the process of the rolling of busbar/tire during its longitudinal disturbed motion, can be obtained by the same path. Let us assign within the zone of contact of function u and w of which the first now must be symmetrical, and the second skew-symmetric relative to line

$z=0$, in the form

$$u = \xi(t) + x\mu(t); \quad w = 0, \quad (10)$$

where $\xi(t)$ the shift the contact zone lengthwise as of rigid body, $\mu(t)$ - deformation of the material of busbar/tire lengthwise.

Let functions (10) satisfy equations (2) and (3) at point with coordinates $x=0$, $z=0$. Then between variables $\xi(t)$, $\mu(t)$ and the parameters of the disturbed motion of the housing of wheel there is the dependence

$$V_u + \dot{\xi} + V_x + \frac{V}{\omega_0} \omega_z = 0. \quad (11)$$

Let us present function u and w beyond the limits of the contact zone in the form, analogous (6), and let us require the equality of derivatives $\frac{\partial u}{\partial x}$ from both sides of interface in the vicinity of the point of intersection of leading edge with line $z=0$. This leads to the appearance of a linear dependence between variables $\xi(t)$, $\mu(t)$ and $f(t)$:

$$\mu = b_1 \xi + b_2 f, \quad (12)$$

where b_1 and b_2 - constants.

Relationship/ratios (11) and (12) represent by themselves the closed system of equations of the rolling of busbar/tire. The components of reaction to wheel from the side of the earth/ground in

the case in question are expressed linearly through variables, entering equation (12).

Page 91.

In conclusion let us point out to some differences in the processes of the rolling of elastic busbar/tire, characterized by the obtained here equations and the equations, given in work [1]. Let us examine the steady rectilinear rolling of the busbar/tire when the center-line plane of the housing of wheel is turned with respect to velocity vector to angle θ_0 . According to the equations of the rolling of busbar/tire, presented in work indicated above, to busbar/tire under these conditions, must act the same moment of the forces of relatively vertical axle/axis, that also during the rotation of the zone of contact of the quiescent busbar/tire to angle θ_0 relative to the housing of wheel. The value of the same torque/moment, found on the basis of equations (8) and (9), will render/show another, since due to that composing shifts ϵ , that considers shearing strain in the adjacent to the earth/ground part of the busbar/tire, value ϵ and θ_0 will not be equal to each other.

Equations (11) and (12) differ from the taken in work [1] conditions of the rolling of busbar/tire in the case of the longitudinal disturbed motion of wheel by presence in terms of that

composing the shifts of the points of the busbar/tire, designated through $\mu(t)$. Because of this supplement of equation (11) and (12) they reflect the fact of the change in the angular velocity of steady run of the housing of the wheeling wheel under effect of the applied to busbar/tire from the side earth/ground of column load. During the fluctuations of the housing of the wheeling wheel lengthwise or during its angular oscillations relative to rotational axis the acting on busbar/tire from the side of the earth/ground longitudinal force, found on the basis of equations (11) and (12), scatters energy of these fluctuations, which is also connected with the characterizable function $\mu(t)$ by the stretch deformation of busbar/tire in the contact zone.

REFERENCES

1. M. V. Keldysh. Shimmies of the front/nose wheel of tricycle gear. Transactions of TsAGI, No 564, 1945.
2. Yu. N. Neymark, N. A. Pufayev. Dynamics of nonholonomic systems. M., "science", 1967.
3. V. S. Gozdek. To the formulation of the problem of interaction with wheel wheeling earth/ground with elastic busbar/tire during its fluctuations. IAS USSR, 1969, No 5.

THE ACCOUNT OF EXPERIENCE IN OPERATION DURING THE DETERMINATION OF
THE SERVICE LIFE OF CONSTRUCTION.

V. D. Il'ichev.

Page 92.

On the basis of the hypothesis of the linear addition of fatigue failures, is developed the procedure for calculation of the current safe service life of construction and its prolongation without the excess of the assigned/prescribed probability of emergency in park/fleet. Is provided for the use only of not current given full-scale measurements of loads and results of laboratory tests for durability, but also the statistics of the current coating in park/fleet, including leaders's coating.

The proposed method of calculation of the permissible prolongation of the current safe service life of construction (BSS) according to the conditions of fatigue life is instituted on use besides usual given supplementary statistical information. Are

considered the data on the current distribution of coating in park/fleet and on the presence or the absence in the constructions of fatigue failures, the laboratory data on the life of the constructions, which have operation time under actual conditions, including their statistical data operation time.

Let us assume that at all stress levels density distribution of the probabilities of the durability of constructions obeys the law $p^0(\tau)$ with equal to zero average and dispersion ρ^2 . Here

$$\tau = \lg N(\sigma) - \overline{\lg N(\sigma)} = \lg N(\sigma) - \lg N_0(\sigma) = \lg r, \quad (1)$$

where $N(\sigma)$ - the number of cycles of loading before the destruction of the datum of construction on stress level σ [kg/cm²].

$\overline{\lg N(\sigma)}$ - the average logarithm of the number of cycles before destruction on stress level σ .

Let us assume also that the average curve of durability $N_0(\sigma)$, obtained under laboratory conditions, is determined with an accuracy to its position along axis/axis $\lg N$, so forth with an accuracy to random coefficient ξ :

$$|N_0(\sigma)|_{\text{nat}} = \xi |N_0(\sigma)|_{\text{lab}} \quad (2)$$

(random character ξ is connected, in particular, with the diversity of operating conditions of constructions).

In an analogous manner are connected and congruent, i.e., corresponding one and the same to the value of the parameter of the probability of destruction r , durability curves for other levels of the probability of destruction, since $N(\sigma) = r \cdot N_0(\sigma)$.

In accordance with the linear hypothesis of the addition of fatigue failures, life K of construction under these conditions will be expressed by the formula

$$K_{\text{nat}} = K - \frac{r}{\Xi} \xi, \quad (3)$$

where Ξ — the sum of structural fatigue failures relatively average of the curve of durability $N_0(\sigma)$ per hour of standard flight. The probability of destruction during K of hours depends on coefficient of r and it is equal to 0.5 with $r=1$. Consequently, $\bar{K} = \frac{\xi}{\Xi}$ and

$\bar{K}_s = \frac{1}{\bar{\xi}}$ — these are the respectively average life and the average initial (corresponding $\xi=1$) life of construction.

It is obvious that

$$\tau = \lg \frac{N(\tau)}{N_0(\tau)} = \lg r = \lg \frac{K}{K} \quad (4)$$

Consequently, the probability of structural failure during period K is equal to

$$p_A = \int_{-\infty}^{\lg \frac{K}{K}} p^0(\tau) d\tau = \int_{-\infty}^{\lg \frac{K}{K}} p^0\left(\frac{\tau}{\rho}\right) d\left(\frac{\tau}{\rho}\right) = \Phi\left(\frac{1}{\rho} \lg \frac{K}{K}\right) \quad (5)$$

Let us introduce the logarithmic scale of lives K , of coating x of average coating \bar{x} , of the service lives and so forth, utilizing constants k_0 and g :

$$K = k_0 g^x; \quad x = k_0 g^x; \quad \bar{x} = k_0 g^{\bar{x}};$$

$$K_s = k_0 g^{\bar{x}_s}, \quad K = k_0 g^{\bar{x}},$$

then

$$\lg \xi = \lg \frac{K}{K_s} = (\bar{x} - \bar{x}_s) \lg g. \quad (6)$$

Page 94.

Let us examine diagram. Experience in operation of park/fleet from M_1 constructions is reproduced on it in the form M_1 of the points, driving/moving upward along diagonal in the course of time for the operating constructions and fixed for those copied. Motion is limited from above by the value that flow of ESS $x_0(\bar{x}_1)$. Value $x_0(\bar{x}_1)$ is determined from the condition:

$$p_0 = \int_{-\infty}^{(x_0 - \bar{x}) \lg g} p_0(\tau) d\tau. \quad (7)$$

Here p_0 - permissible probability of structural failure during K_0 hours of operation. According to formula (6) $\bar{x} = \bar{x}_0 + \frac{\lg \xi}{\lg g}$, therefore it is necessary to determine value ξ . Density distribution of probabilities $\lg \xi$ can be obtained on Bayes' formula

$$p(\lg \xi) = \frac{P_M(\lg \xi) \cdot p^*(\lg \xi)}{P_A}, \quad (8)$$

where $P_M(\lg \xi)$ - the probability of the "event" of T, i.e., the

actual current distribution of coating and failures in park/fleet under condition assigned/prescribed lg ξ .

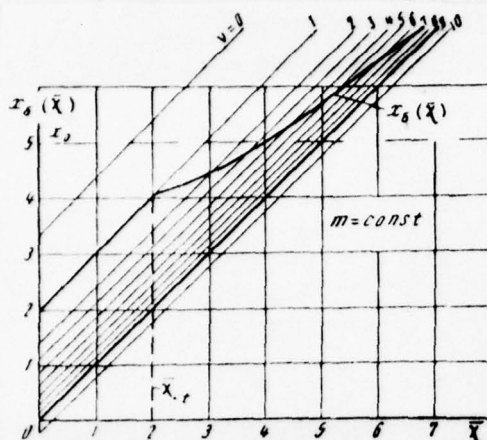
$p^*(\lg \xi)$ — a priori probability distribution lg ξ .

P_A — the normalizing constant, which makes sense of the composite probability of event T.

The current statistics of the operation of park/fleet, i.e., event T, is assigned in the form of the distribution

$$\binom{n_j}{x_j \atop v_j}_{j=1, 2, \dots, j_m}$$

where n_j — the number of constructions with coating x_j , including v_j the constructions, which have fatigue failures.



$p_0 = 0,0013$; $m = 1024$; $\chi_c = 4,8$; $\rho = 0,45$;
 $\lg g = 0,15$; $\Phi^{-1}(p_0) = -3$; $a = 0,483$;
 $x_t = 400$; $p_v = 0,004$; $\delta_v = 1$; $k_0 = 200$; $v_t = 0$

Page 05.

Let us take as a posteriori value $\lg \xi = \lg \xi_a$ to Maud distributions $f(\lg \xi)$, which, as show calculations, somewhat lesser than the expectation $\lg \xi$. Appropriate Maud value $\xi = \xi_a$ (or $\bar{x} = \bar{x}_a$). Equation Maud for determination \bar{x}_a takes the form

$$\frac{(p^*)_x}{p^*} + \frac{(P^*)_v}{P^*_M} = 0. \quad (9)$$

Probability P^*_M it is easy to calculate. Sc, when $v_t = 0$

$$P^*_M = \prod_{j=1}^{J_m} [1 - p(\chi_j - \bar{x})]^{n_j}, \quad (10)$$

where

$$p(\chi_j - \bar{x}) = \int_{-\infty}^{(\chi_j - \bar{x}) \lg g} p^0(\tau) d\tau; \quad \bar{x} = \bar{x}_a + \frac{\lg \xi}{\lg g}. \quad (11)$$

then $v = v_t$

$$P_M^v = \prod_{j=1}^{j_m} [1 - p(\chi_j - \bar{x})]^{n_j'} \prod_{i=1}^{i_m} p^{v_i}(\chi_i - \bar{x}),$$

where

$$\sum_{j=1}^{j_m} n_j' = M_t - v_t; \quad n_j' = n_j - v_j.$$

The probability of the event, which includes besides the already occurred failure v_t of constructions the failure one additional of the remaining $M - v_t$ constructions is defined, as it is easy to show that by the formula

$$P_M^{v_t+1} = P_M^{v_t} \sum_{i=1}^{i_m} n_i \frac{p_i}{q_i},$$

where $p_i = 1 - q_i$

thus, is here taken into account only not current number v_t of the actually broken constructions, but also their operation time, and

is introduced "supply or failures", equal to unit.

Let us introduce the designations

$$\left. \begin{aligned} A_1(\bar{x}) &= -\frac{1}{\ln g} \frac{[p^*(\lg \bar{x})]_x}{p^*(\lg \bar{x})} \\ A_2(\bar{x}) &= -\frac{1}{\ln g} \frac{[P_M'(\chi - \bar{x})]_x}{P_M'(\chi - \bar{x})} \end{aligned} \right\} \quad (12)$$

and equation Maud (9) let us write in the form $A_1(\bar{x}) = A_2(\bar{x})$.

In the simple case when entire park/fleet with a volume of m has the identical coating of χ and v failures, and the life of constructions is distributed according to the logarithmic normal law

$$A_2(\bar{x}) = \frac{m}{p \ln 10} \varphi_N(y) \left[1 - \frac{v}{m} \frac{1}{\Phi_N(y)} \right] \frac{1}{1 - \Phi_N(y)}, \quad (13)$$

where $y = \frac{(\chi - x) \ln g}{p}$; $\Phi_N(y)$ — the normal law $N(0,1)$; $\varphi_N(y) = \Phi_N'(y)$.

Page 96.

Function $A_1(\bar{x})$ is expressed simply only for some special cases.

Let us pause at calculation $p^*(\lg \bar{x})$. Let us assume that we always avail three identical copies of each construction, tested to

life respectively under the actual, laboratory and mixed conditions. The results of the tests of each triad according to formula (2) must satisfy the condition

$$K = u\xi = v + w\xi. \quad (14)$$

Here u - life of the new construction, tested according to the specific program under laboratory conditions (law) of distribution $f(u)$;

w - life under laboratory conditions of the construction, which mastered under actual conditions period v [laws of distribution respectively $\psi(w)$ and $\zeta(v)$].

Consequently,

$$\xi = \frac{v}{u - w} \quad (15)$$

and

$$\lg \xi = \lg v - \lg (u - w), \quad (16)$$

where $u > w$.

With the large relative operation time v/w random variables u and w can be considered independent variables. This assumption occurs

into "supply", since the account to correlation u and w increases value ξ . It is real/actual, let us substitute into formula (15) instead of w value

$$w^* = \alpha u + (1 - \alpha) w, \quad (17)$$

where $0 \leq \alpha \leq 1$, and u and w - independent random quantities. Then, as it is easy to verify that that $\xi(\alpha) = \xi(0) / (1 - \alpha)$, where $\xi(0)$ - initial expression for ξ .

Value α - parameter of the identity of old and new constructions.

In accordance with equality (15), utilizing an assumption about independence v , u and w , we will obtain

$$p^*(\lg \xi) = C \frac{\ln 10}{\xi} \int_0^\infty \zeta(v) v dv \int_0^\infty f^0(u) \psi\left(u - \frac{v}{\xi}\right) du, \quad (18)$$

where C - normalization constant.

Usually distributions $\zeta(v)$, $\psi(w)$ are assigned in discrete form. Then equation (18) takes the form

$$p^*(\lg \xi) = C \frac{\ln 10}{\xi} \sum_{i=1}^{J_1} \zeta_i v_i \left[\sum_{j=1}^{J_2} \psi_j f^0 \left(w_j + \frac{v_i}{\xi} \right) \right]. \quad (19)$$

Page 97.

Here ζ_i — the relative number of constructions with operation time v_i , tested before failure in laboratory, $\sum_{i=1}^{J_1} \zeta_i = 1$;

ψ_j — the relative number of constructions with operation time, which showed during testing in laboratory life w_j , $\sum_{j=1}^{J_2} \psi_j = 1$.

According to initial assumptions, distribution $f^0(u)$ can be expressed through $p^0(r)$.

The value that flow of ESS of x_0 after determination \bar{x}_0 is expressed according to formula (5) in the form

$$x_0 = \bar{x}_0 + p \frac{\Phi^{-1}(p_0)}{\lg g}, \quad (20)$$

where $\Phi^{-1}(p_0)$ — the function, reverse/inverse $\Phi(y)$.

For the case, illustrated by diagram, function $x_0(\gamma)$

asymptotically approaches or top a direct/straight, parallel diagonal, i.e.

$$\bar{x}_3 \approx \bar{\gamma} + \bar{x}_{a.c} - \bar{\gamma}_c, \quad (21)$$

where $\bar{x}_a(\gamma_c) = \bar{x}_{a.c}$.

Consequently,

$$x_6 = \gamma + \left[\bar{x}_{a.c} - \bar{\gamma}_c + \frac{\rho^{(p-1)}(p_0)}{\lg g} \right]. \quad (22)$$

However, so that current ESS and the future it was not necessary to reduce, it is necessary to establish/install the tendency of change $x_6(\gamma)$ in $\bar{\gamma}$, i.e., to extrapolate function $x_6(\gamma)$ from instantaneous value in point $\bar{\gamma}_c$. After determining the permissible probability p_0 of the failure of each construction in park/fleet with a volume of M_0 during entire initial ESS K_0 , we thereby establish/installed the risk of operation P_0 , i.e., the permissible probability at least of one failure in park/fleet of M_0 constructions

$$P_0 = 1 - (1 - p_0)^{M_0} \approx 1 - e^{-M_0 p_0} \text{ with small } p_0, \quad (23)$$

the average permissible density of fractures in park/fleet M_0 to

flying hour

$$\bar{p}_v = \frac{M_0 p_0}{K_0} \quad (24)$$

and the maximum permissible density of the fractures

$$p_v = \frac{M_0 p_0 + \beta_0 \sqrt{M_0 p_0}}{K_0} \quad (25)$$

The respectively average and maximum permissible number of fractures will comprise

$$v_0 = M_0 p_0 \quad \text{and} \quad \max v = M_0 p_0 + \beta_0 \sqrt{M_0 p_0} \quad (26)$$

Page 98.

Therefore let us consider v as continuous the parameter.

For simplification in the lining/calculations during extrapolation $x_0(\gamma)$ let us determine event T_{skn} "equivalent" to event T in the sense that

$$\bar{x}_s(T_{\text{skn}}) = \bar{x}_s(T) = \bar{x}_{s, \text{skn}} \quad (27)$$

Event T_{skn} lies in the fact that in certain park/fleet with a

volume of m_{KB} all the constructions have a coating \bar{x} and the number of fatigue failures in park/fleet is equal to $v = v_f$. Value m_{KB} is determined from equations (27). Equation Maud (9) in this case strongly is simplified [see expression (13)].

Extrapolation $\bar{x}_a(\gamma)$ from the current torque/moment is conducted for an equivalent park/fleet with a constant volume of m_{KB} , the number of fractures in which with coating increases over v_f so that an increase in the fractures is equal

$$\Delta v = \rho_s (\bar{x} - x_f) + \delta_v \quad \text{with} \quad \bar{x} > \bar{x}_f. \quad (28)$$

Here δ_v — the "supply on fractures", which can be introduced for the larger guarantee of safety. Then $\bar{x}_{a, \text{KB}}(\delta_v \neq 0) < \bar{x}_{a, \text{KB}}(\delta_v = 0)$.

If dependence $x_0(\gamma)$ when $\bar{x} > \bar{x}_f$ proves to be decreasing, i.e.,

$$\frac{dx_0}{d\gamma} < 0 \quad \text{with} \quad \bar{x} = \bar{x}_f. \quad (29)$$

then as BSS it cannot be taken $x_0(\gamma_i)$ in formula (20),

$$x_0 = \bar{x}_{a. \text{ KB}} + \frac{\rho \Phi^{-1}(p_0)}{\lg g} \quad \text{with} \quad \bar{\lambda} = \bar{\lambda}_r \quad (30)$$

Current BSS in this case is determined by the value of the minimum of function $\bar{x}_0(\bar{\lambda})$ when $\bar{\lambda} > \bar{\lambda}_r$:

$$x_0 = \min_{\bar{\lambda} > \bar{\lambda}_r} \left[\bar{x}_{a. \text{ KB}}(\bar{\lambda}) + \rho \frac{\Phi^{-1}(p_0)}{\lg g} \right] \quad (31)$$

With the review that flow of BSS at following torque/moment, is considered already new current statistics 1 and, possibly, the supplemented data on the endurance test of constructions, on the calculation procedure it remains previous.

Supplementary possibilities for the prolongation of BSS can be opened, for example, during an improvement in the fatigue data of constructions, i.e., with an increase x_0 (work hardening, etc.), during a change in operating conditions (periodic flaw detection). In the latter case can be calculated and accepted as p_0 greater than p_0 , the permissible probability of the occurrence of fatigue crack, since under conditions of periodic flaw detection crack initiation does not still indicate fracture. Crack with the specific probability can be

DOC = 78103906

PAGE ~~24~~ 219

reveal/detected, and the assigned/prescribed level of the risk of operation, i.e., probability of one or more fractures and park/fleet during K_0 hours, it will be preserved.

The manuscript entered 18/IX 1969.

Page 09.

APPROXIMATION METHOD OF THE CALCULATION OF AXISYMMETRIC INTERACTION
OF THE FREELY SPRAYING JET WITH BARRIER

V. I. Blagcsklonov.

Is proposed the approximation method of the solution of the problem of interaction of supersonic underexpanded jet with barrier/obstacle. This problem is reduced to the problem of the flow around sphere of the steady flow of gas. Is given the procedure of the determination of mach number and a radius of sphere. The results of calculation by approximation method are compared with experimental data.

The problem of interaction of the freely expanded gas jet with barrier/obstacle is theoretically still little investigated, only recently appeared several numerical methods of its solution. So, in work [1] it is solved by reverse/inverse method. Effective render/showed the method of integral relationship/ratios which was used in works [2] and [3]. At mechanics's 3rd All-Union congress/descent about the solution of this task, made a report M. R. Lebedev and K. G. Savinov, which used method of the establishment of

K. I. Babenko and V. V. Rusanov. In this article unlike the mentioned above works, is proposed the method, which does not require use EtsVM; the problem of axisymmetric interaction of supersonic jet with barrier/obstacle (sphere or plane) is reduced to the problem of the flow around sphere of the steady flow of gas. As initial are utilized the data on the distribution of the parameters in the freely expanded supersonic jet and the flow around sphere of uniform supersonic flow, which are, for example, in work [4].

Let us examine the flow around sphere of the steady flow of gas (Fig. 1a). During flow appears the detached shock wave and between the wave front and the body surface is formed region ABCO of subsonic flow. In the case of adiabatic flow, the system of equations, which describes the flow of gas, can be written in the form

$$\left. \begin{aligned} (u^2 - a^2) \frac{\partial u}{\partial x} + uv \left(\frac{\partial u}{\partial y} + \frac{\partial v}{\partial x} \right) + (v^2 - a^2) \frac{\partial v}{\partial y} &= a^2 \frac{v}{y}; \\ \frac{\partial v}{\partial x} - \frac{\partial u}{\partial y} &= -\frac{1}{2} \gamma R \frac{ds}{d\psi} \end{aligned} \right\} \quad (1)$$

where R - a radius of sphere; u, v - comprising velocities in the direction of x and y axes; a - speed of sound; ψ - the function of current; ρ - density.

Problem consists of the determination of unique and continuous solution of the region in question. Its boundaries on which are

placed the corresponding conditions, are the shock wave ABD, the axis of symmetry AO, the duct/contour of body OC. Survey/coverage of methods of solution of this problem is given in work [4].

Page 100.

Now let us examine the flow around sphere of gas jet. Here, as during the flow around sphere of the steady flow, appears the detached shock wave and between the wave front and the body is formed the region of subsonic flow. Systems of equations, which describe the motion of gas, and boundary conditions on the axis of symmetry and on the surface of the sphere, streamlined with the steady flow and gas jet, the same. The specific character of the problem of the flow around sphere of gas jet consists of satisfaction to boundary conditions on jump ABD. Along gallop changes both very velocity of incident flow and its direction. Let the solution of the problem of the flow around sphere of gas jet be known. Let us attempt to determine, to which radius of sphere and in which Mach number of the uniform incident flow this solution most of all corresponds.

Let us take a radius of the sphere, streamlined with the steady flow, by such so that the departure/withdrawal of shock wave would be equal to the departure/withdrawal of the shock wave of the sphere, streamlined with gas jet. This radius of sphere let us call/name

equivalent and let us designate F_0 .

Let us pass to the system of coordinates sr , where s - arc length, measured along the duct/contour of body, n - a standard to it. Regions $ABDCO$ and $A'E'D'C'C'$ will take the form, represented on fig. 1c, d.

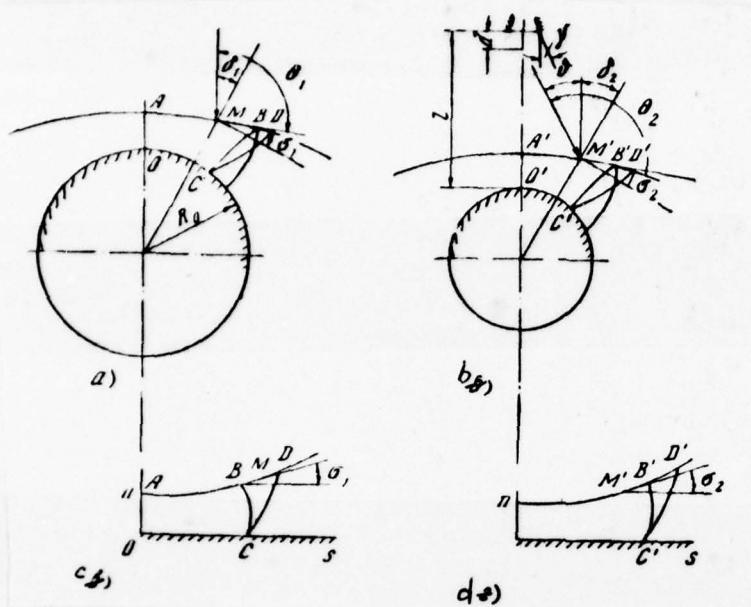


Fig. 1.

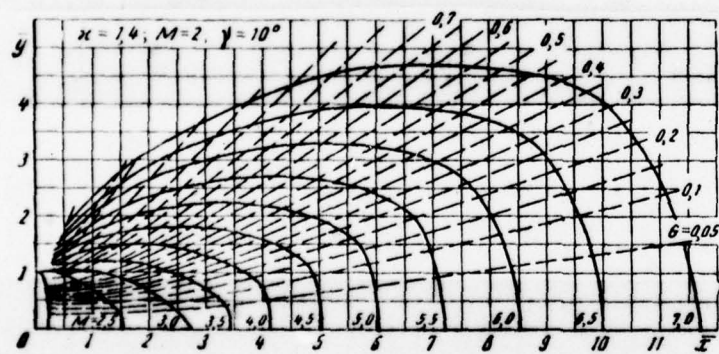


Fig. 2.

If stated problem had exact solution, then these regions would coincide. In this case the Mach number along the length jump must be by constant and equal to Mach number of uniform flow, the angles of the slope of jump σ_1 and σ_2 by x -axis must be equal. The angles, formed by velocity vectors from tangent to jump, θ_1 and θ_2 must be also equal. Is averaged the module/modulus of velocity of the incident flow according to any law. The value of this velocity let us call/name V_1 . This averaging weakly will pronounce during the final solution of problem, if $M_1 = V_1/a$ is sufficiently great, which usually is in this problem, since for the sphere, streamlined with the steady flow of gas, the dependence of solution on Mach number at its sufficiently high values is weak.

From Fig. 1, it is evident that

$$\theta_1 = \delta_1 + \frac{\pi}{2} - \sigma_1, \quad (2)$$

$$\theta_2 = \delta + \frac{\pi}{2} - \sigma_2 + \delta_3. \quad (3)$$

From formulas (2) and (3) it follows that

$$\delta_1 = \delta + \delta_3, \quad (4)$$

but

$$\delta_1 = \frac{s}{R_0}, \quad (5)$$

$$\delta_2 = \frac{s}{R}, \quad (6)$$

For θ - the angle of the slope of velocity to the axle/axis of jet - analytical expression, no, but from the analysis of the numerical calculation of jets, it follows that the distribution of the angles of the slope of the velocity in the vicinity of barrier/obstacle can be approximated by the distribution, which corresponds to source with pole on the axis of symmetry. Distance from nozzle edge to the center of source d should be taken for each specific case, utilizing numerical calculations of jets.

With this approximation

$$\theta = \operatorname{arctg} \left(\frac{s}{R - \epsilon} \right) \approx \frac{s}{R_1 - \epsilon}, \quad (7)$$

where ϵ - distance from shock wave to barrier/obstacle; $R_1 = l - d$;

l - distance from the axle/axis of OT nozzle to barrier/obstacle. All linear dimensions are referred to a radius of nozzle.

After substituting expressions (5)-(7) into equation (4), we will obtain:

$$\frac{1}{R_0} = \frac{1}{R_1 - \epsilon} + \frac{1}{R}. \quad (8)$$

If in jet stands plate, then, by transfer/converting in equation (8) to apparatus for R, we will obtain $R_0 = R_1 - \epsilon(s)$. Thus, is found a radius of sphere and a mach number of the incident flow, i.e., is approximately solved stated problem.

On the basis of the aforesaid, it is possible to propose the following procedure of the flow-field analysis of plate or sphere by gas jet with sufficiently large underexpansion.

1. Through assigned/prescribed position of plate or sphere, we find center of fictitious source. In this case, it is necessary to use the numerical calculations of jets (Fig. 2).

2. We find R_0 through formula $R_0 = R_1(1 - \epsilon)$.

3. We construct dependence $\epsilon = \epsilon(x)$. In this case, it is possible to use the material, available in work [4], or by curve/graph Fig. 3.

We more precisely formulate values R_0 and R_1 .

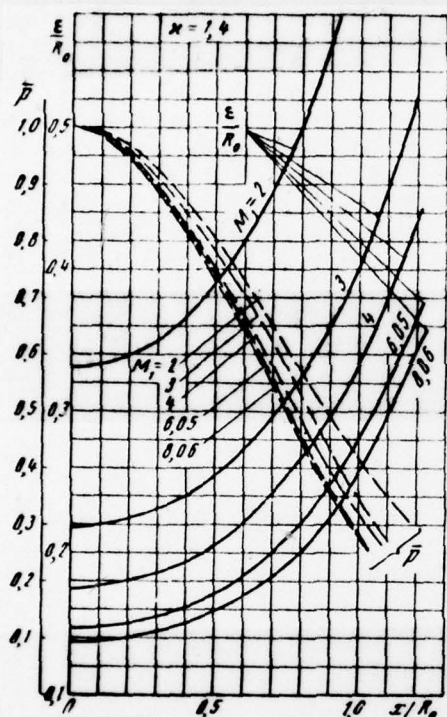


Fig. 3.

Page 102.

We construct the necessary dependences for a sphere with a radius of R_0 in the steady flow. These dependences are simultaneously dependences on plate or sphere in gas jet.

Since for jet-edge problems it is accepted pressure to relate to pressure in nozzle edge, then for obtaining its this dimensionless

pressure it is necessary to multiply by the ratio of stagnation pressure at critical point to pressure in nozzle edge. Having data of the calculation of jet and departure/withdrawal of jump from body, this can be made with the aid of the tables of gas-dynamic functions.

For checking the correctness of the procedure presented was designed interaction of flat/plane plate with the gas jet, escaping behind nozzle with $M_a = 2$ and $\alpha = 1.4$ when $l = 3.9; 4.6; 5.3; 6.0; 6.6; 10.0$. The law of averaging was undertaken similar so that the momentum of the part of the jet, flowing into subsonic region, before and after averaging would remain identical.

The results of calculation are given to Fig. 4. On this same figure are plotted/applied the points, obtained in experiment. On photo Fig. 5, are plotted/applied the points, which correspond to the shock wave, shown on Fig. 4. The results of calculation and experiment converge satisfactorily. In the region of supersonic flow with an increase in an error in the method grows/rises. This is connected with the fact that the lines of equal Mach numbers sharply are run up/turned to the side of nozzle, and in this zone of flow no longer is similar to the flow around sphere of the steady flow, but it approaches a flow of radial jet from slit into the medium with low variable pressure. Calculations according to approximation method should be carried out from $l > 3 + 5$ radii of nozzle.

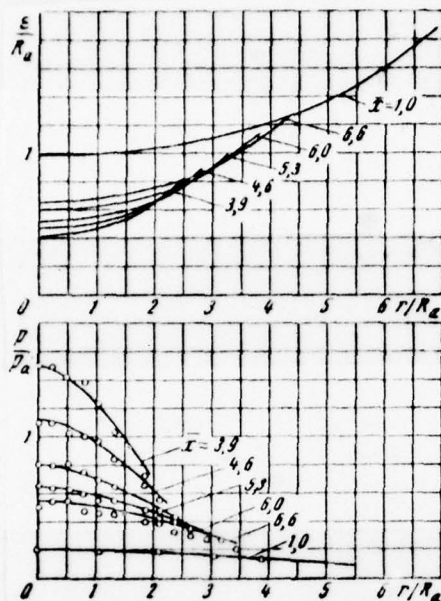


Fig. 4.



Fig. 5.

Fig. 5.

Key: (1). [illeg.]

REFERENCES

1. D. W. Eastman, I. E. Ecnema . Flowfield of a highly underexpanded impinging on surface. AIAA J, v 4, No 7, 1966.

2. N. Ye. Khranov. Calculation of interaction of the axisymmetric supersonic underexpanded jet with barrier/obstacle. MZhG, 1966, No 5.

3. N. Ye. Khranov. Flow-field analysis of sphere of the nonuniform flow of gas. FHM, Vol. 29, iss. 1, 1965.

4. Flow around blunted bodies of supersonic flow of gas. Coll. of article pcd. ed. O. E. Beltserskivskogo. CC of the AS USSR, 1966.

The manuscript entered 6/X 1969.

Page 103.

WORK OF GAS EJECTOR IN THE DISSIMILAR PHYSICAL PARAMETERS OF THE
MIXED GASES.

F. A. Kukanov, I. I. Mezhiro.

Are given the equations of ejection at the dissimilar values of the adiabatic index κ , of heat capacity at constant pressure c_p and the temperatures of stagnation T_0 of the mixed gases. It is shown, that with preservation/retention/maintaining by the

constant/invariable of the given velocities and pressures at the entrance into ejector the value of the coefficient of ejection changes inversely proportional to the parameters

$$\eta = \sqrt{\frac{c_{p1} T_{01}}{c_p T_0}} \quad \text{and} \quad b = \sqrt{\frac{1 - \frac{1}{\gamma_1^2}}{1 - \frac{1}{\gamma^2}}}$$

Are given the results of the experimental investigation of supersonic gas ejector at constant temperature of braking ejection gas ($T'_0=280^\circ\text{K}$) and the different values of the temperature of stagnation of ejected gas ($T_{01}=280-2000^\circ\text{K}$). It is established/installed that with $T_{01}=1500-2000^\circ\text{K}$ characteristic of ejector it is considerably worse than calculated.

It is shown, that the water injection into the jet of low-pressure gas improves the characteristics of ejector and gives them into conformity with calculated.

1. Let us examine gas ejector, in which are mixed two flows of ideal gas, that have different physical parameters (adiabatic indices and specific heat) and temperature of braking. Let us make the following assumptions:

the mixing chamber cylindrical;

in the mixing chamber, occurs the complete mixing of gases, which is not accompanied by chemical reactions and a change in the state of aggregation.

the parameters of the gas flows, which enter the mixing chamber and which emerge from it, are distributed evenly over the appropriate sections.

friction on the chamber walls of mixing and heat exchange with the environment are absent.

The use of equations of mechanics for the mass of gas, which is located in the mixing chamber, leads to the following relationship/ratios, which relate parameters of gases at the entrance into ejector and at output from it:

$$z = \frac{q(\lambda_1, x_1) + \alpha z(\lambda') q(\lambda', x')}{(1 + \alpha) q(\lambda'', x'')} f \quad (1)$$

(flow equation with the use of equation of conservation of energy):

$$\frac{z(\lambda_1) q(\lambda_1, x_1) + \alpha z(\lambda') q(\lambda', x')}{q(\lambda_1, x_1) + \alpha q(\lambda', x')} = z(\lambda'') f \quad (2)$$

(equation of momentum with the use of equation of conservation of energy):

$$k \vartheta b = \frac{q(\lambda_1, x_1)}{a \gamma q(\lambda', x')} \quad (3)$$

(equation of the relation between the parameters of the gases, which enter the mixing chamber).

Page 104.

Here:

$$\begin{aligned} \sigma &= \frac{p_0'}{p_{01}}; \quad \varepsilon = \frac{p_0''}{p_{01}}; \quad q(\lambda, x) = \lambda \left(1 - \frac{x-1}{x+1} \lambda^2\right)^{\frac{1}{x-1}}; \\ \vartheta &= \sqrt{\frac{c_{p1} T_{01}}{c_p' T_0'}}; \quad f = \frac{(1+k\vartheta)(1+kcb)}{(1+kc)(1+k\vartheta b)} \sqrt{(1+\Delta_0)(1+\Delta_x)}; \\ z(x) &= x + \frac{1}{x}; \quad c = \frac{c_{p1}}{c_p'}; \quad b = \frac{B_1}{B'}; \quad B = \sqrt{1 - \frac{1}{x^2}}; \\ \Delta_0 &= \frac{z(\vartheta) - 2}{z(k\vartheta) + 2}; \quad \Delta_x = \frac{z\left(\frac{x_1}{x'}\right) - 2}{x_1 x' B_1 B' [x(kcb) + 2]} + \frac{z(b) - 2}{z(kcb) + 2}; \end{aligned}$$

p - pressure, T - absolute temperature, $\lambda = \frac{W}{a_*}$ - the given velocity, W - velocity, a_* - critical speed, $x = \frac{c_p}{c_v}$ - adiabatic index, c_p and c_v - specific heat capacities at constant pressure and volume, $\alpha = F'/F_1$, F - cross-sectional area of jet, $k = Q_1/Q'$ - coefficient of ejection, Q - mass flow rate. Prime designates the ejection gases, double prime - gas mixture at output from ejector,

index "1" - the ejected gas, zero - isentropically stagnation gas.

Relationship/ratios (1)-(3) differ from the appropriate expressions for the case of ejector with the identical values T_0 , λ , c_p of the mixed gases in terms of the presence of factor f in the right side of equations (1) and (2) and by certain dependence of function q on λ (at subsonic and small supersonic values λ this dependence very weak). These factors, as is shown the analysis of equations (1) and (2), with the specific relationships of the parameters at the mixing chamber inlet, can lead to the fact that the velocity of mixture at output from ejector will be sonic. This operating mode limits the possibility of further increase in the coefficient of ejection during the decrease of pressure at output from ejector and in this sense is maximum. However, thus far this conditions/mode is not achieved/reached, the effect of the factors indicated on the work of ejector in many instances is small.

Another possible maximum mode of operation of ejector is, as is known, the so-called "critical" conditions/mode, discovered by M. D. Millicentsikov and G. M. Byatinkov, who corresponds to the acceleration/dispersal of the ejected gas in the beginning of the mixing chamber to the transonic speed as a result of the expansion of the supersonic flow of the ejection gas.

The supplementary limitation, which critical behavior is superimposed on the parameters of gases at the mixing chamber inlet, can be expressed by the following approximate relationship/ratios:

$$k_{0b} = \frac{z(\lambda_2) - z(\lambda)}{z(\lambda_1) - 2}; \quad (4)$$

$$q(\lambda_2, x) = \frac{\alpha q(\lambda_1, x_1) q(\lambda', x')}{q(\lambda_1, x_1)(1 + \alpha) - q(\lambda_1, x_1)} \quad (5)$$

FOOTNOTE 1. Yu. N. Asil'yev. Theory of supersonic gas ejector with the cylindrical mixing chamber. In the collection "rotodynamic machines and jet apparatuses". Iss. 2. M., "machine-building", using 1967. ENDFOOTNOTE.

Page 105.

Here λ_2 - average value of the given velocity of the ejection gas in the section where in the ejected gas is reached the speed of sound.

From equations (3) and (4) it follows further that a difference between parameters T_0, γ, c_p the mixed gases at any mode of operation of ejector will affect most strongly the coefficient of ejection, so that when the effect of the parameters of gas on values $q(\lambda, x)$ and f small, it is possible to count that

$$k_{0, b=1} = \frac{k_{0, b=1}}{0.6} \quad (6)$$

Value k_{0b} can be named the given coefficient of ejection. From relationship/ratio (6) it follows that if we present the characteristics of the ejectors, which have the identical parameters σ , λ' , p'_0/p''_0 , in the form of dependences $k_{0b} = \Phi(\sigma)$, then, in spite of a difference in the parameters of the ejection and ejected gases, these characteristics will virtually coincide.

This position is retained until are disrupted the conditions on basis of which are obtained those given above relationship. Chief among them it is supposition about the complete mixing of gases in the chamber of mixing of ejector.

2. Effect of difference in temperatures of stagnation and physical properties of gases on work of ejector was investigated on model of ejector with cylindrical mixing chamber with a diameter of $d=294$ mm. Gas mixture was discarded from ejector in the atmosphere through the subsonic exit cone/diffuser. As the ejection gas was utilized the air ($T'_0=280^\circ K$, $\gamma' = 1.4$), which entered the ejector through the supersonic annular nozzle ($\lambda' \approx 1.88$) on the periphery of the mixing chamber.

The temperature of stagnation of the ejected gas which entered ejector from gas generator along cylindrical channel, could change in the range $T_{01}=280-2000^{\circ}\text{K}$ (corresponding values of adiabatic index $\kappa \approx 1.4-1.33$). The specific heat of the mixed gases were approximately identical.

The given coefficient of ejection k_{eb} was determined from the formula

$$k_{eb} = A \frac{p_{01} q(\lambda_1, \kappa_1)}{Q'}$$

where A - constant, depending on the physical constants of gases and geometric dimensions of ejector.

During experiments were realized/accomplished all the measurements, necessary for determining of the fundamental characteristics of ejector.

The results of experiments, obtained at total pressure $p'_{01} \approx 5.7$ atm (abs.), are represented on Fig. 1 in the form of dependences $k_{eb} = f(\theta)$. At the total pressure indicated high-pressure gas and the identical temperatures of stagnation of the mixed gases, the ejector

worked in critical behavior in all investigated range of a change in the coefficients of ejection.

Calculated curve, which corresponds to critical behavior of the work of ejector, designed on formulas (3)-(5), is plotted/applied on Fig. 1 in the form of solid line. It is evident that the experimental points, obtained at the identical temperatures of stagnation of the mixed gases, well will agree with calculation data. The results, obtained with $T_{01} \approx 800^\circ\text{K}$, are also close to calculated. However, the dependences, which correspond to the higher temperatures of ejected gas ($T_{01} = 1500-2000^\circ\text{K}$), sharply differ from calculated curve with $\sigma \geq 5$, ejector transfer/converts in these two cases to the subcritical operating mode. The attempt to improve the characteristics of ejector via an increase in the length of the mixing chamber from $l = 5$ to the diameters of the camera/chamber to $l = 10$ to diameters did not give the results (see Fig. 1).

This the which contradicts calculation charge in the characteristics of ejector can be explained by deterioration in the process of the mixing of gases with the increase of the temperature of low-pressure gas. On Fig. 2, is represented the dependence of the velocity of ejected gas a_{*1} in the section where during critical behavior of work it reaches the speeds of sound, from temperature T_{01} . Here noted average value of the velocity of the ejection gas in

the same section W'_2 (with $T'_0=280^\circ\text{K}$). It is evident that with an increase in temperature T_{01} , the difference in velocities in this section decreases and with $T_{01}\approx 1000^\circ\text{K}$ they are equalized.

Thus, the conducted experimental investigation detects sharp deterioration in the process of mixing during the equalization of the velocities of the mixed flows in the beginning of the camera/chamber of ejector.

Page 106.

Let us note that the equality gas velocities at the entrance into ejector and, consequently, also deterioration in the mixing, can be not only with a difference in the temperatures of stagnation, but also at difference BETWEEN specific heat c_p and the adiabatic indices γ of the mixed gases.

3. One of methods of improvement in mixing of jets with $W_1\approx W'$ and high values T_{01} , is cooling low-pressure gas before its feed into chamber of mixing which can be realized via water injection into low-pressure circuit.

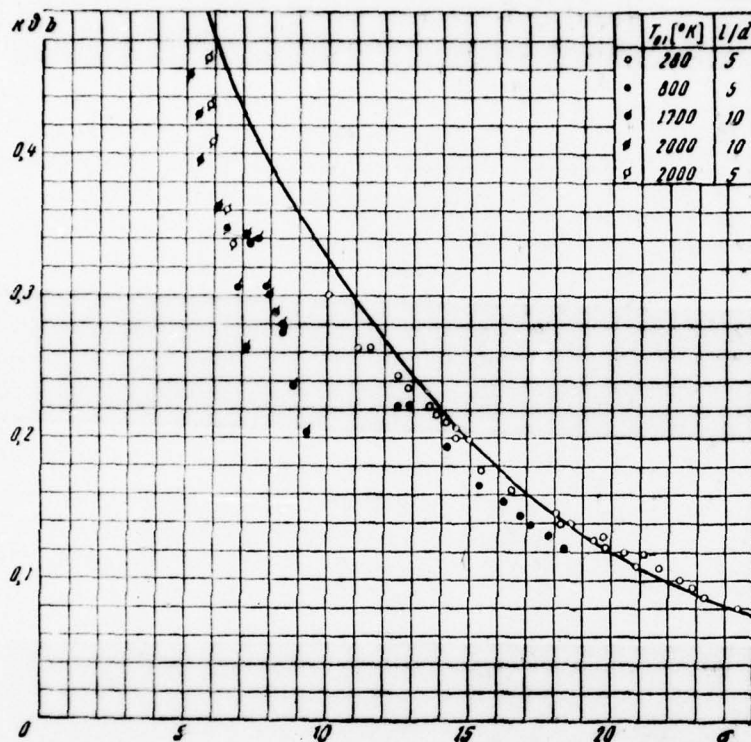


Fig. 1.

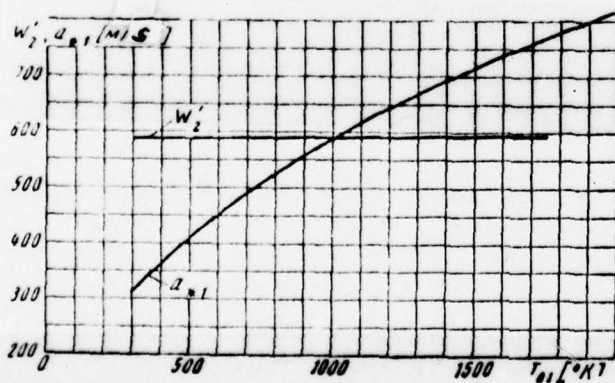


Fig. 2.

Page 107.

Water injection into the jet of hot low-pressure gas affects the process of ejection as follows:

as a result of evaporating water decreases temperature of stagnation T_{01} and, consequently, also critical speed a_{*1} . This contributes to an improvement in the process of mixing in ejector;

water injection increases the weight flow rate of the ejected gas, raises the coefficient of ejection k and, therefore, contributes to the decrease of compression ratio of ejector;

a temperature decrease T_{01} leads to the decrease of parameter $\eta = \sqrt{\frac{c_{p1} T_{01}}{c_p T_{01}}}$, which in turn, leads to an increase in compression ratio;

The total effect of water injection on compression ratio with complete mixing is determined by a change in the given coefficient of ejection $k\eta$.

On Fig. 3, is represented dependence $\frac{Q_n}{Q_1} = f(\Delta T)$, where $\frac{Q_n}{Q_1}$ — the consumption of water to the unit of the mass of low-pressure gas, its required for reduction of temperature on ΔT [$^{\circ}\text{K}$] during the complete evaporation of water. During calculations it was accepted that the initial temperature of gas was equal to 2023°K , and the initial temperature of water of 303°K . Certain representation of value ΔT , required for restoring good mixing, gives Fig. 4, where are given dependence $a_{\text{mix}}/W' = f(\Delta T)$ with the same as are above, the original values of the temperatures of gas and water, also, at $W' = 620 \text{ m/s}$ ($\lambda' = 2$ with $T'_0 = 230^{\circ}\text{K}$).

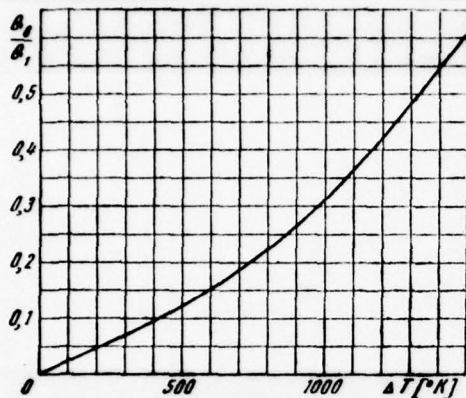


Fig. 3.

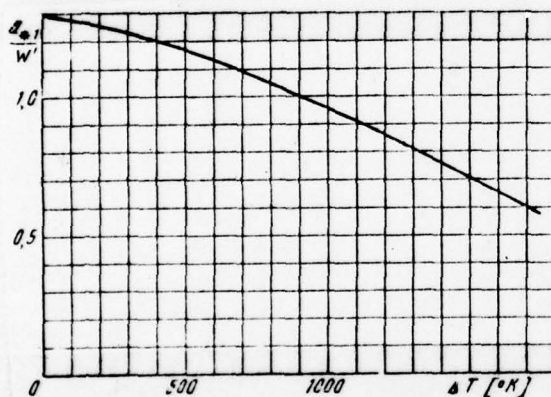


Fig. 4.

Page 108.

The effect of water injection on the given coefficient of ejection is illustrated Fig. 5, where is given dependence $k_{\text{eb}}/(k_{\text{eb}})_0 = f(\Delta T)$; $(k_{\text{eb}})_0$ corresponds to initial state of the gas without injection. during the complete evaporation of water, the given coefficient of

ejection even somewhat descends.

Experiments confirmed the effectiveness of water injection into the hot ejected gas for restoring the mixing in ejector. To Fig. 6, is given experimental dependence $(k\dot{t})_0 = f(\epsilon)$, obtained with injection into hot water jet with relative consumption $\frac{Q_0}{Q_1} = 0.35 \div 0.52$. Datum temperature $T_{01} = 1700K$, pressure $p'_0 \approx 6.5$ atm (abs.). By the shaded band is shown the experimental dependence for critical behavior, obtained with $T_{01} = T'_0$. It is evident that the water injection led to the restoration/reduction of critical behavior of the work of ejector.

Data are acquired at the length of the supplying circuit of the steam-gas mixture $L = 5$ m and the relative length of the chamber of mixing of ejector $\frac{l}{d} = 11.5$.

FOOTNOTE 1. The completeness of the evaporation of water is determined at the assigned/prescribed gas velocity by the absolute length of the conduit/manifold, in which occurs the evaporation, i.e., by the retention time of the drops of water in hot gas.

ENDFOOTNOTE.

During these experiments is noted certain deterioration in the characteristics of ejector in the case $T_{01} = T'_0$ in comparison with initial characteristics, which is explained apparently, by an

increase in the nonuniformity of inlet velocities into the mixing chamber, by the caused elongation of feeders during the organization of water injection (exemplary/approximate length of the supplying low-pressure channel of 30 bores, and high-pressure - 50 bores).

In the case of good fields at the entrance into ejector, one should expect an even larger improvement in its characteristics with water injection into the hot jet of low-pressure gas, i.e., the decrease of the required pressure p'_0 in the work of ejector in critical behavior.

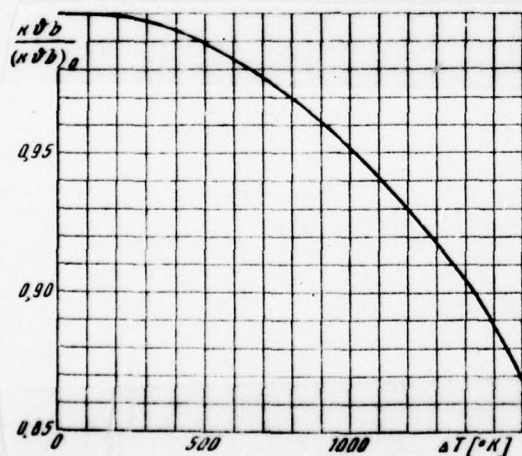


Fig. 5.

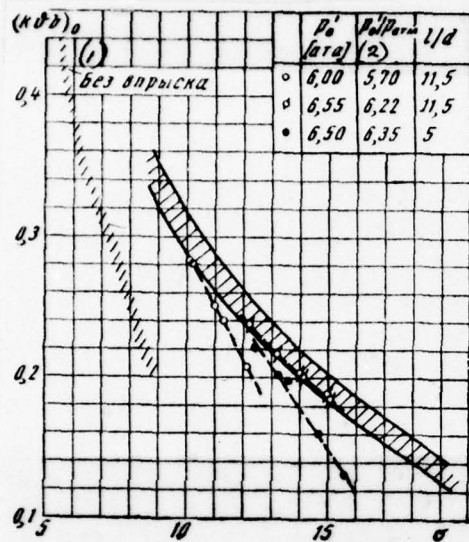


Fig. 6.

Key: (1). Without injection. (2). [atm(ahs.)].

The manuscript entered 6/X 1969.

~~10520 REVISION FROM 11-22-78 TO 11-22-78~~

Page 109.

EFFECT OF WING VORTEX SYSTEM IN THE ABSENCE OF LIFT ON ITS
STREAMLINING AT LOW ANGLES OF ATTACK.

K. K. Fedyaevskiy, N. N. Fomin.

it is experimental that the character of the flow around thick rectangular low-aspect-ratio wing flat-topped at zero angle of attack in many respects is determined and the character of its flow at low angles of attack and, therefore, affects lift formation.

The existing methods of calculation of the bearing capacity of wing do not consider the character of its flow in the absence of lift. Meanwhile it is already long revealed/detected that the wings with symmetrical airfoil/profile at zero angle of attack possess the system of the end eddy/vortices, caused by detached flow of end/faces. Since during transition from zero angle of attack to small angles the vortex/eddy system cannot completely be broken and disappear, it is of interest to explain that in which measure

vortex/eddy system at low angles of attack retains the features, which are inherent in it at zero angle.

Was investigated the flow around of the wing of rectangular planform with elongation $\lambda=1$, with airfoil/profile NACA-0018. Chord b and the span of wing were equal to 0.8 m. Wing had flat/plane end/faces. Testings were conducted in a return-flow wind tunnel with the open test section at the angles of attack, equal to zero and 5° , and the rate of flow $V_0=40$ m/s ($Re=2.2 \cdot 10^6$). Wing was fastened to the special installation, connected with coordinate spacer apparatus, to two brackets in the middle of lower surface. Thus, brackets did not affect the flow around suction side of wing, end/faces and lower surface near end/faces. Fig. 1, shows the adopted system of coordinates.

Complete, dynamic and static pressures and local downwashes in vertical and horizontal planes near the wing surface were measured with the aid of the five-ribbed nozzle, fasten/strengthened in the coordinate spacer apparatus, making it possible to move nozzle in the direction of the connected with model axle/axes Ox_1 , Oy_1 and Oz_1 , and to rotate it around the axle/axis, coinciding with the direction of axle/axis Oz_1 .

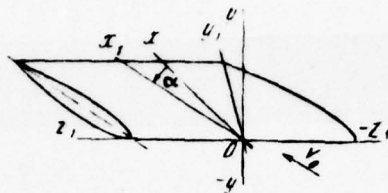


Fig. 1.

Page 110.

On the measured dynamic pressures and local downwashes in vertical and horizontal planes, were determined transverse component of local velocity, i.e., the components of rate, lying at the planes, parallel to plane z_1Oy_1 .

Although the study of wing vortex system by field measurement of velocities and pressure around wing is very laborious, it has known advantages before the study of wake with the aid of spindle, since it gives the more complete picture of the formation of eddy/vortices, their intensity and direction of rotation.

The lines of equal static pressures (isobar) and of the field of transversing speeds near wing with $\alpha=0$ are represented in Fig. 2 and 3. On these curve/graphs are shown the values and the position of

minimum pressure near the wing which in the first approximation, determines the position of vortex core relative to wing.

In leading edge where its thickness increases (see Fig. 2), and transversing speeds are directed from wing, the flow around the edges of end/face leads to breakaway and to formation on the end/face of two eddy/vortices of large intensity. However, these eddy/vortices sufficiently rapidly lose their intensity, they are sucked to the edges of end/faces and diffuse.

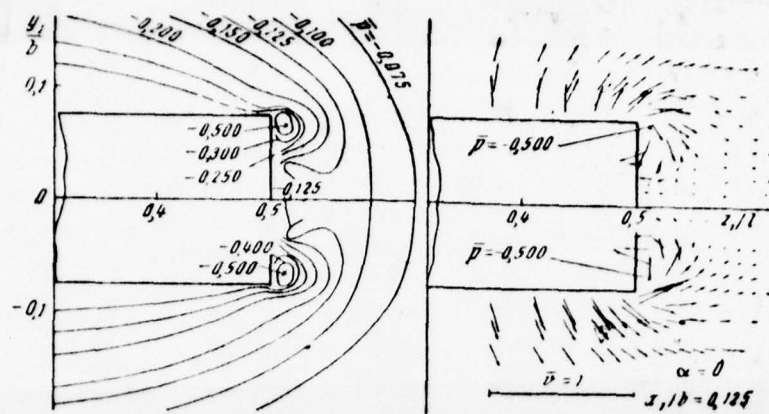


Fig. 2.

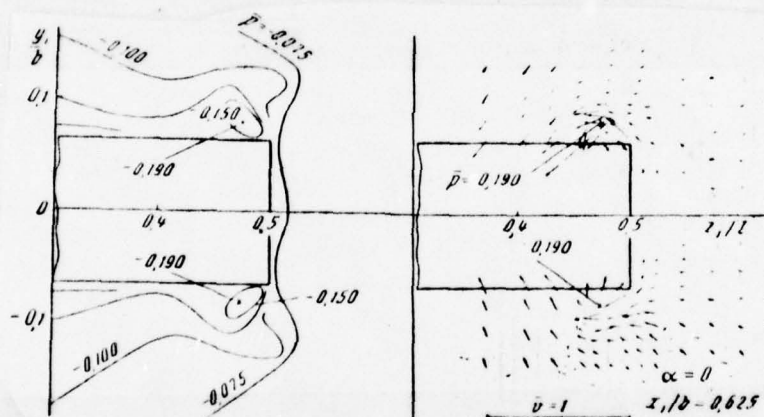


Fig. 3.

Page 111.

In area after the greatest thickness of the airfoil/profile (see Fig. 3), where the transversing speeds are directed toward wing, the

flow around the edge of end/face leads to the emergence of two symmetrically arranged/located eddy/vortices above the upper and under pressure side of wing. These eddy/vortices have opposite direction of rotation in comparison with eddy/vortices on the front of the wing and they sufficiently rapidly lose their intensity.

Isobars and the fields of transversing speeds it near covered at $\alpha=5^\circ$ were given in Fig. 4 and 5. At this angle just as at zero angle so, as at zero angle of attack, near the wing leading edge are formed two end eddy/vortices of different intensity. In this case, the upper end eddy/vortex of weak intensity and clockwise rotation rapidly diffuses.

On the picture of the field of transversing speeds, one can see well the overflowing from lower surface to upper. Because of the flow around the lower sharp edge of the end/face of wing is formed the eddy/vortex of the large power of counterclockwise rotation, who near trailing edge loses its intensity.

On suction side of wing near end/face, in area of the greatest profile thickness $x_1/b=0.375$, arises the eddy/vortex of the large intensity of identical direction of rotation with lower end eddy/vortex. This eddy/vortex converges from trailing wing edge near end/face.

Fig. 6, shows the position of the minimums of pressure in vortex core relative to the end/face of wing along its chord which in the first rough approximation make it possible to judge the location of vortex core relative to wing.

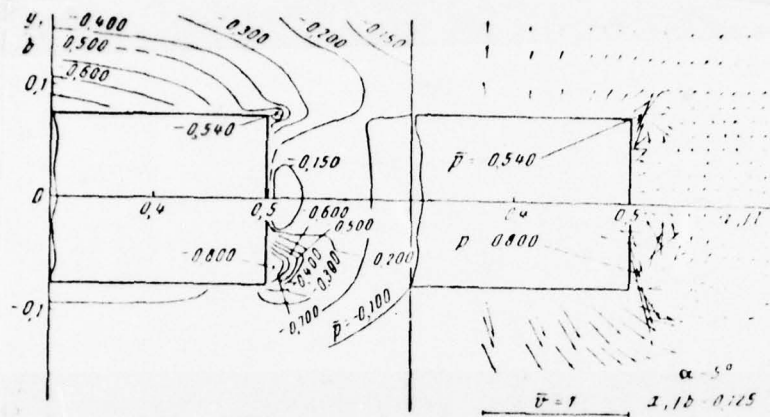


Fig. 4.

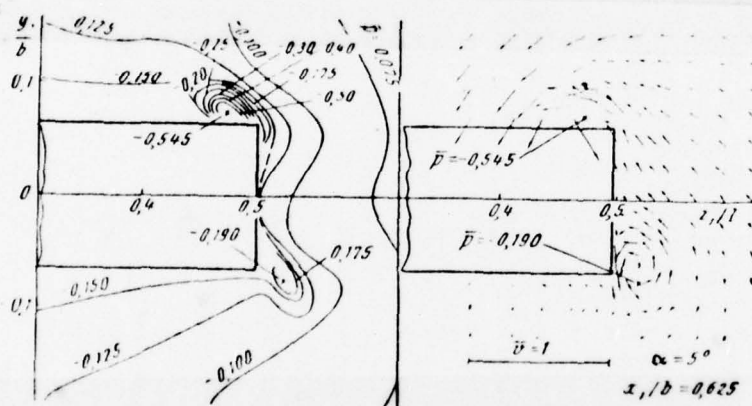


Fig. 5.

Page 112.

The comparison of the fields of transversing speeds at $\alpha=0$ and 5° shows that the character of flow around of the wing at zero angle

of attack in many respects determines the character of flow at the angle of attack of 5° . In fact, the comparison Fig. 2 and 4 shows that about the wing leading edge the end eddy/vortices, discovered with $\alpha=0$, are retained at $\alpha=5^\circ$. In this case, the end eddy/vortex, arranged/located nearer to pressure side of wing, during transition from $\alpha=0$ to $\alpha=5^\circ$ it becomes more intense, whereas the intensity of the eddy/vortex, arranged/located is nearer to upper surface, it virtually remains constant/invariable. The location of the centers of end eddy/vortices in these sections also little is changed during transition from $\alpha=0$ to $\alpha=5^\circ$ (see Fig. 6). Only in section with $x_1/b=0.375$ at the angle of attack of $\alpha=5^\circ$ eddy/vortex is considerably more intense. Thus, the character of flow around of the wing the zero angle of attack affects lift formation.

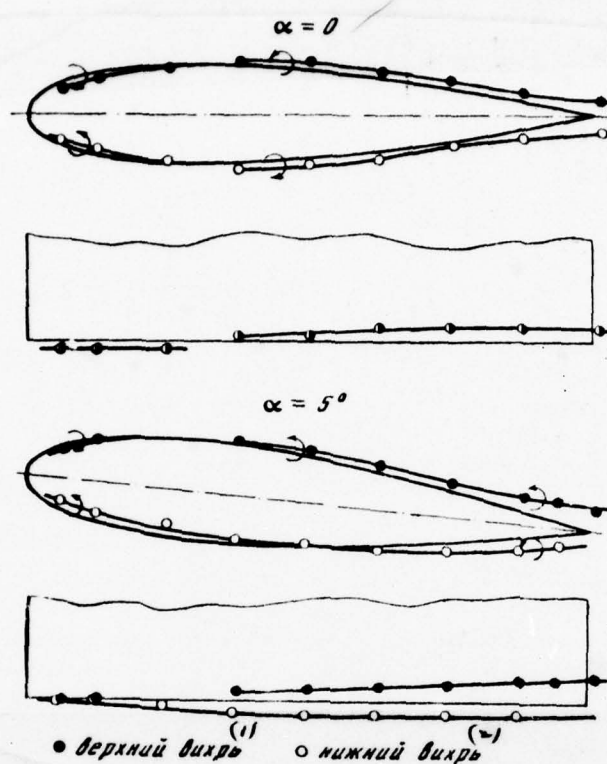


Fig. 6.

Key: (1). Upper eddy/vortex. (2). lower eddy/vortex.

Received 13/VIII 1969.

Page 113.

STUDY OF THE VORTEX SYSTEM OF HELICOPTER ROTOR.

V. G. Kolkov.

By the method of visualization is investigated the vortex/eddy system of helicopter rotor with its circular blowing over a wide range of the flight speeds and values of specific load. Is establish/installated the dependence of the form of vortex/eddy system on the rate of the undisturbed flow and on specific load on screw/propeller. Are determined the forms of vortex systems in different modes of operation of rotor. Are establish/installated the limits of the applicability of the existing models of vortex systems.

Helicopter rotor flows itself both at small and at large positive and negative angles of attack ($-90^\circ \leq \alpha \leq +90^\circ$) over a wide range of flight speeds, including the mode of operation of screw/propeller on the spct. In connection with this is observed the diversity of the forms of the vortex/eddy system of screw/propeller with very complex problem of induced velocities into surrounding screw/propeller space. The analysis of this field is important for

determining of the aerodynamic characteristics of rotor and systems of screw/propellers taking into account their mutual induction, and also for the solution of the number of questions of the interference of the rotor, wing and other cell/elements of helicopter. Therefore the experimental study of the vortex/eddy system of rotor in different modes of its operation represents practical interest and it makes it possible to a certain extent to explain the essence of the occurring in flow physical processes.

One of the effective methods of the study of the vortex/eddy system of screw/propeller is the method of visualization the fume of the eddy/vortices, which disappear from blade tips. The first experiments on the basis of this method were carried out A. S. D'yachenko [1] in 1957 on the model of screw/propeller in oblique flow with small α and under conditions of vertical descent.

In this article are given some results of the study of the forms of vortex/eddy system with the circular blowing of screw/propeller in the vertical wind tunnel of TsAGI.

The tests were carried out on the model of two-bladed propeller 2.1 m in diameter. For the visualization of vortex/eddy system, was utilized the oil fume, produced from blade tip. Propeller hub was equipped by extensometric balance for measuring the total aerodynamic

characteristics of screw/propeller. In the process of experiment, was conducted the high-speed filming of the visualized vortex/eddy system.

Fig. 1, depicts the climb regime on vertical line with a low speed of lift of $\tilde{V}_\infty = \frac{V_\infty}{\omega R} \approx 0.05$, where V_∞ - a speed of flow in wind tunnel, ω - the angular rate of rotation of screw/propeller, R - a radius of screw/propeller. It is evident that in this case is valid the vortex/eddy diagram, it is proposed to N. E. Joukowski.

Page 114.

N. Ye. Zhukovskiy's vortex/eddy diagram occurs, also, during the sufficiently rapid reduction when rate of descent $\tilde{V}_\infty = \frac{V_\infty}{v_n} < -2.5$, where v_n - average on the swept disk induced velocity while hovering. In these conditions/modes the induced velocities, created by screw/propeller, are low in comparison with the rate of the undisturbed flow.

Under conditions of reduction with low speed, the flow pattern of screw/propeller significantly changes. In this case the caused by free vorticity are commensurable with the rates of the motion of vortex elements. The cell/elements of free vortices move so slowly that they manage to be broken in close to the screw/propeller of

area. Is observed the expansion of vortex/eddy system, caused by the fact that the limited as a result of diffusion system of free vortices induces the rates radial components which are directed toward periphery. This expansion can occur, obviously, only in viscous fluid.

With an increase in the rate of descent, vortex/eddy system approaches a plane of the rotation of screw/propeller (Fig. 2a). In connection with this the induced velocities in this plane grow/rise. And vortex/eddy vortex cores have complex spiral-shaped form. Is observed the conditions/mode "vortex ring", special feature/peculiarity of which is the annular motion of the masses of air around vortex bands. Free vortices under these conditions create in flow high turbulence, which causes the increased agitation of helicopter.

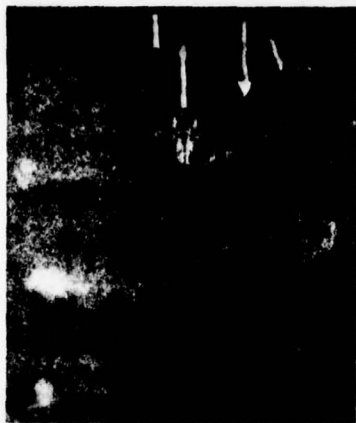


Fig. 1. Conditions/mode of vertical lift:

$\alpha = -90^\circ$; $c_T = 0.0086$; $V_{co} \approx 1$

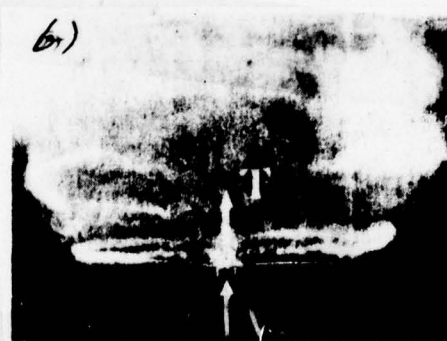
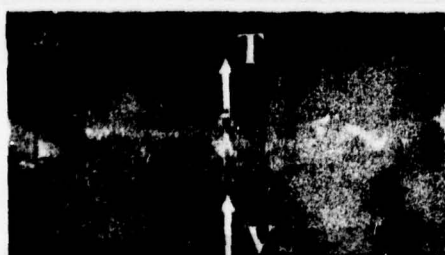


Fig. 2. Conditions/modes of the vertical descent:

a) $\alpha = 90^\circ$; $c_T = 0.013$; $V \approx -1.5$
 b) $\alpha = 90^\circ$; $c_T = 0.013$; $V \approx -1.76$

Page 115.

With further increase in the rate of descent, free vortices are

taken away upstream (Fig. 2b), which leads to the decrease of induced velocities. The observed expansion of vortex/eddy system can be explained by different action of the individual sections of this system on each other. The vortex elements, arranged/located far from the plane of the rotation of screw/propeller, produce near screw/propeller the induced velocities radial components which are directed outside, which leads to the expansion of system after screw/propeller. The cell/elements of eddy/vortices, located near screw/propeller, produce at the outlying eddy/vortices the induced velocities radial components which are directed toward screw axis, which with respect gives to certain contraction of the expanded vortex/eddy system. As network for these conditions/modes, it is possible to accept the approximate theoretical diagram, assumed by Ye. S. Vozhdaev [2].

The visualization of the tip vortices of screw/propeller with different values V_∞ and $\bar{v}_n = \frac{v_n}{\omega R} = -0.5 \sqrt{c_T}$ (where $c_T = \frac{T}{\frac{\rho_0}{2} (\omega R)^2 \pi R^2}$ - force coefficient of propeller thrust, T - the thrust of screw/propeller, ρ_0 - air density of the earth/ground) it shows that the essential transformation of the vortex/eddy system of screw/propeller occurs at the rates of descent, which correspond to interval $-2.5 < \bar{V}_\infty < -0.5$. Out of this range of rates, is valid the cylindrical vortex/eddy diagram, proposed to N. Ye. Zhukovskiy.

Under conditions of oblique blowing, the rotor tested over a wide range of angles of attack ($-60^\circ \leq \alpha \leq 60^\circ$).

In large negative angles of attack (Fig. 3) real vortex/eddy system satisfactorily corresponds to the vortex/eddy model of rotor in oblique flow, proposed by G. I. Maykapar [3]. In these conditions/modes the vortex elements are arranged/located at considerable removing from plane the rotation of screw/propeller. The produced by them induced velocities in this plane are small. Under the conditions of the oblique blowing of screw/propeller at angle $\alpha=0$ (Fig. 4a) the observed deviation of vortex/eddy system from the plane of rotation occurs only due to the presence axial component induced velocity which is commensurable with the rate of the undisturbed flow. The angle of the slope of the obtained in this case vortex/eddy cylinder depends both on the velocity of the incident to screw/propeller undisturbed flow and from the value of load on screw/propeller. At high flight velocity $\left(\mu = \frac{V_\infty \cos \alpha}{\omega R} \geq 0,15 \right)$ vortex/eddy system can be considered plane (Fig. 4b).

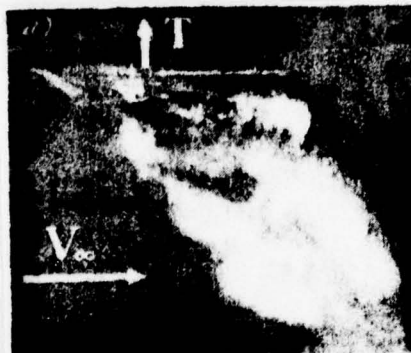


Fig. 3. Climb with $\alpha = -60^\circ$.
 $\mu \approx 0,05$, $c_T = 0,0123$

Fig. 4. Flat/plane vortex/eddy system with $\alpha=0$ and $c_T = 0,0095$.
a) $\mu \approx 0,05$; b) $\mu \approx 0,25$

Page 116.

Induced velocities in these conditions/modes are negligible in comparison with the rate of the incident or screw/propeller undisturbed flow. According to given L. S. Sil'dgrube [4], the vortex sheet will be virtually flat/plane, if $\mu \geq 1,15 / c_T$. When $c_T = 0,0095$ we find $\mu > 0,112$. Thus, this relationship/ratio is satisfactorily confirmed by

experiment.

Considerable interest represents the investigation of the insufficiently studied conditions/modes of the steep glide. During gliding/planning at angle of $\alpha=30^\circ$ with $\mu=0.05$ and light load on screw/propeller, the form of vortex/eddy system is close to the theoretical schematic of oblique vortex/eddy cylinder (Fig. 5a). With an increase in the load on screw/propeller, the rate of the motion of the cell/elements of free vortices becomes less, that leads to more intense eddy diffusion as a result of the grown effect of the forces of viscosity (Fig. 5b) and to the destruction of vortex/eddy system.

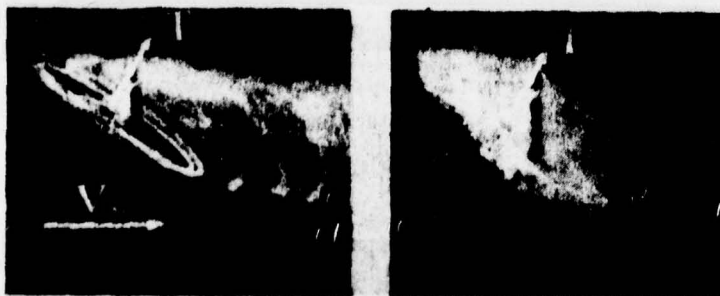


Fig. 5. Gliding conditions with $\alpha=30^\circ$ and $\mu \approx 0.05$.

a) $c_T = 0.0055$; b) $c_T = 0.015$

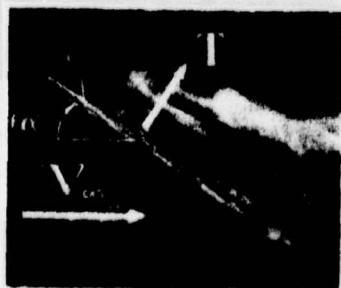


Fig. 6.

Fig. 6. Gliding condition with $\alpha = 30^\circ$, $\mu \approx 0.1$, $c_f = 0.0087$

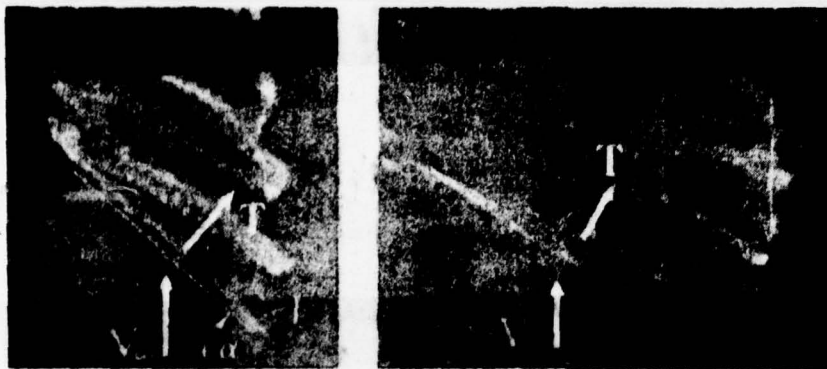


Fig. 7. Conditions/modes of the steep glide at $\alpha = 60^\circ$ and $\mu \approx 0.05$:

a) $c_f = 0.0087$, b) $c_f = 0.0174$

Page 117.

Thus, usual vortex conceptions prove to be inapplicable to the calculation of these conditions/modes. Calculation according to the schematic of oblique vortex/eddy cylinder here it is possible to carry out only with very low values of the quantity of specific load on screw/propeller. At larger gliding speed (Fig. 6) is noticeable end of vortex deformation bands, caused by interaction of vortex elements with each other. For these conditions/modes, apparently, one should apply the nonlinear calculation methods, which consider the deformation of vortex elements.

During the investigation of the conditions/modes of the steep glide at angle of $\alpha=60^\circ$ (Fig. 7) was observed the nonuniformity of the motion of the cell/elements of free vortices along the disk of screw/propeller. The rate of the motion of vortex elements, exiting/waste from the rear end of the disk of screw/propeller, is smaller than the rate of the motion of vortex elements, exiting/waste from its front/leading part. Vortex/eddy cylinder is retained at considerable removing from the plane of the rotation of screw/propeller, and the noted nonuniformity of the motion of vortex elements is observed within the limits of the oblique vortex/eddy cylinder (see Fig. 7a). With high value specific load on the screw/propeller (see Fig. 7b) vortex elements in the rear end of the disk of screw/propeller transfer/convert under the plane of rotation. Thus, vortex/eddy system is arranged/located from two sides from the plane of the rotation of screw/propeller.

Fig. 7b, shows the dark vortex core of the blade/vane, from which the fume was not discharged. As we see, fume does not fall from without into vortex core. This means that the vortex filament near screw/propeller consists of one and the same particles of the air (vortex filament is moved together with air), that it corresponds to Helmholtz' second theorem. Thus, in this case the effect of diffusion near screw/propeller is small and it can be disregarded.

REFERENCES

1. B. E. Baskin, A. S. D'yachenko, G. I. Maykapar, A. I. Martynov. Study of air flow and blade loadings of the screw/propeller of helicopter in level flight. by "eng. jour." the AS USSR, Vol. III of iss. 3, 1963.

2. Ye. S. Vozhdayev. Theory of rotor under conditions "vortex ring", BNI of TsAGI, iss. 1184, 1970.

3. G. I. Maykapar. Vortex conception of rotor. Collection of works on the theory of propellers. BNI of TsAGI, 1953.

4. L. S. Vil'dgrube. Aerodynamic design of helicopters. Transactions of TsAGI, 1954.

Received 2/VII 1969.

Page 118.

FLUCTUATIONS OF LIQUID IN CYLINDRICAL CONTAINERS WITH CIRCULAR BAFFLE.

I. V. Kclin.

Is examined determination by the method of direct/straight dynamic characteristics of the fluctuations of the liquid, which partially fills cylindrical cavity with circular partition/baffle. Is given the comparison of the results of calculation with the results of experiment.

For an increase of oscillation damping of liquid in cavities, are establish/installated different damping baffles: circular, longitudinal, perforate/punched and so forth [1]. Since the theoretical analysis of the dynamics of liquid in such cavities is complex, at present during determining of the dynamic characteristics of the fluctuations of liquid (natural vibration frequency ω , the moving mass of liquid m , the coordinate of the point of the application/appendix of flow forces l) in cavities with partition/baffles the dominant role plays experiment. Experiments showed that the setting in the cavity of circular partition/baffles

during the fluctuations of liquid leads to the appearance of the eddy/vortices whose intensity determines the dissipation of kinetic energy, i.e., the attenuation of its fluctuations. Furthermore, introduction into cavity with the liquid of the damping baffles leads to a change in the dynamic characteristics of the fluctuations of liquid ω, μ, λ .

The approximate theoretical studies of the dynamics of liquid in cylindrical cavity with the circular partition/baffles of small width is given in work [2].

In this article is examined the solution by the method of the straight lines of the problem of the fluctuations of liquid in cavity with the circular partition/baffle arbitrarily of width. This method makes it possible to rate/estimate a change in the dynamic characteristics of the fluctuations of liquid during introduction into cavity with the liquid of circular partition/baffle. Calculations by the method of straight lines showed that on the levels, close to partition/baffle, the characteristics of the fluctuations of liquid differ significantly from the appropriate characteristics in cavity without partition/baffle.

The results of calculation by the method of straight lines satisfactorily will agree with the results of experiment.

§1. Derivation of the equation of the frequencies of liquid.

In cavity at a distance h_n under free surface of liquid is establish/installed circular partition/baffle by width d_n (Fig. 1).

It is known that the problem of the natural oscillations of liquid is formulated as follows:

$$\Delta\varphi = 0 \text{ в объеме жидкости } \tau; \quad (1)$$

$$j \frac{\partial \varphi}{\partial x} + \frac{\partial^2 \varphi}{\partial t^2} = 0 \text{ на свободной невозмущенной поверхности жидкости } \Xi; \quad (2)$$

$$\frac{\partial \varphi}{\partial n} = 0 \text{ на смачиваемой поверхности } S, \quad (3)$$

Key: (1). In the volume of liquid τ . (2). on free undisturbed surface of liquid. (3). on hydrophilic surface of S .

where $S = S_1 + S_+ + S_-$ (S_1 - hydrophilic surface of cavity without partition/baffle, S_+ and S_- - upper and lower surfaces of the damping baffle); $\varphi = \Phi(r, r_0, x) e^{i\omega t}$ - velocity potential of liquid [(r, r_0, x) - cylindrical coordinates]; \bar{n} - unit normal to S .

Page 119.

let the cavity represent by itself direct/straight circular

cylinder with flat/plane bottom. Boundary-value problem for determination $\Phi(r, \eta, x)$ takes the form (see Fig. 1)

$$\Delta\Phi = r^2 \frac{\partial^2 \Phi}{\partial r^2} + r \frac{\partial \Phi}{\partial r} + \frac{\partial^2 \Phi}{\partial \eta^2} + r^2 \frac{\partial^2 \Phi}{\partial x^2} = 0 \quad \text{в } \tau; \quad (4)$$

$$j \frac{\partial \Phi}{\partial x} - \omega^2 \Phi = 0 \quad \text{при } x = 0; \quad (5)$$

$$\frac{\partial \Phi}{\partial r} = 0 \quad \text{при } r = R; \quad (6)$$

$$\frac{\partial \Phi}{\partial x} = 0 \quad \text{при } x = -H; \quad (7)$$

$$\frac{\partial \Phi}{\partial x} = 0 \quad \text{на } S_+ \text{ и } S_-.$$

Key: (1). V. (2). with. (3). on.

Let us examine the plane, passing through the damping baffle. It divides volume τ into two volume τ_+ and τ_- , arranged/located above and below partition/baffle. Let us designate velocity potentials in τ_+ through $\Phi_+(r, \eta, x)$, in τ_- - through $\Phi_-(r, \eta, x)$. Taking into account the continuity of a change in the velocity potentials and the vertical velocities of liquid during transition from τ_- in τ_+ , for determining the potentials Φ_+ and Φ_- it is possible to formulate following boundary-value problems;

$$I. \Delta\Phi_+ = 0 \quad \text{в } \tau_+; \quad (8)$$

$$\frac{\partial \Phi_+}{\partial r} = 0 \quad \text{при } r = R; \quad (9)$$

$$\frac{\partial \Phi_+}{\partial x} = 0 \quad \text{при } x = -h_n, \quad (R - d_n) < r < R; \quad (10)$$

$$\Phi_+ = \Phi_- \quad \text{при } x = -h_n, \quad 0 < r < (R - d_n); \quad (11)$$

$$j \frac{\partial \Phi_+}{\partial x} - \omega^2 \Phi_+ = 0 \quad \text{при } x = 0; \quad (12)$$

$$II. \Delta\Phi_- = 0 \quad \text{в } \tau_-; \quad (13)$$

$$\frac{\partial \Phi_-}{\partial r} = 0 \quad \text{при} \quad r = R; \quad (14)$$

$$\frac{\partial \Phi_-}{\partial x} = 0 \quad \text{при} \quad x = -h_0; \quad (R - d_0) \leq r < R; \quad (15)$$

$$\frac{\partial \Phi_+}{\partial x} = \frac{\partial \Phi_-}{\partial x} \quad \text{при} \quad x = -h_0; \quad 0 < r < (R - d_0); \quad (16)$$

$$\frac{\partial \Phi_-}{\partial x} = 0 \quad \text{при} \quad x = -H. \quad (17)$$

Key: (1) - V. (2) - with. (3) - with.

$a_{\pm i}, b_{\pm i}$ - unknown constants.

Let us introduce the designations

$$c_i^0 = a_i - a_{-i}, \quad c_i = a_i + a_{-i} \quad (19)$$

from conditions (12) and (17) it follows

$$c_i = c_i^0 \omega^2 \frac{R}{j \xi_i}; \quad b_{-i} = b_i \exp \left(-2 \xi_i \frac{H}{R} \right). \quad (20)$$

General solutions for the potentials Φ_+ and Φ_- taking into account (20) take the form

$$\Phi_+ = \sum_{i=1}^{\infty} J_i \left(\xi_i \frac{r}{R} \right) c_i \left[\operatorname{ch} \left(\xi_i \frac{x}{R} \right) + \omega^2 R (j \xi_i)^{-1} \operatorname{sh} \left(\xi_i \frac{x}{R} \right) \right] \cos \eta_i \quad (21)$$

$$\Phi_- = \sum_{i=1}^{\infty} J_i \left(\xi_i \frac{r}{R} \right) b_i \left[\exp \left(\xi_i \frac{x}{R} \right) + \exp \left(-2 \xi_i \frac{H}{R} \right) \exp \left(-\xi_i \frac{x}{R} \right) \right] \cos \eta_i \quad (22)$$

During this selection of solutions, boundary conditions (8), (9), (12), (13), (14), (17) are satisfied. The unknown values c_i and b_i are determined from boundary conditions (10), (11) and (15), (16). Subsequently in general solutions (21) and (22) is considered n of the first terms. Boundary conditions (10), (11), (15), (16) are considered in the discrete number of points $(r_k - h_n)$ - at the points of intersection of vertical straight lines with the plane of the partition/baffle (see Fig. 1).

In matrix recording these conditions take the form

$$A_1 X - \omega^2 j^{-1} A_2 X = A_3 Y, \quad (23)$$

$$B_1 X - \omega^2 j^{-1} B_2 X = B_3 Y, \quad (24)$$

where

$$X = \begin{bmatrix} c_1 \\ c_2 \\ \vdots \\ c_n \end{bmatrix}; \quad Y = \begin{bmatrix} b_1 \\ b_2 \\ \vdots \\ b_n \end{bmatrix}. \quad (25)$$

Matrix elements A_i and B_i take the form

$$a_{1ik} = \begin{cases} J_1\left(\xi_i \frac{r_k}{R}\right) \operatorname{ch}\left(\xi_i \frac{h_n}{R}\right) & k = 1, 2, \dots, p; \quad i = 1, 2, \dots, n; \\ \xi_i R^{-1} J_1\left(\xi_i \frac{r_k}{R}\right) \operatorname{sh}\left(\xi_i \frac{h_n}{R}\right); & k = (p+1), \dots, n; \quad i = 1, 2, \dots, n; \end{cases} \quad (26)$$

$$a_{2ik} = \begin{cases} R \xi_i^{-1} J_1\left(\xi_i \frac{r_k}{R}\right) \operatorname{sh}\left(\xi_i \frac{h_n}{R}\right) & k = 1, 2, \dots, p; \quad i = 1, 2, \dots, n; \\ J_1\left(\xi_i \frac{r_k}{R}\right) \operatorname{ch}\left(\xi_i \frac{h_n}{R}\right); & k = (p+1), \dots, n; \quad i = 1, 2, \dots, n; \end{cases}$$

$$a_{3ik} = \begin{cases} J_1\left(\xi_i \frac{r_k}{R}\right) \left[\exp\left(-\xi_i \frac{h_n}{R}\right) + \exp\left(-2\xi_i \frac{H}{R}\right) \exp\left(\xi_i \frac{h_n}{R}\right) \right] & k = 1, 2, \dots, p; \quad i = 1, 2, \dots, n; \\ 0; & k = (p+1), \dots, n; \quad i = 1, 2, \dots, n; \end{cases}$$

$$b_{1ik} = \begin{cases} \xi_i R^{-1} J_1\left(\xi_i \frac{r_k}{R}\right) \operatorname{sh}\left(\xi_i \frac{h_n}{R}\right); & k = 1, 2, \dots, p; \quad i = 1, 2, \dots, n; \\ 0; & k = (p+1), \dots, n; \quad i = 1, 2, \dots, n; \end{cases} \quad (27)$$

$$b_{2ik} = \begin{cases} J_1\left(\xi_i \frac{r_k}{R}\right) \operatorname{ch}\left(\xi_i \frac{h_n}{R}\right); & k = 1, 2, \dots, p; \quad i = 1, 2, \dots, n; \\ 0; & k = (p+1), \dots, n; \quad i = 1, 2, \dots, n; \end{cases}$$

$$b_{3ik} = -\xi_i R^{-1} J_1\left(\xi_i \frac{r_k}{R}\right) \left[\exp\left(-\xi_i \frac{h_n}{R}\right) - \exp\left(-2\xi_i \frac{H}{R}\right) \exp\left(\xi_i \frac{h_n}{R}\right) \right]; \quad i, k = 1, 2, \dots, n.$$

Components Y are determined from the uniform system of the algebraic equations

$$(A_1 - A_3 B_3^{-1} B_1) Y - \omega^2 j^{-1} (A_2 - A_3 B_3^{-1} B_2) Y = 0. \quad (28)$$

The equation of frequencies takes the form

$$[(A_1 - A_3 B_3^{-1} B_1) - \omega^2 j^{-1} (A_2 - A_3 B_3^{-1} B_2)] = 0. \quad (29)$$

The given above formulas are suitable only when $h_n > 0$. When $h_n = 0$ the problem is solved by the method, presented in work [3]. Thus, determination by the method of the direct/straight velocity potentials and frequencies of liquid in cavity with circular partition/baffle is reduced to the problem against the intrinsic numbers and the vectors of some matrix/dies.

Knowing the velocity potentials of liquid, it is possible to determine the moving mass of liquid and the coordinate of the point of application/appendix l , of the resultant of flow forces [4]:

$$m = \rho \frac{\omega^2}{j} \left(\int_{\Sigma} z \varphi dS \right)^2 \bigg/ \int_{\Sigma} \varphi^2 dS, \quad (30)$$

$$l = \frac{j}{\omega^2} \int_{\Sigma} \varphi (x n_z - z n_x) dS \bigg/ \int_{\Sigma} z \varphi dS. \quad (31)$$

§2. Results of calculation.

For the evaluation of accuracy/precision and effectiveness of

the method of straight lines, was carried out the calculation of cylindrical cavity with the partition/baffle of width $d_n = 0,3 R$, establish/installated at a distance $1.45R$ from bottom. Fig. 2, gives the results of calculation ($n=20$) of the frequencies of the first (0, curve 1), second (Δ , curve 2) tones of the fluctuations of liquid. There are given the results of the calculation of moving masses (x, curve 3) and the coordinates of the points of the application/appendix of hydrodynamic pitchforks (\square , curve 4) the results of the calculation of values $\frac{\omega_1^2 R}{j}$ and $\frac{l_1}{R}$ were compared with the results of experiment (0, \blacksquare).

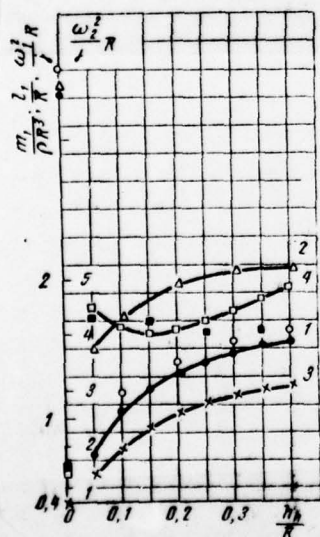


Fig. 2.

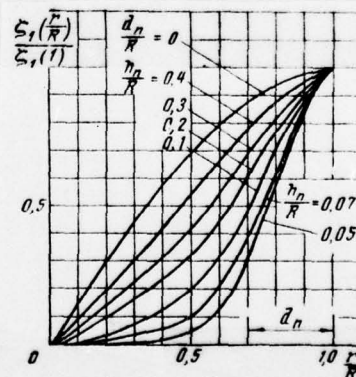


Fig. 3

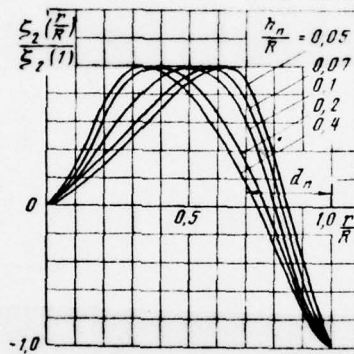


Fig. 4

Page 122.

During the comparison of theoretical and experimental results, is observed a good coincidence. It should be noted that during the approach/approximation of the level of filling to partition/baffle from above the frequency of liquid it decreases, which is explained by the effect of the flat/plane bottom, created by partition/baffle. During the coincidence of free surface of liquid with the plane of

partition/baffle, the frequency of liquid in cavity with partition/baffle is higher than the frequency in cavity without partition/baffle on the same level of filling.

Fig. 3 and 4, give $\zeta_1(r)$ and $\zeta_2(r)$ - computed values of the forms of free surface of liquid, which correspond to the first and second tones of fluctuations. the fields-unit vectors of rates near partition/baffle, that corresponds to the first tone of the fluctuations of liquid, is given to Fig. 5.

The satisfactory coincidence of theoretical results with experimental data shows that the method of straight lines with sufficient for technical application/appendices accuracy/precision can be applied for the calculation of the cavities of rotation with circular partition/baffles.

AD-A066 206

FOREIGN TECHNOLOGY DIV WRIGHT-PATTERSON AFB OHIO
SCIENTIFIC NOTES FROM THE CENTRAL AERO-HYDRODYNAMIC INSTITUTE (--ETC(U)
AUG 78

F/G 20/4

UNCLASSIFIED

FTD-ID(RS)T-1039-78

NL

4 OF 4

AD
A099208



END
DATE
FILMED
5-79
DDC

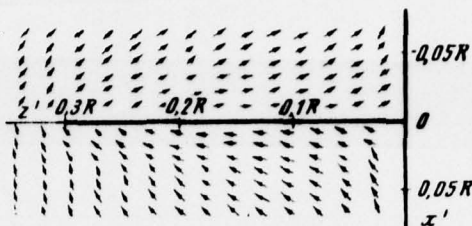


Fig. 5.

REFERENCES

1. J N Mills. Ring Damping of free surface cseillations in circular tank. J Appl. Mech., 1958, v 25, No 2.

2. H F Bauer. Zur Elastising Tragheitsmoment Erhounng und Schwaerenmassenreduktion durch Dastungsringe in Treibstofftank. Raumfahrtforschung, HF 4, 1967.

3. I. V. Kolin, V. N. Sukhov. Solution of the problem of the fluctuations of liquid in the cavities of rotation by the method of straight lines, "scientific notes of TsAGI", No 3, 1970.

4. G. N. Mikishev, B. I. Fabinovich. dynamics rigid body with the cavities, partially filled by liquid. M., "machine-building", 1968.

DOC = 78103907

PAGE

~~38~~ 284

Received 14/XII 1969.

end section.

~~SECRET 14100 NT VERSION PROG 11 APR 78 ETC 006 04 12 78~~

Page 123.

DETERMINATION OF THE REQUIRED ACCURACY OF THE AUTONOMOUS ANGULAR MEASUREMENTS AND ESTIMATION POWER CONSUMPTION FOR THE TRAJECTORY CORRECTION OF SPACE VEHICLE DURING APPROACH TO PLANET.

S. V. Petukhov.

Is examined the task of the determination of the required accuracy of angular measurements for purpose of obtaining of estimating the parameters of the motion of space vehicle relative to destination planet. It is assumed that the information about the motion of space vehicle enters from its edge discretely in the form of some angular values, measured at the assigned/prescribed moment of time. Is investigated the dependence of the required accuracy of measurements from the program of conducting measurements and from the parameters, which determine the motion of the center of mass of space vehicle, taking into account the restrictions placed on the width of the corridor of entry in the atmosphere of planet. Is given the estimation of the expenditures of characteristic velocity on one and two-pulse correction.

1. Let us examine motion of space vehicle on section of approach to planet when is correct assumption about the fact that on vehicle acts only attraction of destination planet, and disturbance/perturbations, caused by solar gravity and other planets, can be considered negligible. In this case the trajectory of approach represents by itself hyperbola with focus in the gravitational center of planet. xyz - planet-centered right-handed coordinate system (Fig. 1). Z axis is directed in parallel to the asymptote of the hyperbola of approach (towards the velocity vector of space vehicle at infinite removal/distance from planet). Plane XY represents plane of figure in which is arranged/located the vector of sighting range \vec{W} - perpendicular, omitted from the origin of coordinates to the asymptote of the hyperbola of approach. Sighting range $w = |\vec{W}|$ determines the small distance of the flight/span of space vehicle from planet without the account of its attraction [1, 2]. Value w at given speed \vec{V}_∞ is unambiguously connected with pericentric distance r_p (by conditional pericenter). Between the standard deviation of pericentric distance $(\delta r_p)_{\max}$ and the width of the corridor of entry in the atmosphere δH_{ex} there is communication/connection, which is determined by many values (change in the atmospheric density in height/altitude, the lift-drag ratio of space vehicle, the height/altitude of conditional pericenter, etc.). Subsequently for

simplicity, let us set/assume $(\delta r_p)_{\max} = \delta H_{\text{BX}}, r_p = r_{\text{H.1}} (r_{\text{H.1}} - \text{a radius of planet}).$

$$\delta r_p = \dot{r}_p \delta w. \quad (1)$$

Page 124.

The deviation of conditional pericenter is recounted to deviation in plane of figure δw with respect to the formula

where $\dot{r}_p = \left(\frac{\partial r_p}{\partial w} \right) = \left(1 + \frac{\mu}{w V_\infty^2} \right)^{-\frac{1}{2}}$ - particular derivative of r_p according to w , calculated from nominal trajectory when $V_\infty = \text{const}$ [3], μ - the gravitational constant of planet (for Mars $\mu = 42.88 \cdot 10^3 \text{ km}^3/\text{s}^2$). In series of problems, connected with navigation and trajectory correction of space vehicle during approach to planet, it is more preferable to utilize as the corrected parameter sighting range w instead of r_p : at sufficiently large distance from planet flight speed V constant (Fig. 2), moreover $V_x = V_y = 0; V_z = V = V_\infty$, therefore $\delta w = (\delta V_x^2 + \delta V_y^2)^{1/2} T$, where T - flight time to plane of figure. This makes it possible to simplify the algorithm of processing the results of trajectory measurements [4] and allow/assumes comparatively idle time, also, at the same time sufficiently precise calculation the sublimity of corrective momentum/impulse/pulses [5].

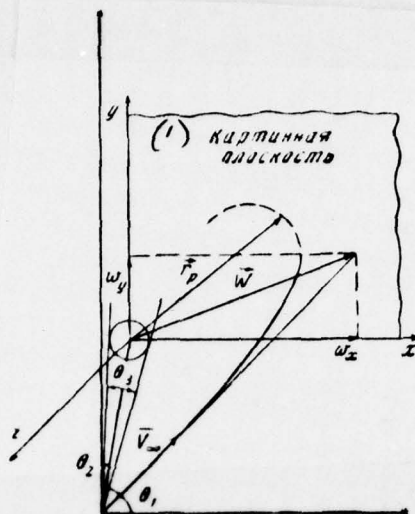


Fig. 1.

Key: (1). Picture plane.

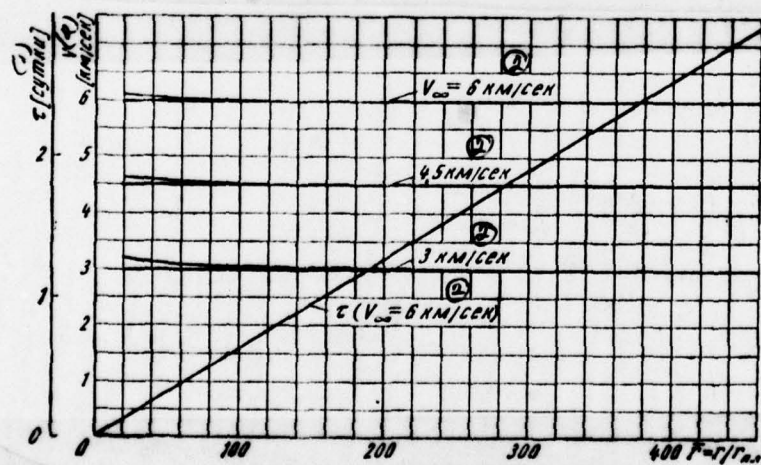


Fig. 2.

Key: (1). days. (2). km/s.

Page 125.

Let us determine position and the velocity of space vehicle in the selected system of coordinates xyz by state vector

$\vec{R} = (x, y, z, V_x, V_y, V_z)^T$ (T indicates transposition). At zero time $R(0) = R_0 + \delta R_0$, where $R_0 = (x_0, y_0, z_0, 0, 0, -V_\infty)^T$, and δR_0 - vector of the random initial deviations, distributed according to normal law with zero mathematical expectation and known correlation matrix/die K_{R_0} .

2. For examination of disturbed motion, let us pass to osculating cell/elements, i.e., to parameters q_1, q_2, \dots, q_6 , which uniquely determine trajectory and are constant values, with exception/elimination of torque/moments of time, when is conducted trajectory correction. The parameters of trajectory let us select in such a way that the first two parameters would be corrected. As such parameters let us examine the components of vector \vec{W} of sighting range in plane of figure $q_1 = w_x, q_2 = w_y$ (see Fig. 1). Those linearized relative to the supporting trajectory of the equation of the disturbed motion of space vehicle take the form

$$\frac{d}{dt} \delta \vec{q} = A \cdot \vec{u}. \quad (2)$$

Here

$\delta \vec{q} = (\delta q_1, \delta q_2, \dots, \delta q_6)^T$ - the random vector of the deviations of the parameters of trajectory.

\vec{u} - vector of the control pressures, $\vec{u} = \Delta \vec{V} \delta(t-\tau)$, where $\Delta \vec{V}$ - vector of the corrective momentum/impulse/pulse of velocity, $\delta(t-\tau)$ - δ -function.

A - matrix/die 6x6 of partial derivatives (6 - dimensionality of the vector of the control pressures).

At zero time $M(\delta \vec{q}_0) = 0$, and correlation matrix/die is determined from the formula

$$K_0 = M(\delta \vec{q}_0, \delta \vec{q}_0^T) = Q_0 K_{R_0} Q_0^T, \quad (3)$$

where Q_0 - matrix/die 6x6 of partial derivatives $\frac{\partial q_i}{\partial R_j}$ ($i, j=1, \dots, 6$) of parameters q_i according to the components of state vector, calculated at the initial moment $t=0$; K_{R_0} - correlation matrix/die of the probable deviations of state vector with $t=0$. Two upper diagonal of matrix element K_0 represent the initial (a priori) dispersions of the components of the vector of sighting range $\sigma_{q_{10}}^2$ and $\sigma_{q_{20}}^2$. In the

case of statistical independence δw_x and δw_y , the a priori dispersion of deviation in plane of figure is calculated from the formula

$$\sigma_{w_0}^2 = \Sigma_0 = \sigma_{q_{10}}^2 + \sigma_{q_{20}}^2.$$

Let at the previously known moment of time t_1, \dots, t_N with the aid of on-board means be measured the angles between directions in two stars and in the center of planet θ_1 and θ_2 , the angular diameter of planet θ_3 (see Fig. 1). In linear approach/approximation for any moment of time t , it is possible to write:

$$\delta \vec{\theta}_l = \psi_l \delta \vec{q}_l + \vec{\zeta}_l \quad (l = 1, 2, \dots, N), \quad (4)$$

where $\vec{\theta}_l = (\theta_{1l}, \theta_{2l}, \theta_{3l})^T$ - a vector of the measured values; $\vec{\zeta}_l = (\zeta_{1l}, \zeta_{2l}, \zeta_{3l})^T$ - vector of measuring errors; ψ_l - matrix/die 3×6 of particular derivatives of the measured values from the parameters of the trajectory q_1, q_2, \dots, q_6 , computed at torque/moment t .

Let us assume that the measurements contain the random errors $\zeta_1, \zeta_2, \zeta_3$, each of which has normal distribution, moreover at the any moment of time $t_l (0 < l \leq N)$ value $M(\vec{\zeta}_l) = 0$, and correlation matrix/die is diagonal:

$$\Lambda_l = M(\vec{\zeta}_l, \vec{\zeta}_l^T) = \sigma_{\theta_l}^2 P_l. \quad (5)$$

Here $\sigma_{\theta_l}^2$ - the dispersion of single measurement; P_l - known matrix/die of the weights of measuring errors:

$$P_i = \begin{bmatrix} 1/p_1 & 0 & 0 \\ 0 & 1/p_2 & 0 \\ 0 & 0 & 1/p_3 \end{bmatrix}. \quad (6)$$

Page 126.

According to the results of the measurements of values θ_i ($i=1, \dots, N$) it is possible to obtain the estimation of the deviations of the parameters of trajectory with the use of methods of statistical linear analysis [6] or with the aid of the optimum theory of filtration [7]. As a result of the adopted assumptions $M(\delta \vec{q}_0) = M(\delta \vec{R}_0) = 0$, $M(\vec{r}_i) = 0$ the probable deviations are determined with the aid of the dispersion of estimation. In particular, maximum deviation in plane of figure with probability 0.9973 can be determined by rule $(\delta w_N)_{\max} = 3\sigma_{w_N}$, where $\sigma_{w_N}^2 = \sigma_{q_{1N}}^2 + \sigma_{q_{2N}}^2$ - dispersion of deviation in plane of figure, calculated after conducting all N of measurements.

Let us formulate the following task: to determine the greatest permissible errors for angular measurements $(\delta \theta_{\max} = 3\sigma_\theta)$, conducted at the assigned moment of time t_1, t_2, \dots, t_N so that the dispersion of deviation in plane of figure, obtained on the basis of all measurements, would satisfy the condition:

$$\sigma_{w_N}^2 = \left(\frac{\delta r_{p \max}}{3\tilde{r}_p} \right)^2, \quad (7)$$

where $\tilde{r}_{p \max}$ - the maximum standard deviation of pericentric

distance; $\frac{dr_p}{dw}$ - particular derivative of r_p with respect to deviation in plane of figure.

3. With made above assumptions about error distribution for trajectory measurements and of initial deviations from nominal trajectory $\delta \vec{R}_0$, formulated problem is solved by using recurrence formulae, obtained in works [4] and [8]. Correlation matrix/die K_{i+1} of the errors for the estimation of the deviations of the parameters of trajectories q_1, q_2, \dots, q_6 to torque/moment t_{i+1} is calculated taking into account equations (2), (4) and (5) for the formula

$$K_{i+1} = K_i [E - \psi_{i+1}^T (\Lambda_i + \psi_{i+1} K_i \psi_{i+1}^T)^{-1} \psi_{i+1} K_i], \quad (8)$$

where K_i - correlation matrix/die, calculated for the torque/moment of time t_i ;

ψ_{i+1} - the matrix/die 3x6 of the particular derived measured values $\theta_1, \theta_2, \theta_3$ according to the parameters of trajectory q_1, q_2, \dots, q_6 , calculated for the torque/moment of time t_{i+1} ;

$\Lambda_i = \sigma_{\theta_i}^2 P_i$ - the correlation matrix/die of the dimensionality 3x3 of the measuring errors of values $\theta_1, \theta_2, \dots, \theta_3$.

At the first space is utilized the a priori matrix/die K_0 , determined on formula (3). Then for arbitrary value q_0 is conducted

N of calculations with the aid of recursion formula (8), as a result of which is obtained matrix/die K_N . Two First upper of the cell/element of diagonal matrix/die K_N give the representation of the root-mean-square deviation of the components of the corrected parameter - vector of sighting range. Condition (7) is checked with the help of these matrix elements K_N . If

$$\sqrt{\sigma_{q_{1N}}^2 + \sigma_{q_{2N}}^2} \leq \frac{\delta r_{p \max}}{3\varepsilon_p},$$

then process is repeated with new value σ_θ and so forth, until with the assigned/prescribed accuracy/precision is fulfilled the condition

$$\sqrt{\sigma_{q_{1N}}^2 + \sigma_{q_{2N}}^2} = \frac{\delta r_{p \max}}{3\varepsilon_p}.$$

Obtained in this case value σ_θ determines the maximum root-mean-square error for angular measurements $\delta\theta_{\max} = 3\sigma_\theta$, at which with a probability of 0.9973 the condition $|\delta w| \leq \frac{\delta r_{p \max}}{3\varepsilon_p}$ is satisfied. On remaining four diagonal matrix elements K_N it is possible to determine the root-mean-square deviations of the uncorrected parameters q_3, q_4, q_5, q_6 .

Let us note that the use of recurrence formula (8) unlike the method of least squares makes it possible to solve task with the arbitrary intervals of measurements $t_{i+1} - t_i$ ($i=0, 1, \dots, N$) and with the variable composition of measurements $(\theta_1, \theta_2, \dots, \theta_n)$ it is important only so that at each moment of time would be previously known the correlation matrix/die of measuring errors A_{i+1} .

Page 127.

The obtained as a result of the solution of the formulated problem matrix elements (K_i) ($i=1, 2, \dots, N$) at the moment of time t_1, t_2, \dots, t_N are memorized for the calculation of the value of the corrective momentum/impulse/pulses and determination of their optimum position in trajectory.

4. In simpler setting task in question admits analytical solution. Let be measured only two angles - θ_1 and θ_2 - (see Fig. 1) at the moment of time t_1, t_2, \dots, t_N are determined only corrected parameters $q_1 = w_x$ and $q_2 = w_y$. It is possible to show that in this case matrix/die $\psi_k = \frac{\partial \theta_i}{\partial q_j}$ will be determined as follows:

$$\psi_k = \frac{1}{r_k} E, \quad (9)$$

where E - unit matrix (2×2) , r_k - a distance from space vehicle to planet at the moment of conducting the measurements.

The matrix/die of partial derivatives \tilde{Q}_k is simplified:

$$\tilde{Q}_k = \frac{\partial (q_1, q_2)}{\partial r, \partial \vec{V}} = \begin{vmatrix} 1 & 0 & 0 & r_k/V_\infty & 0 & 0 \\ 0 & 1 & 0 & 0 & r_k/V_\infty & 0 \end{vmatrix}.$$

If the correlation matrix/die of initial deviations K_{R_0} takes the diagonal form, moreover $\sigma_{x_0}^2 = \sigma_{y_0}^2 = \sigma_{z_0}^2 = \sigma_{r_0}^2$, $\sigma_{x_0}^2 = \sigma_{y_0}^2 = \sigma_{z_0}^2 = \sigma_{V_0}^2$, then we will obtain:

$$K_0 = \tilde{Q}_0 K_{R_0} Q^T = \begin{vmatrix} \sigma_{q_1}^2 & 0 \\ 0 & \sigma_{q_2}^2 \end{vmatrix}, \quad (10)$$

where $\sigma_{q_{10}}^2 = \sigma_{q_{\infty}}^2 - \sigma_{v_0}^2 + \frac{r_0^2}{V_{\infty}^2} \sigma_{V_0}^2$; r_0 - initial distance of planet.

With previous assumptions about measuring errors, let us assume that the correlation matrix of measuring errors takes the form

$$\Lambda = \begin{bmatrix} \sigma_0^2 & 0 \\ 0 & \sigma_0^2 \end{bmatrix} = \sigma_0^2 E = \text{const},$$

where E - unit matrix (2x2).

Recursion formula (8) is reduced to the form

$$K_{i+1} = K_i \left[E + \frac{1}{r_{i+1}^2} \left(\sigma_0^2 + \frac{\sigma_{q_i}^2}{r_{i+1}^2} \right)^{-1} \sigma_{q_i}^2 E \right], \quad (11)$$

where σ_{q_i} - diagonal matrix elements K_i at the i space. After using formula (11) consecutively N once, under initial condition (10) after simplifications we will obtain

$$\sigma_{q_N}^2 = \frac{\sigma_{q_0}^2}{1 + \frac{\sigma_{q_0}^2}{\sigma_0^2} \sum_{i=1}^N \frac{1}{r_i^2}}, \quad (12)$$

where $r_i = r_0 - \Delta r$, $r_2 = r_0 - 2\Delta r, \dots$, $r_N = r_0 - N\Delta r$; $\Delta r = \frac{r_0 - \Delta t_k V_{\infty}}{N}$ - a space of measurements, $\Delta t_k = t_1 - t_N$.

This same result it is possible to obtain with the use of formulas of linear statistical analysis [9] or with the aid of Kalman's filter by transition from the continuous to discrete measurements [10].

With $\Delta r/r_0 \ll 1$ we will obtain $\sum_{i=1}^N \frac{1}{r_i^2} = \frac{N-1}{r_0 r_N}$. Then from equation (12) we determine the permissible error for the angular measurements:

$$\sigma_\theta = \frac{\sigma_{w_0} \sigma_{w_N}}{\sqrt{\sigma_{w_0}^2 - \sigma_{w_N}^2}} \sqrt{\frac{N-1}{r_0 r_N}}, \quad (13)$$

where $\sigma_{w_0} = \sigma_{w_N} / \sqrt{2}$, while σ_{w_N} it is determined from condition (7). If we assume $\sigma_{w_0} \gg \sigma_{w_N}$, then taking into account (7) we will obtain convenient formula for calculating the permissible root-mean-square error for angular measurements (in radians)

$$\sigma_\theta = \frac{\delta r_{p \max}}{3 \varepsilon_p} \sqrt{\frac{N-1}{r_0 - r_N}}, \quad (14)$$

where r_0, r_N - the distances, which correspond to beginning toward the end of the measurements.

N - number of measurements.

$\delta r_{p \max}$ - the maximum standard deviation of pericentric distance,

$$\delta r_p = \frac{\partial r_p}{\partial w}.$$

With the aid of formula (14) it is possible to rate/estimate requirements for measuring systems depending on the parameters of the trajectory of approach to planet (r_p, V_x, V_p) and the standard deviation of pericentric distance $\delta r_{p \max}$ at predetermined program of trajectory measurements (r_0, r_N, N).

5. Let us determine permissible measuring errors and necessary expenditures of characteristic velocity on trajectory correction of space vehicle during approach to Mars under condition

$$(\delta w)_{\max} \leq \frac{1}{\xi_p} \delta r_{p \max}. \quad (15)$$

Parameters of the trajectory: the velocity of approach $V_\infty = 6$ km/s; pericentric distance $r_p = r_{\min} = 3332.1$ km, in this case $\xi_p = 0.0935$. Let be measured the angles θ_1, θ_2 and the angular diameter of planet θ_3 (see Fig. 1). Weight coefficients in the correlation matrix/die of measuring errors (5) let us accept equal with respect to the following values: $p_1 = p_2 = 1, p_3 = 0.1$. Measurements begin at a distance r_0 , equal to a radius of the sphere of effect (for Mars $r_{\text{сф. вл}} = 1.8$ million km), they are carried out through equal time intervals and they conclude after $\tau_N = 1, 2$ and 3 days to approach by planet. The number of performances of measurements let us take as equal to 25. Initial errors are characterized by values

$$\sigma_{r_0} = \sigma_{x_0} = \sigma_{y_0} = 1000 \text{ km}, \quad \sigma_{V_0} = \sigma_{z_0} = 1 \text{ m/s}.$$

The necessary expenditures of characteristic velocity on correction let us calculate for one- and two-pulse correction under the condition

$$P \sum_{i=1}^2 |\Delta V_i| < U) = \alpha, \quad (16)$$

where $|\Delta V_i|$ - a module/modulus of the momentum/impulse/pulse of

velocity, U - the necessary supply of characteristic velocity for correction (power consumption); α - number, which characterizes the level of the probability of event (-) (let us accept $\alpha=0.9973$). For the calculation of the expenditures of characteristic velocity on correction, we will use the formulas, obtained in work [11] on the assumption that each momentum/impulse/pulse must completely remove more precisely formulated deviation in plane of figure. During the analysis of the effect of performing errors δV , let us consider that they are distributed according to normal law and do not depend on the value of the momentum/impulse/pulse of correction, moreover

$$M(\delta V) = 0; \quad M(\delta V^2) = \sigma_{\delta V}^2.$$

The results of the calculations of the permissible error for angular measurements σ_θ without the account of performing errors are given in table 1 and 2.

Page 129.

The permissible error for angular measurements, as in the simplified setting [see formula (14)], it is proportional to standard deviation in plane of figure $\delta r_{p \max}$. If we compare obtained values σ_θ with those calculated according to formula (14), then it is possible it will ascertain that the expansion of the composition of the measurements by adding the angle θ , makes it possible to lower

requirements for the accuracy/precision of angle measurement θ_1 and θ_2 , even despite the fact that in our example the angle θ_2 is measured rougher ($\sigma_{\theta_2} = 10 \sigma_{\theta_1} = 10 \sigma_{\theta_2}$). For example, for $N=25$,

$\delta r_{p \max} = 25 \text{ km}$, $r_N = 518400 \text{ km}$ ($\tau_N = 1$ days) on formula (14) we will obtain

$\sigma_{\theta} = 44.605$, and from table 2 $\sigma_{\theta} = 119,515$.

The permissible error for angular measurements is inversely proportional $\sigma_N = \sqrt{\frac{r_N}{V_{\infty}}}$. This fact is explained by the fact that for scattering in plane of figure is superimposed condition (7); therefore the further from the planet conclude the measurements, that more precise must be determined the parameters of trajectory. The effect of the number of measurements on σ , with $r_0 = \text{const}$, $r_N = \text{const}$ can be establish/installed on formula (13): the permissible measuring error increases proportionally $\sqrt{N-1}$.

Table 1.

knocks;

 $N = 25$; $\tau_N = 1$ сек; $\sigma_{\delta V} = 0$

$\delta r_{p \max}$ [км]	σ_0	\bar{U}_I	\bar{U}_{II}	$\bar{U}_{I II}$	$\tau_{I II}$ [сутки]	$N_{I II}$
25	119,515	51,265	23,118	19,061	2,681	8
20	95,586	51,265	22,387	19,081	2,681	8
15	71,675	51,265	21,571	18,405	2,779	7

Key: (1). days.

Table 2.

 $N = 25$; $\delta r_{p \max} = 25$ км; $\sigma_{\delta V} = 0$

$\delta \tau_N$ [сутки]	σ_0	\bar{U}_I	\bar{U}_{II}	$\bar{U}_{I II}$	$\tau_{I II}$ [сутки]	$N_{I II}$
1	119,515	51,265	23,118	19,061	2,681	8
2	37,273	25,632	18,261	16,723	3,059	7
3	7,985	17,088	16,028	15,517	3,302	9

Key: (1). days.

Table 3.

 $N = 25$; $\delta r_{p \max} = 25$ км; $\tau_N = 1$ сек

$\delta \tau_N$ [м.сек]	σ_0	\bar{U}_I	\bar{U}_{II}	$\bar{U}_{I II}$	$\tau_{I II}$	$N_{I II}$
0	119,515	51,265	23,118	19,061	2,681	8
0,05	12,711	51,265	23,347	19,807	2,582	9
0,10	7,999	51,266	21,940	18,402	2,779	7

Key: (1). m/s.

Note. In the tables are accepted the following designations:

 \bar{U}_I - power consumption during the single-impulse correction, in

reference to σ_{V_0}

\bar{U}_{II} - the energy expenditures during the two-pulse correction,
in reference to σ_{V_0}

$\bar{U}_{I II}$ - power consumption to the first momentum/impulse/pulse
during the two-pulse correction, related to σ_{V_0}

τ_V - the remaining flight time to planet after the n
measurement.

$\tau_{I II}$ - the remaining flight time after conducting of the first
correction (during two-pulse correction).

$N_{I II}$ - the number of performances of measurements to conducting
of the first correction (during two-pulse correction).

Page 130.

Value power consumption in the case of single-impulse correction
in effect depends only on initial spread in plane of figure $\Sigma_0 = \sigma_{r_0}^2 +$
 $+ \left(\frac{r_0}{V_\infty}\right)^2 \sigma_{V_0}^2$ and from flight time to planet τ_V which remained
after conducting of the correction (conducting correction in time
coincides with the termination of last/latter measurement). It is

real/actual, power consumption in the case of single-impulse correction are determined from the formula (see [11]) $U_1 = \frac{3}{\tau N} \sqrt{\Sigma_0 - \Sigma_N}$.

Taking into account formula (12) (during measurement only θ_1 and θ_2) we will obtain

$$U_1 = \frac{3}{\tau N} \sqrt{\Sigma_0 - 0,5 \Sigma_0 \left(1 + \frac{0,5 \Sigma_0}{\sigma_0^2} \frac{N-1}{r_0 r_N}\right)^{-1}} = \frac{3}{\tau N} \sqrt{\Sigma_0 - \left(\frac{\delta r_{p \max}}{3 \xi_p}\right)^2}.$$

But since $\Sigma_0 > \Sigma_N$ ($\Sigma_0/\Sigma_N \approx 10^4$), approximately it is possible to count $U_1 = \frac{3}{\tau N} \sqrt{\Sigma_0}$, therefore effect N and $\delta r_{p \max}$ on power consumption is very insignificant (see Table 1 and 2).

In the case of two-pulse correction, the time of the application/appendix of the first momentum/impulse/pulse was located via sorting points on planes $(\Sigma_i, f_i = \frac{1}{\tau_i})$, in which can be carried out correction [11]. These points correspond to the torque/moments of conducting the measurements. The second momentum/impulse/pulse was applied at torque/moment t_N immediately after the termination of all measurements when is satisfied condition (7). The criterion of the selection of the time of conducting the first correction is the minimum of total the power consumption:

$$U_{11} = \min_{0 < i < N} [U_{11}(t_N) + U_{21}(t_i)] = 3 \sqrt{\frac{\pi}{2}} [M(|\Delta V_1|) + M(|\Delta V_2|)].$$

This expression is correct, when one of the momentum/impulse/pulses is that predominate. The results of

calculations show that the first momentum/impulse/pulse is that predominate (see Table 1 and 2); therefore the dependence of total power consumption on time τ_N is exhibited in smaller measure than in the case of single-impulse correction, and limitation on $\delta r_{p \max}$ acts more noticeably, since this limitation affects the character of dependence $\Sigma \left(\frac{1}{\tau} \right)$ and, therefore, for the redistribution of momentum/impulse/pulses. But as a whole during change $\delta r_{p \max}$ the total expenditures are little affected. The total expenditures during two-pulse correction half than in the case of single-impulse.

In such a manner, as during single-impulse correction total power consumption in essence are determined by initial correlation matrix/die $\Sigma_0 \gg \Sigma_N$. But this limitation to a high degree affects the permissible errors for angular measurements. To decrease this effect is possible by the appropriate selection of parameters N , τ_0 , τ_N [see formula (14)].

The effect of the performing errors in essence affects the permissible accuracy of the trajectory measurements: the variance of error for the determination of scattering in plane of figure at the moment of conducting the last/latter correction must satisfy the condition

$$\Sigma_N + \sigma_{\Delta V}^2 \tau_N^2 = \left(\frac{\delta r_{p \max}}{3 \xi_p} \right)^2.$$

Page 131.

After substituting this expression into equation (14), we will obtain

$$\sigma_0 = \left[\left(\frac{\delta r_{p \max}}{3 \tau_N \epsilon_p} \right)^2 - \sigma_{\delta V}^2 \tau_N^2 \right] \sqrt{\frac{N-1}{r_0 - r_V}}.$$

Therefore, when $\sigma_{\delta V} \rightarrow \frac{\delta r_{p \max}}{3 \tau_N \epsilon_p}$, measurements must be ideal ($\sigma_0 = 0$), otherwise will not be fulfilled condition (7). In this case, the consumption by correction decrease due to decrease σ_0 . Moreover during single-impulse correction it is insignificant (as a result of predominant effect Σ_0), while with two-pulse - in larger measure (as a result of a change in the position of the first momentum/impulse/pulse). The results of calculation σ_0 and total power consumption taking into account performing errors are given in table 3.

REFERENCES

1. E. L. Akin, T. M. Enyev. Parameter determination of the motion of space vehicle along the data of trajectory measurements. "space investigations", Vol. I, iss. 1, 1963.
2. M. L. Lidov, D. Ye. Okhotsimskiy, N. M. Teslenko. Study of one class of the trajectories of the bounded three-body problem.

"space investigations", Vol. II, iss. 6, 1964.

3. P. Ye. El'yasberg. Introduction into the theory of the flight of artificial Earth satellites. M., "science", 1966.

4. C R Gates, H J Gordon. Planetary approach guidance. J Spacecraft and Rockets, v 2, No 2, 1965.

5. K. A. Platonov. Study of the properties of the correction maneuvers in interplanetary flights. "space investigations", Vol. IV, iss. 5, 1966.

6. T. Anderson. Introduction into multidimensional statistical analysis. M., Fizmatgiz, 1963.

7. R. E. Kalman, B. S. Bussey. New results in linear filtration and the theory of prediction. Transactions of the American Society of Mechanical Engineers. Series D. "Technical mechanics" (Russ. trans.). Vol. 83, No 1, M., publ. foreign of lit., 1961.

8. V. A. Yaroshevskiy. Synthesis of the statistically optimum linear control systems final of the parameters. Transactions of TsAGI, iss. 1090, 1968.

9. I. A. Boguslavskiy. On the synthesis of stochastic optimum control. Coll. the "contemporary design concepts automatic control systems". Edited by B. N. Petrov, E. V. Solodovnikov, Yu. A. Topchiyev. M., "machine-building", using 1967.

10. S. V. Petukhov. Effect is the composition of trajectory measurements for the trajectory correction of the flight of space vehicles. "space investigations", Vol. VI, iss. 3, 1968.

11. V. A. Yaroshevskiy, G. V. Parysheva. Optimum distribution of the corrective momentum/impulse/pulses during one-parameter correction. "space investigations", Vol. III, iss. 6, 1965; Vol. IV, iss. 1, 1966.

Received 15/VII 1969.

Page 132.

No typing.

END MT/ST-78-1039.

DISTRIBUTION LIST

DISTRIBUTION DIRECT TO RECIPIENT

<u>ORGANIZATION</u>	<u>MICROFICHE</u>	<u>ORGANIZATION</u>	<u>MICROFICHE</u>
A205 DMATC	1	E053 AF/INAKA	1
A210 DMAAC	2	E017 AF/RDXTR-W	1
E344 DIA/RDS-3C	9	E403 AFSC/INA	1
C043 USAMIIA	1	E404 AEDC	1
C509 BALLISTIC RES LABS	1	E408 AFWL	1
C510 AIR MOBILITY R&D	1	E410 ADTC	1
LAB/FIO		E413 ESD	2
C513 PICATINNY ARSENAL	1	FTD	
C535 AVIATION SYS COMD	1	CCN	1
C591 ESTC	5	ASD/FTD/NICD	3
C019 MIA REDSTONE	1	NIA/PHS	1
D008 NISC	1	NICD	2
H300 USAICE (USAPEUP)	1		
P005 ERDA	1		
P005 CIA/CPS/ADB/SD	1		
NAVOEDSTA (50L)	1		
NASI/KSI	1		
AFIT/ID	1		